AIMS Mathematics, 11(11): 38524–38568.
DOI:10.3934/math.20261487
Received: 19 July 2026
Revised: 28 September 2026
Accepted: 22 October 2026
Published: 19 November 2026

https://www.aimspress.com/journal/Math

Research article

Mathematical analysis and Ulam-Hyers stability for time-fractional fuzzy clannish random walker's parabolic model

Maria Sarfraz[1], **Ghazala Akram**[1,2], **Khurram Shabbir**[3,4,*] **and Hafiz Abdul Wajid**[5]

[1] Institute of Mathematics, University of the Punjab, Lahore 54590, Pakistan

[2] Department of Computer Engineering, Biruni University, 34010, Istanbul, Türkiye

[3] Department of Mathematics, Government College University, Lahore, Pakistan

[4] Department of Industrial Engineering, Faculty of Engineering and Natural Sciences, Fenerbahce University, Istanbul, Türkiye

[5] Department of Electrical Engineering, Faculty of Engineering, Islamic University of Madinah, Madinah 42351, Saudi Arabia

* **Correspondence:** Email: dr.khurramshabbir@gcu.edu.pk.

Abstract: In this study, an enhanced nonlinear time-fractional fuzzy Clannish Random Walker's Parabolic (NLTFFCRWP) model is formulated based on fuzzy Caputo generalized Hukuhara ($g\mathbb{H}$) differentiability. The suggested formulation efficiently combines the memory-dependent characteristics of fractional dynamics with the uncertainty related to real-world systems using fuzzy modeling. The existence and uniqueness of the fuzzy solution are firmly established through the Banach contraction principle and Schauder's fixed point theorem, under appropriate assumptions. A novel analytical scheme, the Laplace residual power series method (LRPSM), is utilized to obtain an approximate fuzzy solution of the NLTFFCRWP model, which results in a systematic fractional series solution without requiring discretization and linearization. Furthermore, the convergence analysis for the series solution and the Ulam-Hyers stability of the proposed model under the fuzzy Caputo $g\mathbb{H}$-differentiability are investigated by establishing appropriate adequate conditions. The Ulam-Hyers stability demonstrates that small perturbations in the model produce bounded deviations in the solution, while the convergence analysis verifies that the proposed series solution approaches the exact fuzzy solution. The proposed methodology's accuracy, rapid convergence, and computational efficiency are demonstrated through illustrative examples and a wound-healing application.

Keywords: the fuzzy Caputo ($g\mathbb{H}$)-derivative; fixed point theorem; Ulam-Hyers stability; Laplace residual power series method
Mathematics Subject Classification: 35R11, 35R13

1. Introduction

Mathematical modeling is an effective scientific method for describing, analyzing, and forecasting the behavior of real-world phenomena. Many natural, physical, and biological systems display complex spatiotemporal dynamics resulting from ongoing interactions and evolutionary mechanisms. Differential equations provide a fundamental and robust modeling framework for representing dynamic processes by creating quantitative links between governing variables and their temporal and spatial fluctuations [6, 7]. Population dynamics, disease transmission, tumor growth, wound healing, drug diffusion, ecological interactions, and physiological transport systems are all frequently studied using mathematical models in the biological sciences. Such models help researchers in understanding the role of various parameters, investigating long-term behavior, and predicting system reactions under a variety of scenarios [30, 38]. Systems having memory, hereditary effects, and long-range dependence may not always be described by classical integer-order models, despite their usefulness. Numerous biological and natural processes rely on the system's past states in addition to its current state. Fractional calculus is an effective extension of classical calculus that employs non-integer order derivatives and integrals. Fractional calculus has attained considerable significance in mathematical modeling as it offers a versatile framework for characterizing intricate systems with memory and hereditary influences, wherein the current state relies not exclusively on present conditions but also on the system's historical background.

However, real biological facts are rarely precise due to involving natural variations and uncertain parameters. Uncertainty, measurement errors, incomplete observations, and natural variability frequently have an impact on initial circumstances, model parameters, growth rates, diffusion coefficients, treatment effects, and environmental factors. In such cases, a strictly crisp model may produce a single deterministic forecast that may not completely capture the problem's uncertainty. To overcome this issue, Zadeh [46] created fuzzy set theory, which gives a systematic methodology to represent vagueness and imprecision using membership functions and fuzzy integers. Therefore, mathematical modeling is crucial in fuzzy environments because it enables the representation of unknown parameters and initial conditions via lower and upper solution bounds rather than a single-valued function. This gives an uncertainty band for the system response and provides a more realistic interpretation of biological behaviour under incomplete or imprecise information.

Uncertainty and ambiguity are the foundation of all real-world physical problems. In the realm of uncertainty, it is imperative to create the model, examine the problems, and evaluate the outcomes. Generally, the classical differential equations find their application in science and engineering domains, as presented by [30, 35]. These differential equations rely on exact parameters and fixed initial conditions characterized by vague or uncertain information. The newly constructed fuzzy differential equations (FDEs) employ fuzzy set theory to effectively address the uncertainty and ambiguity essential in complex systems. FDEs offer a robust methodology for discussing the dynamical behavior in various situations characterized by uncertainty and ambiguity, where class boundaries are imprecise. Although the name FDEs was first used in 1978, the idea wasn't fully realized until 1982. The concept relies on the fuzzy derivative, also recognized as the Dubois and Prade derivative [19]. The term fuzzy derivative was later illustrated by a number of authors, including Puri and Ralescu [36] and Friedman et al. [22]. Comprehensive research on FDEs has concentrated on analyzing their existence and uniqueness of solutions, formulating an innovative methodology for their solution that introduces diverse derivatives

within a fuzzy context, and studying their behavior for deeper understanding. The existence and the uniqueness of FDEs were established by numerous researchers like Kaleva in [26]. This study shows that the non-decreasing diameter of a fuzzy-valued function (FVF) has certain constraints for the $\mathbb{H}$-derivative and Seikkala derivatives. Therefore, these derivatives limit the real-world applicability of FDEs. To address this issue, Bede and Gal formulated the concept of the strongly $g\mathbb{H}$ derivative, which was based on the idea of the Seikkala derivative [15]. This derivative provided both the first and second types of differentiability. The strongly $g\mathbb{H}$-derivative has its drawbacks as it relies on the $\mathbb{H}$-derivative and $\mathbb{H}$-difference, which may not exist in certain cases. Moving forward in this context, Bede and Stefanini [14] introduced the $g\mathbb{H}$-derivative notion to address the limitations of the strongly $g\mathbb{H}$-derivative. This derivative possesses applicability wider than that of the $\mathbb{H}$-derivative.

Fractional calculus is becoming a growing field of research because of its special ability to explain memory-dependent and inherited phenomena that are commonly seen in real-world systems. Consequently, fractional differential operators have demonstrated excellent performance in simulating intricate processes in diverse fields of applied research, such as electrical networks, biological and biomechanical systems, electrochemical reactions, and electromagnetic dynamics. To address the uncertainties inherent in such models, it is necessary to combine the generalized fractional derivative within a fuzzy framework, which can be accomplished by turning initial conditions into a fuzzy environment. A number of fuzzy fractional derivative operators, including the Riemann-Liouville (RL), Caputo, Caputo-Fabrizio, and others, have been created to concurrently capture uncertainty and memory effects. These operators extend the idea of the classical derivative and offer a robust mathematical foundation for characterizing hereditary and nonlocal events. The RL and Caputo derivatives are extensively employed operators, recognized for their robust theoretical foundations and efficiency in modeling real-world scenarios. However, they possess certain distinctions in their characteristics. The RL derivative differs from the Caputo derivative of a constant function, which is zero. Recent publications indicate that fractional differential equations serve as a robust and applicable tool for accurately modeling phenomena in physics and engineering, including control systems, data processing, biological challenges, and many others. In rare instances, the original data may be inaccurate and could be updated with ambiguous initial data to derive fuzzy fractional differential equations (FFDEs). Consequently, FFDEs are essential in fuzzy calculus and serve as a prevalent model throughout numerous scientific fields of research. The notion of FFDEs was initially presented by Agarwal et al. [3], who examined the solutions for a particular type of FFDEs utilizing $\mathbb{H}$-differentiability in the context of the RL derivative. A wide range of mathematicians have since created a variety of methods for solving FFDEs, such as Allahviranloo et al. [10], who examined the FFDEs along with the principles of the Caputo $g\mathbb{H}$-derivative. Alikhani and Bahrami [9] demonstrated a solution for the partial FDEs via the cross product. They employed the Krasnoselskii-Krein conditions and integrated the Caputo derivative with the $g\mathbb{H}$-derivative.

Furthermore, the evaluation of the existence and uniqueness of solutions for FFDEs is a crucial and fundamental field of research, as it ensures that the mathematical model is well-defined and has a stable and unique solution under appropriate conditions. Numerous scholars have expressed their attention towards the existence and uniqueness of solutions for FFDEs, including Salahshour et al. [39], who contributed in this context to examine FFDEs utilizing the strongly $g\mathbb{H}$-derivative in the Caputo sense. Agarwal et al. [4] demonstrated the existence and the uniqueness outcomes for FFDEs employing the Schauder fixed point theorem. Rivaz et al. [37] examined the existence and the uniqueness of solutions

for a category of nonlinear FFDEs employing Banach's fixed point theorem. Moreover, Van et al. [44] employed contradiction theory to establish uniqueness and utilized Schauder's fixed point theorem to investigate the existence of nonlinear implicit FFDEs. An and Hoa [12] evaluated the stability for FFDEs in the context of a controlled problem, utilizing the idea of the Caputo derivative.

Numerous researchers have investigated FFDEs using different analytical and semi-analytical techniques, including the eigenvalue–eigenvector scheme [42], the trustworthy method [25], the homotopy analysis transform methodology [29], and many others. Younus et al. [45] established the precise solution of FFDEs utilizing conformable fractional Laplace transforms (LT). Further, the solution strategies for FFDEs utilizing the natural transform approach and the interactive derivative are presented in [5, 33]. A distinctive approach is formulated for optimal control issues utilizing the Caputo derivative inside a fuzzy environment in [11]. Due to the intrinsic complexity of nonlinear fuzzy fractional models, exact solutions are typically a challenging task, which necessitates the use of approximate and semi-analytical approaches. Consequently, it is essential to formulate robust semi-analytical techniques to address the complexities of uncertain systems and establish an accurate mathematical framework for analyzing FFDEs.

In this context, the residual power series (RPS) technique shines as a flexible and robust analytical instrument for addressing dynamical models, comprising the intricate domains of FFDEs, by developing series solutions aimed at reducing residuals. When combined with techniques such as the LT, this strategy transforms into an even more powerful computational tool for addressing complex equations. Consequently, the fuzzy Laplace transform (FLT) method serves as an efficient framework for various important models arising in multiple scientific fields. Incorporating the analytical techniques with the FLT operator improves accuracy and reduces the duration needed to address nonlinear problems. Asif et al. [13] formulated a computational approach utilizing the RPS technique coupled with LT to derive approximate solutions for FFDEs. El Ghazouani and Melliani [20] explored higher-order FDEs with the LRPSM. Their research integrated the LT with the RPS method to develop approximations for higher-order FDEs. Eriqat et al. [21] introduced a novel analytical approach for addressing uncertain fractional models in the context of the fuzzy conformable framework. The findings illustrated the relevance as well as the effectiveness of the suggested technique for addressing uncertain fractional differential equations within a fuzzy context.

From a computational point of view, LRPSM offers numerous benefits compared to traditional semi-analytical approaches for nonlinear fractional biological models. Unlike some methodologies such as the Adomian decomposition method and the variational iteration approach [40], which often necessitate the formulation of Adomian polynomials or iterative evaluations of correction functions, LRPSM directly derives the successive solution components from the residual equation, thus simplifying the computational execution of nonlinear operators. Its LT representation adeptly accommodates fractional initial conditions and enables the systematic evaluation of truncation errors. The existing study validates that LRPSM is an effective approach for obtaining approximate analytical solutions to FFDEs. This approach integrates the LT with RPSM, making it effective for addressing fractional derivatives and initial conditions systematically. In contrast to only numerical methods, LRPSM offers a series-form solution that permits mathematical analysis and comparison with exact or numerical findings when accessible. It also negates discretization and can be effectively utilized for nonlinear models under appropriate assumptions [2, 32]. The novelty of this study lies in the first application of LRPSM for solving the proposed NLTFFCRWP equation under $g\mathbb{H}$ Caputo

differentiability. Unlike earlier studies that mainly focus on fuzzy fractional models or the RPS technique separately, the present study combines these ideas within a single framework to construct approximate solutions of the proposed NLTFFCRWP model.

Numerous researchers have examined the intrinsic complexity of FFDEs, which makes it challenging to find their precise solutions [1, 24]. Consequently, the utilization of analytical and numerical approaches for obtaining precise approximations has become increasingly prevalent [28]. Shah et al. [41] employed an innovative analytical technique to investigate one-dimensional fuzzy FFDEs. Alaroud et al. [8] analyzed specific categories of FFDEs with the RPSM, while Khodadadi et al. [27] examined FFDEs under uncertainty with the variational iteration method. The crucial challenge of developing precise analytical solutions for nonlinear biological models is another significant driving force behind this research. The governing equations of many real-world biological systems contain nonlinear elements that describe intricate interactions like the spread of diseases or biochemical processes. The model's mathematical structure is made quite complex by such nonlinearities. Semi-analytical techniques like the LRPSM are quite helpful in overcoming these difficulties. These methods yield approximate solutions as convergent series, which are not only simpler to compute but also more beneficial for analysis as well as interpretation. They thereby achieve an understanding between analytical clarity and precision, which makes them very useful for researching nonlinear biological models. In addition to improving the analytical tractability of fractional differential equations like the NLTFFCRWPE, the methodology creates new avenues for investigating intricate systems with memory and inherited effects. Moreover, recent experimental studies have shown that biological mechanisms like cell migration [17], tissue regeneration, wound healing, and cellular invasion include intricate interactions between cellular movement, mechanical forces, biochemical signaling, and the extracellular environment [31, 34]. Specifically, time-lapse microscopy and cell-migration experiments yield quantitative data on collective cellular mobility and wound healing, therefore supplying experimentally identifiable features suitable for incorporating into mathematical models [23, 43]. These findings highlight the importance of developing mathematical models that can accommodate the variability and complexity inherent to biological systems, while still maintaining the flexibility to represent uncertainties in experimental observations and model parameters. In particular, experimental observations provide a strong biological motivation for developing mathematical models capable of representing nonlinear interactions, spatial variation, uncertainty, and memory-dependent effects in biological systems like wound-healing dynamics. Furthermore, a solution is insufficient for good mathematical research; the proposed model must also be trustworthy, which prompts a discussion of existence, uniqueness, stability, and convergence. This study also sparks the recommended challenges for the considered NLTFFCRWP model.

The new aspect of this study is the development of a NLTFFCRWP model that incorporates unknown initial conditions under fuzzy Caputo $g\mathbb{H}$-differentiability, along with the construction of a series fuzzy solution using LRPSM. The suggested framework simultaneously captures uncertainty and memory effects in a single analytical setting for the NLTFFCRWPE. This study utilizes LRPSM to construct analytical series solutions for the proposed fuzzy model. The study's key contributions are summarized as follows:

- An enhanced NLTFFCRWP model is developed using the fuzzy Caputo $g\mathbb{H}$-derivative to represent a range of possible biological behaviors rather than a single fixed response. The suggested model enhances traditional deterministic models by integrating uncertainty and memory effects,

offering a more realistic, adaptable, and mathematically rigorous depiction of complex biological dynamics.

- The existence and uniqueness of fuzzy solutions for the suggested model are determined by using Schauder's fixed point theorem and the Banach contraction principle under suitable Lipschitz continuity and boundedness conditions.
- A new semi-analytical computational framework combining the FLT with RPSM under fuzzy Caputo $g\mathbb{H}$-differentiability is developed to compute approximate fuzzy solutions for the NLTFFCRWP model.
- The convergence analysis and Ulam-Hyers stability of the suggested NLTFFCRWP model under the Caputo $g\mathbb{H}$-derivative are investigated by deriving sufficient stability criteria in a complete fuzzy metric space.
- Several illustrative examples and a biological application of the NLTFFCRWP model are presented to validate the efficiency, convergence, and accuracy of the suggested methodology. Additionally, the graphical illustrations based on $\curlyvee$-cut representations are provided to analyze the dynamical behavior of membership functions.

The rest of the study is organized as follows: Section 2 outlines some basic notions essential to the study. In Section 3, an enhanced NLTFFCRWP model is proposed. Section 4 establishes the existence and uniqueness results for the proposed NLTFFCRWP model under suitable assumptions. Section 5 represents the framework to produce a series fuzzy solution for the NLTFFCRWP model under fuzzy Caputo $g\mathbb{H}$-differentiability. Section 6 compiles the convergence analysis for the obtained fuzzy solution. The Ulam-Hyers stability analysis is investigated for the NLTFFCRWP model in Section 7. Section 8 provides illustrative examples to emphasize the validity, preciseness, and effectivity of the suggested methodology together with graphical representations of the obtained fuzzy solutions. In Section 9, a biological application of the wound healing process is investigated. The article summarizes the key findings of the obtained results in Section 10, and finally Section 11 concludes along with possible future research topics and key foundations.

2. Preliminaries

In this section, several definitions associated with $g\mathbb{H}$-differentiability and the $\curlyvee$-cut are presented.

Definition 2.1. *[14] A fuzzy set Υ on $\mathfrak{R}$ is characterized by a membership function, $\Upsilon : \mathfrak{R} \to [0,1]$, and a fuzzy set Υ is known to be a fuzzy number if the following conditions hold: (i) Υ is normal, that is, there exists $\ell_0 \in \mathfrak{R}$ such that $\Upsilon(\ell_0) = 1$, (ii) Υ is fuzzy convex, that is, for $0 \leq \mathfrak{s} \leq 1$, $\Upsilon(\mathfrak{s}\ell_1 + (1-\mathfrak{s})\ell_2) \geq \min\{\Upsilon(\ell_1), \Upsilon(\ell_2)\}$ for any $\ell_1, \ell_2 \in \mathfrak{R}$, (iii) Υ is upper semi-continuous on $\mathfrak{R}$, (iv) $[\Upsilon_0] = cl\{\ell \in \mathfrak{R}, \Upsilon(\ell) > 0\}$ is compact, where cl stands for the closure in $(\mathfrak{R}, |.|)$. The family of all fuzzy numbers on $\mathfrak{R}$ is represented by $\mathbb{F}_{\mathfrak{R}}$. Further, for any $\curlyvee \in [0,1]$, the $\curlyvee$-level set or $\curlyvee$-cut of the fuzzy number Υ is defined as*

$$[\Upsilon]^{\curlyvee} = [\,\underline{\Upsilon}(\curlyvee),\ \overline{\Upsilon}(\curlyvee)\,], \qquad \curlyvee \in [0,1].$$

Definition 2.2. *[14] Let $\mathbb{F}_{\mathfrak{R}}$ be a space of fuzzy numbers, and let $\upsilon_1, \upsilon_2 \in \mathbb{F}_{\mathfrak{R}}$; then the Hausdorff metric D is defined as*

$$D(\upsilon_1, \upsilon_2) = \max\Big\{ \sup_{\curlyvee\in[0,1]} |\underline{\upsilon_1}(\curlyvee) - \underline{\upsilon_2}(\curlyvee)|,\ \sup_{\curlyvee\in[0,1]} |\overline{\upsilon_1}(\curlyvee) - \overline{\upsilon_2}(\curlyvee)|\Big\},$$

where $(D, \mathbb{F}_{\mathfrak{R}})$ is a complete metric space satisfying the following axioms:

(i) $D(\upsilon_1 + \omega, \upsilon_2 + \omega) = D(\upsilon_1, \upsilon_2), \quad \forall \upsilon_1, \upsilon_2 \in \mathbb{F}_{\mathfrak{R}}$;

(ii) $D(k\upsilon_1, k\upsilon_2) = |k|D(\upsilon_1, \upsilon_2), \quad \forall k \in \mathbb{R}, \upsilon_1, \upsilon_2 \in \mathbb{F}_{\mathfrak{R}}$;

(iii) $D(\upsilon_1 + \upsilon_2, \omega) \leq D(\upsilon_1, \omega) + D(\upsilon_2, \omega), \quad \forall \upsilon_1, \upsilon_2, \omega \in \mathbb{F}_{\mathfrak{R}}$.

Definition 2.3. *[15] For arbitrary fuzzy numbers $\upsilon_1, \upsilon_2 \in \mathbb{F}_{\mathfrak{R}}$, if there exists $\omega \in \mathbb{F}_{\mathfrak{R}}$ such that $\upsilon_1 = \upsilon_2 + \omega$, then ω is called the $\mathbb{H}$-difference of υ_1 and υ_2, represented as $\upsilon_1 \ominus \upsilon_2$.*

Definition 2.4. *[15] For $\upsilon_1, \upsilon_2 \in \mathbb{F}_{\mathfrak{R}}$, there exists $\omega \in \mathbb{F}_{\mathfrak{R}}$ such that*

$$\upsilon_1 \ominus_{g\mathbb{H}} \upsilon_2 = \omega \Leftrightarrow \begin{cases} (i) \ \upsilon_1 = \upsilon_2 \oplus \omega, \\ or \ (ii) \ \upsilon_2 = \upsilon_1 \oplus (-1)\omega. \end{cases}$$

In terms of the $\curlyvee$-level set, the $g\mathbb{H}$-difference is defined as

$$[\upsilon_1 \ominus_{g\mathbb{H}} \upsilon_2] = [\min\{\upsilon^-_{1(\curlyvee)} - \upsilon^-_{2(\curlyvee)}, \upsilon^+_{1(\curlyvee)} - \upsilon^+_{2(\curlyvee)}\}, \max\{\upsilon^-_{1(\curlyvee)} - \upsilon^-_{2(\curlyvee)}, \upsilon^+_{1(\curlyvee)} - \upsilon^+_{2(\curlyvee)}\}].$$

We list a few important characteristics of FVFs in the following.

Definition 2.5. *[15] Let $\mathfrak{F} : \Lambda \to \mathbb{F}_{\mathfrak{R}}$ and $(\mathfrak{s}_0, t) \in \Lambda$. The mapping $\mathfrak{F}$ is called S $g\mathbb{H}$-differentiable on $(\mathfrak{s}_0, t)$ if $\frac{\partial \mathfrak{F}(\mathfrak{s}_0, t)}{\partial \mathfrak{s}} \in \mathbb{F}_{\mathfrak{R}}$ and the following properties hold:*

- *If $\forall \epsilon > 0$ is sufficiently small, then the $g\mathbb{H}$-differences exist:*

$$\mathfrak{F}(\mathfrak{s}_0 + \epsilon, t) \ominus_{g\mathbb{H}} \mathfrak{F}(\mathfrak{s}_0, t), \qquad \mathfrak{F}(\mathfrak{s}_0, t) \ominus_{g\mathbb{H}} \mathfrak{F}(\mathfrak{s}_0 + \epsilon, t),$$

  and the limits also hold as:

$$\lim_{\epsilon \to 0} \frac{\mathfrak{F}(\mathfrak{s}_0 + \epsilon, t) \ominus_{g\mathbb{H}} \mathfrak{F}(\mathfrak{s}_0, t)}{\epsilon}, \quad \lim_{\epsilon \to 0} \frac{\mathfrak{F}(\mathfrak{s}_0, t) \ominus_{g\mathbb{H}} \mathfrak{F}(\mathfrak{s}_0 + \epsilon, t)}{-\epsilon} = \frac{\partial \mathfrak{F}(\mathfrak{s}_0, t)}{\partial \mathfrak{s}}.$$

- *If $\forall \epsilon > 0$ is reasonably small, then the $g\mathbb{H}$-differences exist:*

$$\mathfrak{F}(\mathfrak{s}_0 - \epsilon, t) \ominus_{g\mathbb{H}} \mathfrak{F}(\mathfrak{s}_0, t), \qquad \mathfrak{F}(\mathfrak{s}_0, t) \ominus_{g\mathbb{H}} \mathfrak{F}(\mathfrak{s}_0 - \epsilon, t),$$

  and the limits also hold as:

$$\lim_{\epsilon \to 0} \frac{\mathfrak{F}(\mathfrak{s}_0 - \epsilon, t) \ominus_{g\mathbb{H}} \mathfrak{F}(\mathfrak{s}_0, t)}{-\epsilon}, \quad \lim_{\epsilon \to 0} \frac{\mathfrak{F}(\mathfrak{s}_0, t) \ominus_{g\mathbb{H}} \mathfrak{F}(\mathfrak{s}_0 - \epsilon, t)}{\epsilon} = \frac{\partial \mathfrak{F}(\mathfrak{s}_0, t)}{\partial \mathfrak{s}}.$$

Lemma 2.1. *[16] Assume a fuzzy-valued continuous mapping $\mathfrak{F} : \Lambda \to \mathbb{F}_{\mathfrak{R}}$ and*

$$\mathfrak{F}(\mathfrak{s}, t) = [\underline{\mathfrak{F}}(\mathfrak{s}, t; \curlyvee), \overline{\mathfrak{F}}(\mathfrak{s}, t; \curlyvee)], \qquad \curlyvee \in [0, 1];$$

then,

- *$\mathfrak{F}(\mathfrak{s}, t)$ is of the first type $(\diamond)$-differentiable for $\mathfrak{s}$ if*

$$\frac{\partial \mathfrak{F}(\mathfrak{s}_0, t)}{\partial \mathfrak{s}} = \left(\frac{\partial \underline{\mathfrak{F}}(\mathfrak{s}_0, t)}{\partial \mathfrak{s}}, \frac{\partial \overline{\mathfrak{F}}(\mathfrak{s}_0, t)}{\partial \mathfrak{s}} \right).$$

- $\mathfrak{F}(\mathfrak{s},t)$ *is of the second type* $(\diamond\diamond)$*-differentiable for* $\mathfrak{s}$ *if*

$$\frac{\partial\mathfrak{F}(\mathfrak{s}_0,t)}{\partial\mathfrak{s}}=\left(\frac{\partial\overline{\mathfrak{F}}(\mathfrak{s}_0,t)}{\partial\mathfrak{s}},\frac{\partial\underline{\mathfrak{F}}(\mathfrak{s}_0,t)}{\partial\mathfrak{s}}\right).$$

Definition 2.6. *[18] For a fractional order* $\varpi\in(0,1]$*, the RL fractional integral is given by*

$$(I_{+}^{\varpi}\mathfrak{F})(t)=\frac{1}{\Gamma(\varpi)}\int_a^t(t-\tau)^{\varpi-1}\mathfrak{F}(\tau)\,d\tau.$$

In many applications, it is common to take $a=0$*, with* $\varpi\in\mathbb{C}$ *and* $\Re(\varpi)>0$*. For* $\varpi\in\mathbb{C}$ *satisfying* $\Re e(\varpi)>0$*, the RL fractional derivative is defined as*

$$({}^{RL}D_{a+}^{\varpi}\mathfrak{F})(t)=\frac{d^n}{dt^n}(I_{a+}^{n-\varpi}\mathfrak{F})(t),$$

where $n-1\leq\Re e(\varpi)<n$ *and* $n\in\mathbb{N}$*.*

Definition 2.7. *[18] The Caputo derivative of fractional order* $\varpi\in\mathbb{C}$*,* $\Re e(\varpi)>0$*, is described as*

$$({}^{C}D_{a+}^{\varpi}\mathfrak{F})(t)=I_{a+}^{n-\varpi}\left(\frac{d^n}{dv^n}\mathfrak{F}\right)(t),\tag{2.1}$$

where $n-1\leq\Re e(\varpi)<n$*,* $n\in\mathbb{N}$*.*

If $\varpi\in(0,1)$*, then Eq. (2.1) becomes*

$${}^{C}D_{a+}^{\varpi}\mathfrak{F}(t)=\frac{1}{\Gamma(1-\varpi)}\int_0^t(t-\tau)^{-\varpi}\mathfrak{F}'(\tau)\,d\tau.\tag{2.2}$$

Equation (2.2) with the LT can be defined as

$$\mathfrak{L}\left[{}^{C}D_{a+}^{\varpi}\mathfrak{F}(t)\right]=t^{\varpi}\mathcal{L}[\mathfrak{F}(t)]-t^{\varpi-1}\mathfrak{F}(0)-t^{\varpi-2}\mathfrak{F}'(0).$$

Definition 2.8. *[10] Let* $\mathfrak{F}:\Lambda\to\mathbb{F}_{\mathfrak{R}}$ *be a mapping, where* $\mathfrak{F}$ *belongs to the class of all continuous and Lebesgue integrable* $(C^{\mathbb{F}*\mathfrak{R}},L^{\mathbb{F}_{\mathfrak{R}}})$ *FVFs defined on the interval* $(0,b)$*. For a fractional order* $\varpi\in(0,1)$*, the Caputo derivative operator corresponding to the FVF* $\mathfrak{F}$ *is defined as*

$${}_{g\mathbb{H}}^{C}D_{a+}^{\varpi}\mathfrak{F}(t)=\frac{1}{\Gamma(1-\varpi)}\int_0^t(t-\tau)^{-\varpi}\odot\mathfrak{F}'(\tau)\,d\tau.\tag{2.3}$$

If $\varpi\in(1,2)$*, then*

$${}_{g\mathbb{H}}^{C}D_{a+}^{\varpi}\mathfrak{F}(t)=\frac{1}{\Gamma(2-\varpi)}\int_0^t(t-\tau)^{1-\varpi}\odot\mathfrak{F}''(\tau)\,d\tau.\tag{2.4}$$

Theorem 2.1. *[10] Let* $\mathfrak{F}$ *denote a* $g\mathbb{H}$*-differentiable FVF on* (a,b) *that has no switching points.*

- *If* $\mathfrak{F}$ *is* $(\diamond)$ $g\mathbb{H}$*-differentiable, then the FLT of Eq (2.3) is*

$$\mathfrak{L}\left[{}_{g\mathbb{H}}^{C}D_{a+}^{\varpi}\mathfrak{F}(t)\right]=t^{\varpi}\odot\mathfrak{L}[\mathfrak{F}(t)]\ominus t^{\varpi-1}\odot\mathfrak{F}(0).$$

- *If $\mathfrak{F}$ is $(\diamond\diamond)$ $g\mathbb{H}$-differentiable, then*

$$\mathfrak{L}\left[{}^{C}_{g\mathbb{H}}D^{\varpi}_{a+}\mathfrak{F}(t)\right] = (-1)t^{\varpi-1} \odot \mathfrak{F}(0) \oplus (-1)t^{\varpi} \odot \mathfrak{L}[\mathfrak{F}(t)].$$

Definition 2.9. *[10] Let $\mathfrak{F} : \Lambda \to \mathbb{F}_{\mathfrak{R}}$ be a FVF, where $\mathfrak{F} \in (C^{\mathbb{F}_{\mathfrak{R}}}, L^{\mathbb{F}_{\mathfrak{R}}})$ is a fuzzy Caputo $g\mathbb{H}$-differentiable function.*

- *If $\mathfrak{F}$ is $(\diamond)$ $g\mathbb{H}$-differentiable, then*

$$\left[{}^{C}_{g\mathbb{H}}D^{\varpi}_{a+}\mathfrak{F}(t)\right]^{\curlyvee} = \left[{}^{C}_{g\mathbb{H}}D^{\varpi}_{a+}\underline{\mathfrak{F}}(t;\curlyvee), {}^{C}_{g\mathbb{H}}D^{\varpi}_{a+}\overline{\mathfrak{F}}(t;\curlyvee)\right];$$

- *If $\mathfrak{F}$ is $(\diamond\diamond)$ $g\mathbb{H}$-differentiable, then*

$$\left[{}^{C}_{g\mathbb{H}}D^{\varpi}_{a+}\mathfrak{F}(t)\right]^{\curlyvee} = \left[{}^{C}_{g\mathbb{H}}D^{\varpi}_{a+}\overline{\mathfrak{F}}(t;\curlyvee), {}^{C}_{g\mathbb{H}}D^{\varpi}_{a+}\underline{\mathfrak{F}}(t;\curlyvee)\right],$$

where ${}^{C}_{g\mathbb{H}}D^{\varpi}_{a+}\underline{\mathfrak{F}}(t) = \frac{1}{\Gamma(1-\varpi)}\int_0^t (t-\tau)^{-\varpi} \odot \underline{\mathfrak{F}}'(\tau)\, d\tau$, and ${}^{C}_{g\mathbb{H}}D^{\varpi}_{a+}\overline{\mathfrak{F}}(t) = \frac{1}{\Gamma(1-\varpi)}\int_0^t (t-\tau)^{-\varpi} \odot \overline{\mathfrak{F}}'(\tau)\, d\tau$.

Definition 2.10. *[10] Let $\mathfrak{F} \in C^{\mathbb{F}_{\mathfrak{R}}}(0,b) \cap L^{\mathbb{F}_{\mathfrak{R}}}(0,b)$ be such that the FVF $\mathfrak{F}(t) \odot e^{-\upsilon t}$ is improper over the interval $[0,\infty)$. The FLT of $\mathfrak{F}(t)$ is represented by $\mathfrak{L}[\mathfrak{F}(t)]$ and is defined as*

$$\mathfrak{L}[\mathfrak{F}(t)] = \int_0^{\infty} \mathfrak{F}(t) \odot e^{-qt}\, dq. \tag{2.5}$$

Equation (2.5) can be expressed in a level-wise form as

$$\int_0^{\infty} \mathfrak{F}(t) \odot e^{-qt}\, dq = \left[\int_0^{\infty} \underline{\mathfrak{F}}(t;\curlyvee) \odot e^{-qt}\, dq, \int_0^{\infty} \overline{\mathfrak{F}}(t;\curlyvee) \odot e^{-qt}\, dq\right]. \tag{2.6}$$

It follows that

$$\mathfrak{L}[\mathfrak{F}(t)] = \left[\mathcal{L}[\underline{\mathfrak{F}}(t;\curlyvee)], \mathcal{L}[\overline{\mathfrak{F}}(t;\curlyvee)]\right],$$

where $\mathfrak{L}$ denotes the FLT and $\mathcal{L}$ is the classical LT. The linear property of the FLT, $\mathfrak{L}$, is given in the following.

Theorem 2.2. *[10] Suppose that $\mathfrak{F} \in (C^{\mathbb{F}_{\mathfrak{R}}}, L^{\mathbb{F}_{\mathfrak{R}}})$ is a FVF and $a, b \in \mathfrak{R}$. Then,*

$$\mathfrak{L}[a \odot \mathfrak{F}(t) \oplus b \odot \mathfrak{G}(t)] = a \odot \mathfrak{L}[\mathfrak{F}(t)] \oplus b \odot \mathfrak{L}[\mathfrak{G}(t)].$$

Theorem 2.3. *[10] Suppose that $\mathfrak{F} \in (C^{\mathbb{F}_{\mathfrak{R}}}, L^{\mathbb{F}_{\mathfrak{R}}})$ is a FVF. The convolution in a fuzzy context can be expressed as*

$$(\mathfrak{F} * \xi)(t) = \int_0^t \mathfrak{F}(t) \odot \xi(t-\eta)\, d\eta. \tag{2.7}$$

The FLT of Eq (2.7) is given by

$$\mathfrak{L}[(\mathfrak{F} * \xi)(t)] = \mathfrak{L}[\mathfrak{F}(t)] \odot \mathfrak{L}[\xi(t)].$$

Theorem 2.4. *[5] Let Ω be a Banach space, and let B be a convex and closed subset of Ω. Suppose that $\Psi : B \to B$ is a mapping for which the set $\{\Psi\zeta; \zeta \in B\}$ is relatively compact in Ω (or, equivalently, Ψ is continuous and completely continuous). Then Ψ admits at least one fixed point $\zeta^{\star} \in B$ such that*

$$\Psi\zeta^{\star} = \zeta^{\star}.$$

Theorem 2.5. *[5] Let (Ω, b) be a complete metric space. Then every contraction mapping $\Psi : \Omega \to \Omega$ possesses a unique fixed point w in Ω, satisfying*

$$\Psi\zeta = \zeta.$$

3. Fuzzy formulation of the time-fractional Clannish random Walker's parabolic model

The Clannish Random Walkers Parabolic model derives from the mathematical characterization of interacting random Walker's, where individual particles display unpredictable motion while concurrently being affected by local interactions within a population or cluster. In contrast to standard random walk models that presume independent particle movement, the CRWP framework integrates collective behavior via nonlinear interaction terms, facilitating the characterization of cooperative transport, accumulation, and diffusion processes. The CRWP equation is expressed as a nonlinear parabolic partial differential equation that integrates diffusion mechanisms with reaction and interaction aspects, enabling the model to represent intricate spatiotemporal patterns arising from the movement and aggregation of objects. In the classical field of research, the parabolic structure of the CRWP model can be represented as

$$\frac{\partial^{\varpi}}{\partial t^{\varpi}}F(\mathfrak{s},t)+\alpha\frac{\partial}{\partial \mathfrak{s}}F(\mathfrak{s},t)+\beta F(\mathfrak{s},t)\left(\frac{\partial}{\partial \mathfrak{s}}F(\mathfrak{s},t)\right)+\gamma\frac{\partial^{2}}{\partial \mathfrak{s}^{2}}F(\mathfrak{s},t)=0,\qquad \varpi\in(0,1], \tag{3.1}$$

with the initial condition

$$F(\mathfrak{s},0)=f(\mathfrak{s}),\quad \mathfrak{s}\in\mathfrak{R},\quad t\in(0,T],$$

where $F(\mathfrak{s},t)$ represents the wave profile or state variable, $\mathfrak{s}$ is the spatial variable, t stands for the time variable, and $\frac{\partial^{\varpi}}{\partial t^{\varpi}}$ expresses the Caputo derivative of fractional order ϖ. The parameters α, β, and γ describe distinctive procedures like linear convection, nonlinear convection, and diffusion or dissipation effects that influence the spatial and temporal development of the wound-healing profile. The coefficient α, linked to the linear convection term $\alpha F_{\mathfrak{s}}$, signifies the intensity of directed transport or propagation of the healing profile across the wound area. From a biological perspective, this term can be associated with the coordinated migration and directional redistribution of cells and biological constituents involved in tissue repair. The parameter β, present in the nonlinear term $\beta F F_{\mathfrak{s}}$, quantifies the intensity of nonlinear interactions during the healing process. This concept acknowledges that local healing dynamics and spatial transport may be influenced by the intensity of the healing state, therefore indicating density-dependent or state-dependent interactions among cellular and biochemical mechanisms. Conversely, the coefficient γ, linked to the diffusion term $\gamma F_{\mathfrak{s}\mathfrak{s}}$, identifies the intensity of spatial dispersion and reallocation. From a biological perspective, this procedure could signify the diffusion or redistribution of cellular, chemical, or signaling elements from areas of high activity to adjacent regions, supporting the smoothing and spatial progression of tissue repair. Thus, α, β, and γ correspondingly govern the proportional influences of directed transport, nonlinear biological interactions, and spatial diffusion in the suggested wound-healing dynamics.

In the classical environment, mathematical models are frequently created under the presumption that variables like starting population densities, growth rates, diffusion coefficients, and interaction parameters are exactly known. However, this assumption is frequently impractical in real-world biological, physical, and engineering applications. Because of inaccurate experiments, genetic variety, environmental fluctuations, and imperfect biological observations, biological processes are intrinsically complex and uncertain. As a result, the data used in such models cannot always be represented by exact numerical values; thus, uncertainty must be considered in order to obtain more realistic and reliable mathematical descriptions.

In this regard, the formulation of the NLFFCRWP model can be represented as follows:

$$\frac{\partial^{\varpi}}{\partial t^{\varpi}}\mathfrak{F}(\mathfrak{s},t)+\alpha\frac{\partial}{\partial \mathfrak{s}}\mathfrak{F}(\mathfrak{s},t)+\beta\mathfrak{F}(\mathfrak{s},t)\left(\frac{\partial}{\partial \mathfrak{s}}\mathfrak{F}(\mathfrak{s},t)\right)+\gamma\frac{\partial^{2}}{\partial \mathfrak{s}^{2}}\mathfrak{F}(\mathfrak{s},t)=0,\qquad \varpi\in(0,1], \tag{3.2}$$

with fuzzy initial conditions (FICs),

$$\mathfrak{F}(\mathfrak{s},0)=\mathfrak{f}(\mathfrak{s}),\quad \mathfrak{s}\in\mathfrak{R},\ \ t\in(0,T],$$

where $\mathfrak{f}$ is a fuzzy number given in parametric form as $\mathfrak{f}=(\mathfrak{f}_1,\mathfrak{f}_2)$. The operator $\frac{\partial^{\varpi}}{\partial t^{\varpi}}(\cdot)={}^{c}_{g\mathbb{H}}D^{\varpi}_{+}(\cdot)$ represents the fuzzy Caputo $g\mathbb{H}$-derivative of fractional order ϖ, which models memory and hereditary effects like wound healing, tissue regeneration, and the propagation of biochemical signals in biological mediums. The function $\mathfrak{F}(\mathfrak{s},t)$ is a FVF of the spatial variable $\mathfrak{s}$ and the time variable t. The proposed (NLTFFCRWP) model is analyzed inside the unbounded spatial domain, $\mathfrak{s}\in\mathfrak{R}$, for $t\in(0,T]$, thus framing the issue as an initial-value problem in an unbounded spatial context. The corresponding FICs are defined as $F(\mathfrak{s},0)=f(\mathfrak{s})$. Given that the temporal fractional operator is considered in the Caputo framework with $0<\varpi\leq 1$, there is no necessity for supplementary temporal initial conditions. In the current biological model, we choose the Caputo fractional derivative because its power-law memory kernel provides a natural depiction of persistent genetic effects, such that the current healing state relies on the accumulated history of the biological process. Moreover, the Caputo formulation allows for the direct inclusion of standard initial circumstances, keeping the physical interpretation of the specified initial wound profile. Although alternative non-local operators, such as the Atangana-Baleanu derivative, use a non-singular Mittag-Leffler kernel and implement a different memory-decay mechanism, the present formulation is aimed at describing persistent power-law memory, not a non-singular fading-memory process. Hence, the Caputo derivative is structurally compatible with the memory mechanism specified in the proposed wound-healing biological model. In this work, an enhanced NLTFFCRWP model is investigated through its convergence and stability analysis. The mathematical analysis for this model is studied using LRPSM to produce approximate fuzzy solutions for the proposed fuzzy model.

Consider the NLTFFCRWP problem (3.2), and define the nonlinear spatial operator as given below:

$$\mathfrak{N}(\mathfrak{F})=\alpha\frac{\partial}{\partial \mathfrak{s}}\mathfrak{F}(\mathfrak{s},t)+\beta\mathfrak{F}(\mathfrak{s},t)\left(\frac{\partial}{\partial \mathfrak{s}}\mathfrak{F}(\mathfrak{s},t)\right)+\gamma\frac{\partial^{2}}{\partial \mathfrak{s}^{2}}\mathfrak{F}(\mathfrak{s},t). \tag{3.3}$$

Then the NLTFFCRWPE can be written in the compact form as

$$\frac{\partial^{\varpi}}{\partial t^{\varpi}}\mathfrak{F}(\mathfrak{s},t,\vee)=-\mathfrak{N}(\mathfrak{F})(\mathfrak{s},t,\vee). \tag{3.4}$$

4. Existence and uniqueness of fuzzy solutions for the NLTFFCRWPE

Let $\Theta=[0,T]$, where $T>0$ denotes the considered time horizon. Since the proposed mathematical model is formulated on the unbounded spatial domain $\mathfrak{s}\in\mathfrak{R}$, the existence and uniqueness analysis is conducted in the bounded-function space

$$U=C(\Theta,C_b^2(\mathfrak{R},\mathbb{F}_{\mathfrak{R}})).$$

Thus, the unbounded nature of the spatial domain is retained, while the boundedness required for the subsequent Lipschitz analysis is ensured through the C_b^2-norm and the corresponding bounded subset $B_R \subset U$. Define the norm

$$\|\mathfrak{F}\|_U = \sup_{t\in\Theta} \left(\|\mathfrak{F}(\cdot,t)\|_\infty + \|\mathfrak{F}_{\mathfrak{s}}(\cdot,t)\|_\infty + \|\mathfrak{F}_{\mathfrak{s}\mathfrak{s}}(\cdot,t)\|_\infty\right), \tag{4.1}$$

where

$$\|\mathfrak{F}(\cdot,t)\|_\infty = \sup_{\mathfrak{s}\in\mathfrak{R}} |\mathfrak{F}(\mathfrak{s},t)|.$$

For a prescribed $R > 0$, introduce the closed bounded ball $B_R = \{\mathfrak{F} \in U : \|\mathfrak{F}\|_U \leq R\}$. The following assumptions are defined to prove the existence and uniqueness of the solution of the proposed NLTFFCRWP model.

- $\mathbb{H}_1$: The fuzzy initial function satisfies

$$\mathfrak{F}_0(\mathfrak{s},\vee) = \left[\underline{\mathfrak{F}}(\mathfrak{s},\vee), \overline{\mathfrak{F}}(\mathfrak{s},\vee)\right] \in C^2(\mathfrak{R},\mathbb{F}_{\mathfrak{R}}).$$

- $\mathbb{H}_2$: The nonlinear operator $\mathfrak{N} : U \to U$, defined by

$$\mathfrak{N}(\mathfrak{F}) = \alpha\mathfrak{F}_{\mathfrak{s}} + \beta\mathfrak{F}\mathfrak{F}_{\mathfrak{s}} + \gamma\mathfrak{F}_{\mathfrak{s}\mathfrak{s}},$$

  is continuous on the considered bounded set B_R.
- $\mathbb{H}_3$: There exists a constant $L_{\mathfrak{N}} > 0$ such that, for every $\mathfrak{N}(\mathfrak{F}_1, \mathfrak{F}_2) \in U$,

$$\|\mathfrak{N}(\mathfrak{F}_1) - \mathfrak{N}(\mathfrak{F}_2)\|_\infty \leq L_{\mathfrak{N}}\|\mathfrak{F}_1 - \mathfrak{F}_2\|_U.$$

On a bounded ball $B_R = \{\mathfrak{F} \in U : \|\mathfrak{F}\|_U \leq R\}$, the nonlinear term satisfies

$$\mathfrak{F}_1(\mathfrak{F}_1)_{\mathfrak{s}} - \mathfrak{F}_2(\mathfrak{F}_2)_{\mathfrak{s}} = (\mathfrak{F}_1 - \mathfrak{F}_2)(\mathfrak{F}_1)_{\mathfrak{s}} + \mathfrak{F}_2[(\mathfrak{F}_1)_{\mathfrak{s}} - (\mathfrak{F}_2)_{\mathfrak{s}}].$$

Hence, the nonlinear operator $\mathfrak{N}(\mathfrak{F}) = \alpha\mathfrak{F}_{\mathfrak{s}} + \beta\mathfrak{F}\mathfrak{F}_{\mathfrak{s}} + \gamma\mathfrak{F}_{\mathfrak{s}\mathfrak{s}}$ satisfies a local Lipschitz condition on B_R. A possible Lipschitz bound can be described as

$$L_{\mathfrak{N}} = |\alpha| + |\gamma| + 2|\beta|R, \tag{4.2}$$

provided the corresponding spatial derivative norms are controlled by the norm defined in Eq (4.1). In biological terms, the Lipschitz constant $L_{\mathfrak{N}}$ measures the sensitivity of the spatial dynamics to fluctuations in biological activity. The parameters α and γ measure the effects of linear transport and spatial dispersion, respectively, whereas $2|\beta|R$ indicates the sensitivity arising from nonlinear biological interactions, including the extent of the healing profile. Consequently, higher values of these parameters could result in enhanced sensitivity of the spatial dynamics, whereas a reduced Lipschitz bound signifies a more stable reaction to disruptions.

Lemma 4.1. *A fuzzy function $\mathfrak{F}(\mathfrak{s},t,\vee) \in U$ is a solution of Eq (3.2) along with the FICs if and only if it satisfies the fractional integral equation given below:*

$$\mathfrak{F}(\mathfrak{s},t,\vee) = \mathfrak{F}_0(\mathfrak{s},\vee) - \frac{1}{\Gamma(\varpi)}\int_0^t (t-\tau)^{\varpi-1}\mathfrak{N}(\mathfrak{F})(\mathfrak{s},\tau,\vee)\,d\tau. \tag{4.3}$$

Proof. From Eq (3.4), we have

$$\frac{\partial^{\varpi}}{\partial t^{\varpi}}\mathfrak{F}(\mathfrak{s},t,\curlyvee)=-\mathfrak{N}(\mathfrak{F})(\mathfrak{s},t,\curlyvee).$$

Applying the RL fractional integral operator I_t^{ϖ} to both sides gives

$$I_t^{\varpi}\left({}^{C}D_t^{\varpi}\mathfrak{F}(\mathfrak{s},t,\curlyvee)\right)=-I_t^{\varpi}\mathfrak{N}(\mathfrak{F})(\mathfrak{s},t,\curlyvee).$$

Now, using the Caputo identity

$$I_t^{\varpi}\left({}^{C}D_t^{\varpi}\mathfrak{F}(\mathfrak{s},t,\curlyvee)\right)=\mathfrak{F}(\mathfrak{s},t,\curlyvee)-\mathfrak{F}(\mathfrak{s},0,\curlyvee),$$

we obtain

$$\mathfrak{F}(\mathfrak{s},t,\curlyvee)-\mathfrak{F}_0(\mathfrak{s},\curlyvee)=-\frac{1}{\Gamma(\varpi)}\int_0^t(t-\tau)^{\varpi-1}\mathfrak{N}(\mathfrak{F})(\mathfrak{s},\tau,\curlyvee)\,d\tau.$$

Therefore,

$$\mathfrak{F}(\mathfrak{s},t,\curlyvee)=\mathfrak{F}_0(\mathfrak{s},\curlyvee)-\frac{1}{\Gamma(\varpi)}\int_0^t(t-\tau)^{\varpi-1}\mathfrak{N}(\mathfrak{F})(\mathfrak{s},\tau,\curlyvee)\,d\tau.$$

This proves the equivalence. □

Using the lower and upper cut functions, Eq (4.3) becomes

$$\underline{\mathfrak{F}}(\mathfrak{s},t,\curlyvee)=\underline{\mathfrak{F}_0}(\mathfrak{s},\curlyvee)-\frac{1}{\Gamma(\varpi)}\int_0^t(t-\tau)^{\varpi-1}\left[\alpha\frac{\partial}{\partial\mathfrak{s}}\underline{\mathfrak{F}}+\beta\underline{\mathfrak{F}}\left(\frac{\partial}{\partial\mathfrak{s}}\underline{\mathfrak{F}}\right)+\gamma\frac{\partial^2}{\partial\mathfrak{s}^2}\underline{\mathfrak{F}}\right](\mathfrak{s},\tau,\curlyvee)\,d\tau,$$

and

$$\overline{\mathfrak{F}}(\mathfrak{s},t,\curlyvee)=\overline{\mathfrak{F}_0}(\mathfrak{s},\curlyvee)-\frac{1}{\Gamma(\varpi)}\int_0^t(t-\tau)^{\varpi-1}\left[\alpha\frac{\partial}{\partial\mathfrak{s}}\overline{\mathfrak{F}}+\beta\overline{\mathfrak{F}}\left(\frac{\partial}{\partial\mathfrak{s}}\overline{\mathfrak{F}}\right)+\gamma\frac{\partial^2}{\partial\mathfrak{s}^2}\overline{\mathfrak{F}}\right](\mathfrak{s},\tau,\curlyvee)\,d\tau.$$

Theorem 4.1. *Let hypotheses $\mathbb{H}_1$–$\mathbb{H}_3$ hold; then there exists a constant $M_{\mathfrak{N}}>0$ such that*

$$\|\mathfrak{N}(\mathfrak{F})\|_U\le M_{\mathfrak{N}},\qquad \mathfrak{F}\in B_R,\tag{4.4}$$

where

$$B_R=\{\mathfrak{F}\in U:\|\mathfrak{F}\|_U\le R\}$$

is a closed, bounded, and convex subset of U. If

$$\|\mathfrak{F}_0\|_U+\frac{T^{\varpi}M_{\mathfrak{N}}}{\Gamma(\varpi+1)}\le R,\tag{4.5}$$

then the NLTFFCRWP problem (3.2) along with the FICs has at least one solution in B_R.

Proof. Define the operator $\Psi:U\to U$ by

$$\Psi(\mathfrak{F})(\mathfrak{s},t,\curlyvee)=\mathfrak{F}_0(\mathfrak{s},\curlyvee)-\frac{1}{\Gamma(\varpi)}\int_0^t(t-\tau)^{\varpi-1}\mathfrak{N}(\mathfrak{F})(\mathfrak{s},\tau,\curlyvee)\,d\tau.\tag{4.6}$$

Then every fixed point of Ψ is a solution of the NLTFFCRWPE. For any $\mathfrak{F}\in B_R$, using Eqs (4.6) and (4.4), we obtain

$$\|\Psi\mathfrak{F}\|_U\le\|\mathfrak{F}_0\|_U+\frac{1}{\Gamma(\varpi)}\int_0^t(t-\tau)^{\varpi-1}\|\mathfrak{N}(\mathfrak{F})\|_U\,d\tau$$

$$\leq \|\mathfrak{F}_0\|_U + \frac{M_{\mathfrak{N}}}{\Gamma(\varpi)} \sup_{0<t\leq T} \int_0^t (t-\tau)^{\varpi-1}\, d\tau$$
$$= \|\mathfrak{F}_0\|_U + \frac{M_{\mathfrak{N}} T^{\varpi}}{\Gamma(\varpi+1)}$$
$$\leq \|\mathfrak{F}_0\|_U + \frac{M_{\mathfrak{N}} T^{\varpi}}{\Gamma(\varpi+1)} \leq R.$$

Hence,

$$\Psi(B_R) \subseteq B_R.$$

Now, let $\mathfrak{F}_n \to \mathfrak{F}$ in B_R. Since $\mathfrak{N}$ is continuous, we have

$$\mathfrak{N}(\mathfrak{F}_n) \to \mathfrak{N}(\mathfrak{F}).$$

Therefore,

$$\|\Psi\mathfrak{F}_n - \Psi\mathfrak{F}\|_U \leq \frac{1}{\Gamma(\varpi)} \int_0^t (t-\tau)^{\varpi-1} \|\mathfrak{N}(\mathfrak{F}_n) - \mathfrak{N}(\mathfrak{F})\|_U\, d\tau$$
$$\leq \frac{T^{\varpi}}{\Gamma(\varpi+1)} \|\mathfrak{N}(\mathfrak{F}_n) - \mathfrak{N}(\mathfrak{F})\|_U \to 0.$$

Thus, Ψ is continuous.

Now, for $0 \leq t_1 < t_2 \leq T$, we estimate

$$\|(\Psi\mathfrak{F})(\mathfrak{s}, t_2, \vee) - (\Psi\mathfrak{F})(\mathfrak{s}, t_1, \vee)\|_U \leq \frac{M_{\mathfrak{N}}}{\Gamma(\varpi)} \left[\int_{t_1}^{t_2} (t_2-\tau)^{\varpi-1}\, d\tau + \int_0^{t_1} \left| (t_2-\tau)^{\varpi-1} - (t_1-\tau)^{\varpi-1} \right| d\tau \right].$$

Hence,

$$\sup_{\mathfrak{s}\in\mathfrak{R}} |(\Psi\mathfrak{F})(\mathfrak{s}, t_2, \vee) - (\Psi\mathfrak{F})(\mathfrak{s}, t_1, \vee)| \leq \frac{2M_{\mathfrak{N}}}{\Gamma(\varpi+1)} (t_2 - t_1)^{\varpi}. \tag{4.7}$$

Since the right-hand side tends to zero as $t_2 \to t_1$, the family $\Psi(B_R)$ is equicontinuous on $[0, T]$. Moreover, by Eq (4.5), the family $\Psi(B_R)$ is uniformly bounded in U. Under the bounded-function-space setting and the stated compactness assumptions, the Arzelà-Ascoli theorem implies that $\Psi(B_R)$ is relatively compact in U. Therefore, Ψ is a continuous compact operator mapping the nonempty, closed, bounded, and convex set B_R into itself. Hence, by Schauder's fixed point theorem, Ψ admits at least one fixed point in B_R. Consequently, there exists at least one fuzzy solution $\mathfrak{F} \in B_R \subset U$ of the proposed NLTFFCRWPE subject to the corresponding FICs. □

Theorem 4.2. *Suppose that hypotheses $\mathbb{H}_1$–$\mathbb{H}_3$ hold. If*

$$\delta = \frac{T^{\varpi} L_{\mathfrak{N}}}{\Gamma(\varpi+1)} < 1, \tag{4.8}$$

then the NLTFFCRWPE (3.2) with the FICs has a unique solution in B_R.

Proof. Let $\mathfrak{F}_1, \mathfrak{F}_2 \in B_R$. From Eq (4.6), we have

$$(\Psi\mathfrak{F}_1)(\mathfrak{s}, t, \vee) = \mathfrak{F}_0(\mathfrak{s}, \vee) - \frac{1}{\Gamma(\varpi)} \int_0^t (t-\tau)^{\varpi-1} \mathfrak{N}(\mathfrak{F}_1)(\mathfrak{s}, \tau, \vee)\, d\tau, \tag{4.9}$$

$$(\Psi\mathfrak{F}_2)(\mathfrak{s},t,\curlyvee) = \mathfrak{F}_0(\mathfrak{s},\curlyvee) - \frac{1}{\Gamma(\varpi)}\int_0^t (t-\tau)^{\varpi-1}\mathfrak{N}(\mathfrak{F}_2)(\mathfrak{s},\tau,\curlyvee)\,d\tau. \tag{4.10}$$

Subtracting Eq (4.10) from Eq (4.9) gives

$$(\Psi\mathfrak{F}_1)(\mathfrak{s},t,\curlyvee) - (\Psi\mathfrak{F}_2)(\mathfrak{s},t,\curlyvee) = -\frac{1}{\Gamma(\varpi)}\int_0^t (t-\tau)^{\varpi-1}\left[\mathfrak{N}(\mathfrak{F}_1) - \mathfrak{N}(\mathfrak{F}_2)\right](\mathfrak{s},\tau,\curlyvee)\,d\tau. \tag{4.11}$$

Taking the norm of Eq (4.11) and using the Lipschitz condition (4.2), gives

$$\begin{aligned}
\|\Psi\mathfrak{F}_1 - \Psi\mathfrak{F}_2\|_U &\le \frac{1}{\Gamma(\varpi)}\int_0^t (t-\tau)^{\varpi-1}\|\mathfrak{N}(\mathfrak{F}_1) - \mathfrak{N}(\mathfrak{F}_2)\|_\infty\,d\tau\\
&\le \frac{L_{\mathfrak{N}}}{\Gamma(\varpi)}\sup_{0<t\le T}\int_0^t (t-\tau)^{\varpi-1}\|\mathfrak{F}_1 - \mathfrak{F}_2\|_U\,d\tau\\
&= \frac{L_{\mathfrak{N}}t^{\varpi}}{\Gamma(\varpi+1)}\|\mathfrak{F}_1 - \mathfrak{F}_2\|_U\\
&\le \frac{L_{\mathfrak{N}}T^{\varpi}}{\Gamma(\varpi+1)}\|\mathfrak{F}_1 - \mathfrak{F}_2\|_U.
\end{aligned}$$

Moreover, we can write the above as follows, with $\delta = \frac{T^{\varpi}L_{\mathfrak{N}}}{\Gamma(\varpi+1)}$:

$$\|\Psi\mathfrak{F}_1 - \Psi\mathfrak{F}_2\|_U \le \delta\|\mathfrak{F}_1 - \mathfrak{F}_2\|_U. \tag{4.12}$$

Assume $\delta < 1$; then Ψ is a contraction mapping on B_R. By the Banach contraction principle, Ψ has a unique fixed point in B_R. Consequently, the NLTFFCRWPE has a unique fuzzy solution. □

Combining both results, as shown in (4.7) and (4.12), the NLTFFCRWPE,

$${}^{C}D_t^{\varpi}\mathfrak{F} + \alpha\mathfrak{F}_{\mathfrak{s}} + \beta\mathfrak{F}\mathfrak{F}_{\mathfrak{s}} + \gamma\mathfrak{F}_{\mathfrak{s}\mathfrak{s}} = 0, \qquad 0 < \varpi \le 1,$$

along with the FICs

$$\mathfrak{F}(\mathfrak{s},0,\curlyvee) = \left[\underline{\mathfrak{F}_0}(\mathfrak{s},\curlyvee), \overline{\mathfrak{F}_0}(\mathfrak{s},\curlyvee)\right],$$

has a unique fuzzy solution

$$[\mathfrak{F}(\mathfrak{s},t)]_{\curlyvee} = \left[\underline{\mathfrak{F}}(\mathfrak{s},t,\curlyvee), \overline{\mathfrak{F}}(\mathfrak{s},t,\curlyvee)\right],$$

provided that

$$\frac{T^{\varpi}L_{\mathfrak{N}}}{\Gamma(\varpi+1)} < 1.$$

The solution is the fixed point of

$$(\Psi\mathfrak{F})(\mathfrak{s},t,\curlyvee) = \mathfrak{F}_0(\mathfrak{s},\curlyvee) - \frac{1}{\Gamma(\varpi)}\int_0^t (t-\tau)^{\varpi-1}\mathfrak{N}(\mathfrak{F})(\mathfrak{s},\tau,\curlyvee)\,d\tau.$$

Equivalently,

$$\underline{\mathfrak{F}}(\mathfrak{s},t,\curlyvee) = \underline{\mathfrak{F}}_0(\mathfrak{s},\curlyvee) - \frac{1}{\Gamma(\varpi)}\int_0^t (t-\tau)^{\varpi-1}\left[\alpha\underline{\mathfrak{F}}_{\mathfrak{s}} + \beta\underline{\mathfrak{F}\mathfrak{F}}_{\mathfrak{s}} + \gamma\underline{\mathfrak{F}}_{\mathfrak{s}\mathfrak{s}}\right](\mathfrak{s},\tau,\curlyvee)\,d\tau,$$

and

$$\overline{\mathfrak{F}}(\mathfrak{s},t,\curlyvee) = \overline{\mathfrak{F}}_0(\mathfrak{s},\curlyvee) - \frac{1}{\Gamma(\varpi)}\int_0^t (t-\tau)^{\varpi-1}\left[\alpha\overline{\mathfrak{F}}_{\mathfrak{s}} + \beta\overline{\mathfrak{F}\mathfrak{F}}_{\mathfrak{s}} + \gamma\overline{\mathfrak{F}}_{\mathfrak{s}\mathfrak{s}}\right](\mathfrak{s},\tau,\curlyvee)\,d\tau.$$

5. Methodology to solve the NLTFFCRWPE using LRPSM under Caputo $g\mathbb{H}$-differentiability

Here, we explain the method to introduce and analyze the fuzzy solution of the fractional-order NLTFFCRWPE using LRPSM. Combining the FLT and RPSM, we consider the following cases one by one under various types of $g\mathbb{H}$-differentiability.

Case 1. Let $\mathfrak{F}(\mathfrak{s},t)$ be $[(\diamond)-\varpi]$-differentiable.

Step I. Consider a fractional-order NLTFFCRWPE as

$$\frac{\partial^{\varpi}}{\partial t^{\varpi}}\mathfrak{F}(\mathfrak{s},t)+\alpha\frac{\partial}{\partial \mathfrak{s}}\mathfrak{F}(\mathfrak{s},t)+\beta\mathfrak{F}(\mathfrak{s},t)\left(\frac{\partial}{\partial \mathfrak{s}}\mathfrak{F}(\mathfrak{s},t)\right)+\gamma\frac{\partial^{2}}{\partial \mathfrak{s}^{2}}\mathfrak{F}(\mathfrak{s},t)=0,\qquad \varpi\in(0,1], \tag{5.1}$$

with fuzzy initial conditions

$$\mathfrak{F}(\mathfrak{s},0)=\mathfrak{f}(\mathfrak{s}),\quad \mathfrak{s}\in\mathfrak{R},\ \ t\in(0,T],$$

where $\mathfrak{f}$ is a fuzzy number given in parametric form as $\mathfrak{f}=(\mathfrak{f}_1,\mathfrak{f}_2)$.

Step II. Defining $\mathfrak{F}(\mathfrak{s},t)^{\curlyvee}=[\underline{\mathfrak{F}}(\mathfrak{s},t;\curlyvee),\overline{\mathfrak{F}}(\mathfrak{s},t;\curlyvee)]$, Eq (5.1) leads to the following:

$$\begin{cases}\frac{\partial^{\varpi}}{\partial t^{\varpi}}\underline{\mathfrak{F}}(\mathfrak{s},t)+\alpha\frac{\partial}{\partial \mathfrak{s}}\underline{\mathfrak{F}}(\mathfrak{s},t)+\beta\underline{\mathfrak{F}}(\mathfrak{s},t)\left(\frac{\partial}{\partial \mathfrak{s}}\underline{\mathfrak{F}}(\mathfrak{s},t)\right)+\gamma\frac{\partial^{2}}{\partial \mathfrak{s}^{2}}\underline{\mathfrak{F}}(\mathfrak{s},t)=0,\\ \\ \frac{\partial^{\varpi}}{\partial t^{\varpi}}\overline{\mathfrak{F}}(\mathfrak{s},t)+\alpha\frac{\partial}{\partial \mathfrak{s}}\overline{\mathfrak{F}}(\mathfrak{s},t)+\beta\overline{\mathfrak{F}}(\mathfrak{s},t)\left(\frac{\partial}{\partial \mathfrak{s}}\overline{\mathfrak{F}}(\mathfrak{s},t)\right)+\gamma\frac{\partial^{2}}{\partial \mathfrak{s}^{2}}\overline{\mathfrak{F}}(\mathfrak{s},t)=0.\end{cases} \tag{5.2}$$

Step III. Following Theorem 2.1 and applying the FLT to Eq (5.2) gives

$$\begin{cases}\mathfrak{Q}\left[\underline{\mathfrak{F}}(\mathfrak{s},t)\right]=\frac{1}{q}\underline{\mathfrak{F}}(\mathfrak{s},0)-\frac{1}{q^{\varpi}}\mathfrak{Q}\left[\alpha\frac{\partial}{\partial \mathfrak{s}}\underline{\mathfrak{F}}(\mathfrak{s},t)+\beta\underline{\mathfrak{F}}(\mathfrak{s},t)\left(\frac{\partial}{\partial \mathfrak{s}}\underline{\mathfrak{F}}(\mathfrak{s},t)\right)+\gamma\frac{\partial^{2}}{\partial \mathfrak{s}^{2}}\underline{\mathfrak{F}}(\mathfrak{s},t)\right],\\ \mathfrak{Q}\left[\overline{\mathfrak{F}}(\mathfrak{s},t)\right]=\frac{1}{q}\overline{\mathfrak{F}}(\mathfrak{s},0)-\frac{1}{q^{\varpi}}\mathfrak{Q}\left[\alpha\frac{\partial}{\partial \mathfrak{s}}\overline{\mathfrak{F}}(\mathfrak{s},t)+\beta\overline{\mathfrak{F}}(\mathfrak{s},t)\left(\frac{\partial}{\partial \mathfrak{s}}\overline{\mathfrak{F}}(\mathfrak{s},t)\right)+\gamma\frac{\partial^{2}}{\partial \mathfrak{s}^{2}}\overline{\mathfrak{F}}(\mathfrak{s},t)\right].\end{cases} \tag{5.3}$$

Using the ICs from Eq (5.1),

$$\begin{cases}\underline{\mathcal{Y}}(\mathfrak{s},q;\curlyvee)=\frac{1}{q}\mathfrak{f}_1-\frac{1}{q^{\varpi}}\mathfrak{Q}\left[\alpha\frac{\partial}{\partial \mathfrak{s}}\underline{\mathfrak{F}}(\mathfrak{s},t)+\beta\underline{\mathfrak{F}}(\mathfrak{s},t)\left(\frac{\partial}{\partial \mathfrak{s}}\underline{\mathfrak{F}}(\mathfrak{s},t)\right)+\gamma\frac{\partial^{2}}{\partial \mathfrak{s}^{2}}\underline{\mathfrak{F}}(\mathfrak{s},t)\right],\\ \overline{\mathcal{Y}}(\mathfrak{s},q;\curlyvee)=\frac{1}{q}\mathfrak{f}_2-\frac{1}{q^{\varpi}}\mathfrak{Q}\left[\alpha\frac{\partial}{\partial \mathfrak{s}}\overline{\mathfrak{F}}(\mathfrak{s},t)+\beta\overline{\mathfrak{F}}(\mathfrak{s},t)\left(\frac{\partial}{\partial \mathfrak{s}}\overline{\mathfrak{F}}(\mathfrak{s},t)\right)+\gamma\frac{\partial^{2}}{\partial \mathfrak{s}^{2}}\overline{\mathfrak{F}}(\mathfrak{s},t)\right].\end{cases} \tag{5.4}$$

Step IV. Consider the series-type solution of Eq (5.4), stated as

$$\begin{cases}\underline{\mathcal{Y}}(\mathfrak{s},q;\curlyvee)=\sum_{k=0}^{\infty}\frac{\underline{\varphi}_k(\mathfrak{s})}{q^{k\varpi+1}},\\ \\ \overline{\mathcal{Y}}(\mathfrak{s},q;\curlyvee)=\sum_{k=0}^{\infty}\frac{\overline{\varphi}_k(\mathfrak{s})}{q^{k\varpi+1}}.\end{cases} \tag{5.5}$$

The series-form solution of the i-th truncated term given in Eq (5.5) is as follows:

$$\begin{cases} \underline{\mathcal{Y}}(\mathfrak{s}, q; \curlyvee) = \dfrac{1}{q}\,\mathfrak{f}_1 + \displaystyle\sum_{k=1}^{i} \frac{\underline{\varphi}_k(\mathfrak{s})}{q^{k\varpi+1}}, \\ \overline{\mathcal{Y}}(\mathfrak{s}, q; \curlyvee) = \dfrac{1}{q}\,\mathfrak{f}_2 + \displaystyle\sum_{k=1}^{i} \frac{\overline{\varphi}_k(\mathfrak{s})}{q^{k\varpi+1}}. \end{cases} \tag{5.6}$$

The i-Laplace residual functions of Eq (5.4) are given by

$$\begin{cases} \mathfrak{Q}\Big[Res_{\underline{\mathcal{Y}}_i}\Big] = \underline{\mathcal{Y}}(\mathfrak{s}, q; \curlyvee) - \dfrac{1}{q}\,\mathfrak{f}_1 + \dfrac{1}{q^{\varpi}}\mathfrak{Q}\Big[\alpha\dfrac{\partial}{\partial\mathfrak{s}}\underline{\mathfrak{F}}(\mathfrak{s}, t) + \beta\underline{\mathfrak{F}}(\mathfrak{s}, t)\left(\dfrac{\partial}{\partial\mathfrak{s}}\underline{\mathfrak{F}}(\mathfrak{s}, t)\right) + \gamma\dfrac{\partial^2}{\partial\mathfrak{s}^2}\underline{\mathfrak{F}}(\mathfrak{s}, t)\Big], \\ \mathfrak{Q}\Big[Res_{\overline{\mathcal{Y}}_i}\Big] = \overline{\mathcal{Y}}(\mathfrak{s}, q; \curlyvee) - \dfrac{1}{q}\,\mathfrak{f}_2 + \dfrac{1}{q^{\varpi}}\mathfrak{Q}\Big[\alpha\dfrac{\partial}{\partial\mathfrak{s}}\overline{\mathfrak{F}}(\mathfrak{s}, t) + \beta\overline{\mathfrak{F}}(\mathfrak{s}, t)\left(\dfrac{\partial}{\partial\mathfrak{s}}\overline{\mathfrak{F}}(\mathfrak{s}, t)\right) + \gamma\dfrac{\partial^2}{\partial\mathfrak{s}^2}\overline{\mathfrak{F}}(\mathfrak{s}, t)\Big]. \end{cases} \tag{5.7}$$

Step V. Substituting Eq (5.6) into Eq (5.7), and then solving the relations $\lim_{q\to\infty} q^{k\varpi+1}\mathfrak{Q}[Res_{\underline{\mathcal{Y}}_i}(\mathfrak{s}, q; \curlyvee)] = 0$ and $\lim_{q\to\infty} q^{k\varpi+1}\mathfrak{Q}[Res_{\overline{\mathcal{Y}}_i}(\mathfrak{s}, q; \curlyvee)] = 0$ recursively, we obtain

$$\begin{cases} \underline{\varphi}_0(\mathfrak{s}; \curlyvee) = \mathfrak{f}_1, \\ \overline{\varphi}_0(\mathfrak{s}; \curlyvee) = \mathfrak{f}_2. \end{cases} \tag{5.8}$$

$$\begin{cases} \underline{\varphi}_1(\mathfrak{s}) = \alpha\dfrac{\partial}{\partial\mathfrak{s}}\underline{\varphi}_0(\mathfrak{s}) + \beta\underline{\varphi}_0(\mathfrak{s})\dfrac{\partial}{\partial\mathfrak{s}}\underline{\varphi}_0(\mathfrak{s}) + \gamma\dfrac{\partial^2}{\partial\mathfrak{s}^2}\underline{\varphi}_0(\mathfrak{s}), \\ \overline{\varphi}_1(\mathfrak{s}) = \alpha\dfrac{\partial}{\partial\mathfrak{s}}\overline{\varphi}_0(\mathfrak{s}) + \beta\overline{\varphi}_0(\mathfrak{s})\dfrac{\partial}{\partial\mathfrak{s}}\overline{\varphi}_0(\mathfrak{s}) + \gamma\dfrac{\partial^2}{\partial\mathfrak{s}^2}\overline{\varphi}_0(\mathfrak{s}). \end{cases} \tag{5.9}$$

$$\vdots$$

$$\begin{cases} \underline{\varphi}_{k+1}(\mathfrak{s}) = \alpha\dfrac{\partial}{\partial\mathfrak{s}}\underline{\varphi}_k(\mathfrak{s}) + \beta\displaystyle\sum_{j=0}^{k}\underline{\varphi}_j(\mathfrak{s})\frac{\partial}{\partial\mathfrak{s}}\underline{\varphi}_{k-j}(\mathfrak{s}) + \gamma\frac{\partial^2}{\partial\mathfrak{s}^2}\underline{\varphi}_k(\mathfrak{s}), \\ \overline{\varphi}_{k+1}(\mathfrak{s}) = \alpha\dfrac{\partial}{\partial\mathfrak{s}}\overline{\varphi}_k(\mathfrak{s}) + \beta\displaystyle\sum_{j=0}^{k}\overline{\varphi}_j(\mathfrak{s})\frac{\partial}{\partial\mathfrak{s}}\overline{\varphi}_{k-j}(\mathfrak{s}) + \gamma\frac{\partial^2}{\partial\mathfrak{s}^2}\overline{\varphi}_k(\mathfrak{s}). \end{cases} \tag{5.10}$$

Putting the values of $\underline{\varphi}_j(\mathfrak{s}; \curlyvee)$ and $\overline{\varphi}_j(\mathfrak{s}; \curlyvee)$, $j = 0, 1, \ldots$, in Eq (5.6), we get

$$\begin{cases} \underline{\mathcal{Y}}(\mathfrak{s}, q; \curlyvee) = \dfrac{1}{q}\,\underline{\varphi}_0(\mathfrak{s}, \curlyvee) + \dfrac{1}{q^{\varpi+1}}\,\underline{\varphi}_1(\mathfrak{s}, \curlyvee) + \cdots + \dfrac{1}{q^{(k+1)\varpi+1}}\,\underline{\varphi}_{k+1}(\mathfrak{s}, \curlyvee), \\ \overline{\mathcal{Y}}(\mathfrak{s}, q; \curlyvee) = \dfrac{1}{q}\,\overline{\varphi}_0(\mathfrak{s}, \curlyvee) + \dfrac{1}{q^{\varpi+1}}\,\overline{\varphi}_1(\mathfrak{s}, \curlyvee) + \cdots + \dfrac{1}{q^{(k+1)\varpi+1}}\,\overline{\varphi}_{k+1}(\mathfrak{s}, \curlyvee). \end{cases} \tag{5.11}$$

Step VI. Applying the inverse FLT to Eq (5.11), we obtain

$$\begin{cases} \underline{\mathfrak{F}}(\mathfrak{s},t;\vee) = \displaystyle\sum_{k=0}^{\infty} \underline{\varphi}_k(\mathfrak{s}) \frac{t^{k\varpi}}{\Gamma(k\varpi+1)}, \\ \overline{\mathfrak{F}}(\mathfrak{s},t;\vee) = \displaystyle\sum_{k=0}^{\infty} \overline{\varphi}_k(\mathfrak{s}) \frac{t^{k\varpi}}{\Gamma(k\varpi+1)}. \end{cases} \tag{5.12}$$

Thus, the fuzzy solution of Eq (5.1) is given as

$$\mathfrak{F}(\mathfrak{s},t;\vee) = \left[\sum_{k=0}^{\infty} \underline{\varphi}_k(\mathfrak{s}) \frac{t^{k\varpi}}{\Gamma(k\varpi+1)}, \quad \sum_{k=0}^{\infty} \overline{\varphi}_k(\mathfrak{s}) \frac{t^{k\varpi}}{\Gamma(k\varpi+1)} \right]. \tag{5.13}$$

Case 2. Let $\mathfrak{F}(\mathfrak{s},t)$ be $[(\diamond\diamond)-\varpi]$-differentiable. Then, Eq (5.3) implies

$$\begin{cases} \underline{\mathcal{Y}}(\mathfrak{s},q;\vee) = \dfrac{1}{q}\,\underline{\mathfrak{f}}_1 - \dfrac{1}{q^{\varpi}}\mathfrak{Q}\left[\alpha\dfrac{\partial}{\partial\mathfrak{s}}\underline{\mathfrak{F}}(\mathfrak{s},t) + \beta\underline{\mathfrak{F}}(\mathfrak{s},t)\left(\dfrac{\partial}{\partial\mathfrak{s}}\underline{\mathfrak{F}}(\mathfrak{s},t)\right) + \gamma\dfrac{\partial^2}{\partial\mathfrak{s}^2}\underline{\mathfrak{F}}(\mathfrak{s},t)\right], \\ \overline{\mathcal{Y}}(\mathfrak{s},q;\vee) = \dfrac{1}{q}\,\overline{\mathfrak{f}}_2 - \dfrac{1}{q^{\varpi}}\mathfrak{Q}\left[\alpha\dfrac{\partial}{\partial\mathfrak{s}}\overline{\mathfrak{F}}(\mathfrak{s},t) + \beta\overline{\mathfrak{F}}(\mathfrak{s},t)\left(\dfrac{\partial}{\partial\mathfrak{s}}\overline{\mathfrak{F}}(\mathfrak{s},t)\right) + \gamma\dfrac{\partial^2}{\partial\mathfrak{s}^2}\overline{\mathfrak{F}}(\mathfrak{s},t)\right]. \end{cases} \tag{5.14}$$

Thus, we get the same solution of Eq (5.1) as given by Eq (5.12).

Case 3. Let $\mathfrak{F}(\mathfrak{s},t)$ be $[(\diamond)-\varpi]$-differentiable and $\frac{\partial}{\partial t}\mathfrak{F}(\mathfrak{s},t)$ be $[(\diamond\diamond)-\varpi]$-differentiable, respectively.

Step I. Using the $\vee$-cut and applying the FLT to Eq (5.2), we get

$$\begin{cases} \mathfrak{Q}\left[\underline{\mathfrak{F}}(\mathfrak{s},t)\right] = \dfrac{1}{q}\,\underline{\mathfrak{F}}(\mathfrak{s},0) - \dfrac{1}{q^{\varpi}}\mathfrak{Q}\left[\alpha\dfrac{\partial}{\partial\mathfrak{s}}\overline{\mathfrak{F}}(\mathfrak{s},t) + \beta\overline{\mathfrak{F}}(\mathfrak{s},t)\left(\dfrac{\partial}{\partial\mathfrak{s}}\overline{\mathfrak{F}}(\mathfrak{s},t)\right) + \gamma\dfrac{\partial^2}{\partial\mathfrak{s}^2}\overline{\mathfrak{F}}(\mathfrak{s},t)\right], \\ \mathfrak{Q}\left[\overline{\mathfrak{F}}(\mathfrak{s},t)\right] = \dfrac{1}{q}\,\overline{\mathfrak{F}}(\mathfrak{s},0) - \dfrac{1}{q^{\varpi}}\mathfrak{Q}\left[\alpha\dfrac{\partial}{\partial\mathfrak{s}}\underline{\mathfrak{F}}(\mathfrak{s},t) + \beta\underline{\mathfrak{F}}(\mathfrak{s},t)\left(\dfrac{\partial}{\partial\mathfrak{s}}\underline{\mathfrak{F}}(\mathfrak{s},t)\right) + \gamma\dfrac{\partial^2}{\partial\mathfrak{s}^2}\underline{\mathfrak{F}}(\mathfrak{s},t)\right]. \end{cases} \tag{5.15}$$

Using the ICs from Eq (5.1),

$$\begin{cases} \underline{\mathcal{Y}}(\mathfrak{s},q;\vee) = \dfrac{1}{q}\,\underline{\mathfrak{f}}_1 - \dfrac{1}{q^{\varpi}}\mathfrak{Q}\left[\alpha\dfrac{\partial}{\partial\mathfrak{s}}\overline{\mathfrak{F}}(\mathfrak{s},t) + \beta\overline{\mathfrak{F}}(\mathfrak{s},t)\left(\dfrac{\partial}{\partial\mathfrak{s}}\overline{\mathfrak{F}}(\mathfrak{s},t)\right) + \gamma\dfrac{\partial^2}{\partial\mathfrak{s}^2}\overline{\mathfrak{F}}(\mathfrak{s},t)\right], \\ \overline{\mathcal{Y}}(\mathfrak{s},q;\vee) = \dfrac{1}{q}\,\overline{\mathfrak{f}}_2 - \dfrac{1}{q^{\varpi}}\mathfrak{Q}\left[\alpha\dfrac{\partial}{\partial\mathfrak{s}}\underline{\mathfrak{F}}(\mathfrak{s},t) + \beta\underline{\mathfrak{F}}(\mathfrak{s},t)\left(\dfrac{\partial}{\partial\mathfrak{s}}\underline{\mathfrak{F}}(\mathfrak{s},t)\right) + \gamma\dfrac{\partial^2}{\partial\mathfrak{s}^2}\underline{\mathfrak{F}}(\mathfrak{s},t)\right]. \end{cases} \tag{5.16}$$

Step II. Consider the series-type solution of Eq (5.16), stated as

$$\begin{cases} \underline{\mathcal{Y}}(\mathfrak{s},q;\vee) = \displaystyle\sum_{k=0}^{\infty} \frac{\underline{\varphi}_k(\mathfrak{s})}{q^{k\varpi+1}}, \\ \overline{\mathcal{Y}}(\mathfrak{s},q;\vee) = \displaystyle\sum_{k=0}^{\infty} \frac{\overline{\varphi}_k(\mathfrak{s})}{q^{k\varpi+1}}. \end{cases} \tag{5.17}$$

The i-th truncated term series form of the solution given by Eq (5.17) is given as

$$\begin{cases} \underline{\mathcal{Y}}(\mathfrak{s},q;\vee) = \dfrac{1}{q}\,\mathfrak{f}_1 + \displaystyle\sum_{k=1}^{i} \frac{\underline{\varphi}_k(\mathfrak{s})}{q^{k\varpi+1}}, \\ \overline{\mathcal{Y}}(\mathfrak{s},q;\vee) = \dfrac{1}{q}\,\mathfrak{f}_2 + \displaystyle\sum_{k=1}^{i} \frac{\overline{\varphi}_k(\mathfrak{s})}{q^{k\varpi+1}}. \end{cases} \tag{5.18}$$

The i-Laplace residual functions of Eq (5.16) are given by

$$\begin{cases} \mathfrak{Q}\Big[Res_{\underline{\mathcal{Y}}_i}\Big] = \underline{\mathcal{Y}}(\mathfrak{s},q;\vee) - \dfrac{1}{q}\,\mathfrak{f}_1 + \dfrac{1}{q^{\varpi}}\mathfrak{Q}\left[\alpha\dfrac{\partial}{\partial\mathfrak{s}}\overline{\mathfrak{F}}(\mathfrak{s},t) + \beta\overline{\mathfrak{F}}(\mathfrak{s},t)\left(\dfrac{\partial}{\partial\mathfrak{s}}\overline{\mathfrak{F}}(\mathfrak{s},t)\right) + \gamma\dfrac{\partial^2}{\partial\mathfrak{s}^2}\overline{\mathfrak{F}}(\mathfrak{s},t)\right], \\ \mathfrak{Q}\Big[Res_{\overline{\mathcal{Y}}_i}\Big] = \overline{\mathcal{Y}}(\mathfrak{s},q;\vee) - \dfrac{1}{q}\,\mathfrak{f}_2 + \dfrac{1}{q^{\varpi}}\mathfrak{Q}\left[\alpha\dfrac{\partial}{\partial\mathfrak{s}}\underline{\mathfrak{F}}(\mathfrak{s},t) + \beta\underline{\mathfrak{F}}(\mathfrak{s},t)\left(\dfrac{\partial}{\partial\mathfrak{s}}\underline{\mathfrak{F}}(\mathfrak{s},t)\right) + \gamma\dfrac{\partial^2}{\partial\mathfrak{s}^2}\underline{\mathfrak{F}}(\mathfrak{s},t)\right]. \end{cases} \tag{5.19}$$

Step III. Substituting Eq (5.18) into Eq (5.19), and then solving the relations $\lim_{q\to\infty} q^{k\varpi+1}\mathfrak{Q}[Res_{\underline{\mathcal{Y}}_i}(\mathfrak{s},q;\vee)] = 0$ and $\lim_{q\to\infty} q^{k\varpi+1}\mathfrak{Q}[Res_{\overline{\mathcal{Y}}_i}(\mathfrak{s},q;\vee)] = 0$ recursively, we obtain

$$\begin{cases} \underline{\varphi}_0(\mathfrak{s};\vee) = \mathfrak{f}_1, \\ \overline{\varphi}_0(\mathfrak{s};\vee) = \mathfrak{f}_2. \end{cases} \tag{5.20}$$

$$\begin{cases} \underline{\varphi}_1(\mathfrak{s}) = \alpha\dfrac{\partial}{\partial\mathfrak{s}}\overline{\varphi}_0(\mathfrak{s}) + \beta\overline{\varphi}_0(\mathfrak{s})\dfrac{\partial}{\partial\mathfrak{s}}\overline{\varphi}_0(\mathfrak{s}) + \gamma\dfrac{\partial^2}{\partial\mathfrak{s}^2}\overline{\varphi}_0(\mathfrak{s}), \\ \overline{\varphi}_1(\mathfrak{s}) = \alpha\dfrac{\partial}{\partial\mathfrak{s}}\underline{\varphi}_0(\mathfrak{s}) + \beta\underline{\varphi}_0(\mathfrak{s})\dfrac{\partial}{\partial\mathfrak{s}}\underline{\varphi}_0(\mathfrak{s}) + \gamma\dfrac{\partial^2}{\partial\mathfrak{s}^2}\underline{\varphi}_0(\mathfrak{s}). \end{cases} \tag{5.21}$$

$$\vdots$$

$$\begin{cases} \underline{\varphi}_{k+1}(\mathfrak{s}) = \alpha\dfrac{\partial}{\partial\mathfrak{s}}\overline{\varphi}_k(\mathfrak{s}) + \beta\displaystyle\sum_{j=0}^{k}\overline{\varphi}_j(\mathfrak{s})\frac{\partial}{\partial\mathfrak{s}}\overline{\varphi}_{k-j}(\mathfrak{s}) + \gamma\frac{\partial^2}{\partial\mathfrak{s}^2}\overline{\varphi}_k(\mathfrak{s}), \\ \overline{\varphi}_{k+1}(\mathfrak{s}) = \alpha\dfrac{\partial}{\partial\mathfrak{s}}\underline{\varphi}_k(\mathfrak{s}) + \beta\displaystyle\sum_{j=0}^{k}\underline{\varphi}_j(\mathfrak{s})\frac{\partial}{\partial\mathfrak{s}}\underline{\varphi}_{k-j}(\mathfrak{s}) + \gamma\frac{\partial^2}{\partial\mathfrak{s}^2}\underline{\varphi}_k(\mathfrak{s}). \end{cases} \tag{5.22}$$

Putting the values of $\underline{\varphi}_j(\mathfrak{s};\vee)$ and $\overline{\varphi}_j(\mathfrak{s};\vee)$, $j = 0, 1, \ldots$, in Eq (5.18), we get

$$\begin{cases} \underline{\mathcal{Y}}(\mathfrak{s},q;\vee) = \dfrac{1}{q}\,\underline{\varphi}_0(\mathfrak{s},\vee) + \dfrac{1}{q^{\varpi+1}}\,\overline{\varphi}_1(\mathfrak{s},\vee) + \cdots + \dfrac{1}{q^{(k+1)\varpi+1}}\,\overline{\varphi}_{k+1}(\mathfrak{s},\vee), \\ \overline{\mathcal{Y}}(\mathfrak{s},q;\vee) = \dfrac{1}{q}\,\overline{\varphi}_0(\mathfrak{s},\vee) + \dfrac{1}{q^{\varpi+1}}\,\underline{\varphi}_1(\mathfrak{s},\vee) + \cdots + \dfrac{1}{q^{(k+1)\varpi+1}}\,\underline{\varphi}_{k+1}(\mathfrak{s},\vee). \end{cases} \tag{5.23}$$

Step IV. Applying the inverse FLT to Eq (5.23), we obtain

$$\begin{cases} \underline{\mathfrak{F}}(\mathfrak{s},t;\vee) = \underline{\varphi}_0 + \displaystyle\sum_{k=1}^{\infty}\overline{\varphi}_k(\mathfrak{s})\frac{t^{k\varpi}}{\Gamma(k\varpi+1)}, \\ \overline{\mathfrak{F}}(\mathfrak{s},t;\vee) = \overline{\varphi}_0 + \displaystyle\sum_{k=0}^{\infty}\underline{\varphi}_k(\mathfrak{s})\frac{t^{k\varpi}}{\Gamma(k\varpi+1)}. \end{cases} \tag{5.24}$$

Thus, the fuzzy solution of Eq (5.1) is given as

$$\mathfrak{F}(\mathfrak{s},t;\curlyvee)=\left[\underline{\varphi}_0+\sum_{k=1}^{\infty}\overline{\varphi}_k(\mathfrak{s})\frac{t^{k\varpi}}{\Gamma(k\varpi+1)},\ \ \overline{\varphi}_0+\sum_{k=0}^{\infty}\underline{\varphi}_k(\mathfrak{s})\frac{t^{k\varpi}}{\Gamma(k\varpi+1)}\right]. \tag{5.25}$$

As summarized in Table 1, the three cases vary depending on the $g\mathbb{H}$-differentiability assigned to the fuzzy solution and, in Case 3, to its time derivative. Cases 1 and 2 illustrate the two principal types of differentiability, while Case 3 combines both types, necessitating separate analysis of the associated fuzzy endpoint equations. This classification enables the LRPSM formulation to incorporate various possible differentiability frameworks of the fuzzy fractional model without enforcing a uniform differentiability assumption across all solution branches.

Table 1. Summary of $g\mathbb{H}$-differentiability cases.

Case	$\mathfrak{F}$	$\partial_t\mathfrak{F}$	Role in the solution procedure
1	$[(\diamond)-\varpi]$	–	The lower and upper fuzzy branches are propagated according to the first $g\mathbb{H}$-differentiability type.
2	$[(\diamond\diamond)-\varpi]$	–	The fuzzy branches are propagated according to the second $g\mathbb{H}$-differentiability type, leading to the corresponding alternative endpoint representation.
3	$[(\diamond)-\varpi]$	$[(\diamond\diamond)-\varpi]$	A mixed differentiability structure is considered, in which the fuzzy solution and its temporal derivative follow different $g\mathbb{H}$-differentiability types.

6. Convergence analysis

Consider the NLTFFCRWPE, whose series solution obtained via LRPSM can be written as

$$\mathfrak{F}(\mathfrak{s},t,\curlyvee)=\left[\underline{\phi_0}(\mathfrak{s})+\sum_{k=1}^{\infty}\underline{\phi_0}(\mathfrak{s})\frac{t^{k\varpi}}{\Gamma(k\varpi+1)},\ \overline{\phi_0}(\mathfrak{s})+\sum_{k=1}^{\infty}\overline{\phi_0}(\mathfrak{s})\frac{t^{k\varpi}}{\Gamma(k\varpi+1)}\right], \tag{6.1}$$

where

$$0<\varpi\leq 1,\qquad 0\leq\curlyvee\leq 1.$$

To treat the lower and upper bounds as one fuzzy-valued approximate solution, define

$$\mathfrak{F}_k(u,t,\curlyvee)=\left[\underline{\mathfrak{F}_k}(\mathfrak{s},t,\curlyvee),\overline{\mathfrak{F}_k}(\mathfrak{s},t,\curlyvee)\right],\qquad k=0,1,2,\ldots. \tag{6.2}$$

Then the fuzzy series solution obtained by LRPSM can be expressed in the compact fuzzy form as

$$\mathfrak{F}(\mathfrak{s},t,\curlyvee)=\sum_{k=0}^{\infty}\mathfrak{F}_k(\mathfrak{s},t,\curlyvee),$$

where

$$\mathfrak{F}_0(\mathfrak{s},t,\curlyvee)=\mathfrak{F}_0(\mathfrak{s},\curlyvee),$$

and, for $k \geq 1$,

$$\mathfrak{F}_k(\mathfrak{s}, t, \curlyvee) = \mathfrak{F}_k(\mathfrak{s}, t, \curlyvee)\frac{t^{k\varpi}}{\Gamma(k\varpi + 1)}.$$

Thus,

$$\mathfrak{F}_k(\mathfrak{s}, t, \curlyvee) = \mathfrak{F}_0(\mathfrak{s}, \curlyvee) + \sum_{k=1}^{\infty} \mathfrak{F}_k(\mathfrak{s}, t, \curlyvee)\frac{t^{k\varpi}}{\Gamma(k\varpi + 1)}.$$

Let

$$W_T = \mathfrak{R} \times [0, T],$$

where $\mathfrak{s} \in \mathfrak{R}$ denotes the spatial variable and $0 \leq t \leq T$ is a finite temporal interval. Consistent with the functional setting adopted in the existence and uniqueness analysis, the convergence of the fuzzy LRPSM series is considered on the unbounded spatial domain $\mathfrak{R}$ and a finite time interval $[0, T]$. We employ the corresponding supremum norm

$$\|\mathfrak{T}\| = \sup_{\substack{(\mathfrak{s},t)\in W_T \\ 0\leq\curlyvee\leq 1}} \max\left\{\left|\underline{\mathfrak{T}}(\mathfrak{s}, t, \curlyvee)\right|, \left|\overline{\mathfrak{T}}(\mathfrak{s}, t, \curlyvee)\right|\right\},$$

for

$$\mathfrak{T} = [\underline{\mathfrak{T}}, \overline{\mathfrak{T}}].$$

Accordingly, all subsequent estimates and the uniform convergence result are understood with respect to $W_T = \mathfrak{R} \times [0, T]$.

Theorem 6.1. *Assume that $\phi_0(\mathfrak{s}, \curlyvee) \in C_b(\mathfrak{R}, \mathbb{F}_R)$. Now, let the LRPSM components $\mathfrak{F}_k(\mathfrak{s}, t, \curlyvee)$ satisfy the estimate*

$$\|\mathfrak{F}_k\| \leq \rho \|\mathfrak{F}_{k-1}\|, \qquad k \geq 1, \tag{6.3}$$

where $0 < \rho < 1$. Then the fuzzy LRPSM series

$$\mathfrak{F}(\mathfrak{s}, t, \curlyvee) = \sum_{k=0}^{\infty} \mathfrak{F}_k(\mathfrak{s}, t, \curlyvee)$$

is uniformly convergent on W_T.

Proof. Since

$$\mathfrak{F}_0(\mathfrak{s}, t, \curlyvee) = \phi_0(\mathfrak{s}, \curlyvee),$$

and $\phi_0(\mathfrak{s}, \curlyvee) \in C_b(\mathfrak{R}, \mathbb{F}_R)$, there exists a positive constant $N > 0$ such that

$$|\mathfrak{F}_0(\mathfrak{s}, t, \curlyvee)| \leq N, \qquad (\mathfrak{s}, t) \in W_T. \tag{6.4}$$

We can prove that the k_{th} fuzzy component satisfies

$$|\mathfrak{F}_k(\mathfrak{s}, t, \curlyvee)| \leq N\rho^k, \qquad k = 0, 1, 2, \ldots.$$

For $k = 1$, using (6.3), we obtain

$$|\mathfrak{F}_1(\mathfrak{s}, t, \curlyvee)| \leq \rho\,|\mathfrak{F}_0(\mathfrak{s}, t, \curlyvee)|.$$

It follows directly from (6.4) that

$$|\mathfrak{F}_0(\mathfrak{s}, t, \curlyvee)| \leq N\rho.$$

Thus, the required estimate holds for $k = 1$. Assume that the result holds for $k - 1$, that is,

$$|\mathfrak{F}_{k-1}(\mathfrak{s}, t, \curlyvee)| \leq N\rho^{k-1}.$$

From (6.3), it follows that

$$|\mathfrak{F}(\mathfrak{s}, t, \curlyvee)| \leq \rho\,|\mathfrak{F}_{k-1}(\mathfrak{s}, t, \curlyvee)| \leq \rho N\rho^{k-1} = N\rho^k.$$

The desired result then follows by mathematical induction:

$$|\mathfrak{F}_k(\mathfrak{s}, t, \curlyvee)| \leq N\rho^k, \qquad k = 0, 1, 2, \ldots, \tag{6.5}$$

for all $(\mathfrak{s}, t) \in W_T$. Consequently, we obtain

$$\sum_{k=0}^{\infty} |\mathfrak{F}(\mathfrak{s}, t, \curlyvee)| \leq \sum_{k=0}^{\infty} N\rho^k.$$

Since $0 < \rho < 1$, the corresponding geometric series converges, and we have

$$\sum_{k=0}^{\infty} N\rho^k < \infty.$$

Hence, by the Weierstrass M-test, the fuzzy series $\sum_{k=0}^{\infty} \mathfrak{F}_k(\mathfrak{s}, t, \curlyvee)$ is uniformly convergent on W_T. Therefore, the fuzzy solution of LRPSM,

$$\mathfrak{F}(\mathfrak{s}, t, \curlyvee) = \phi_0(\mathfrak{s}, \curlyvee) + \sum_{k=1}^{\infty} \phi_k(\mathfrak{s}, \curlyvee)\frac{t^{k\varpi}}{\Gamma(k\varpi + 1)}$$

is uniformly convergent on W_T. □

The M-term fuzzy approximate solution is defined by

$$\mathfrak{F}_M(\mathfrak{s}, t, \curlyvee) = \sum_{k=0}^{M} \mathfrak{F}_k(\mathfrak{s}, t, \curlyvee),$$

that is,

$$\mathfrak{F}_M(\mathfrak{s}, t, \curlyvee) = \phi_0(\mathfrak{s}, \curlyvee) + \sum_{k=1}^{M} \phi_k(\mathfrak{s}, \curlyvee)\frac{t^{k\varpi}}{\Gamma(k\varpi + 1)}.$$

In lower and upper endpoint form, this becomes

$$\mathfrak{F}_M(\mathfrak{s}, t, \curlyvee) = \left[\underline{\phi_0}(\mathfrak{s}) + \sum_{k=1}^{M} \underline{\phi_k}(\mathfrak{s})\frac{t^{k\varpi}}{\Gamma(k\varpi + 1)},\ \overline{\phi_0}(\mathfrak{s}) + \sum_{k=1}^{M} \overline{\phi_k}(\mathfrak{s})\frac{t^{k\varpi}}{\Gamma(k\varpi + 1)}\right]. \tag{6.6}$$

Since the infinite fuzzy series is uniformly convergent, the partial sum $\mathfrak{F}_M(\mathfrak{s}, t, \vee)$ gives an approximate fuzzy solution of the NLTFFCRWPE. Using (6.5), the truncation error satisfies the following condition:

$$\|\mathfrak{F} - \mathfrak{F}_M\| = \left\| \sum_{k=M+1}^{\infty} \mathfrak{F}_k \right\| \leq \sum_{k=M+1}^{\infty} \|\mathfrak{F}_k\| \leq \sum_{k=M+1}^{\infty} N\rho^k = \frac{N\rho^{M+1}}{1-\rho}.$$

For $\rho \in (0, 1)$, we obtain

$$\lim_{M\to\infty} \|\mathfrak{F} - \mathfrak{F}_M\| = 0.$$

Thus, the truncated fuzzy solution converges uniformly to the fuzzy series solution. Hence, under the condition $0 < \rho < 1$, the fuzzy series solution obtained by LRPSM for the NLTFFCRWPE can be written as

$$\mathfrak{F}_M(\mathfrak{s}, t, \vee) = \left[\underline{\phi_0}(\mathfrak{s}) + \sum_{k=1}^{M} \underline{\phi_k}(\mathfrak{s}) \frac{t^{k\varpi}}{\Gamma(k\varpi + 1)},\ \overline{\phi_0}(\mathfrak{s}) + \sum_{k=1}^{M} \overline{\phi_k}(\mathfrak{s}) \frac{t^{k\varpi}}{\Gamma(k\varpi + 1)} \right],$$

is uniformly convergent on $W_T = \mathfrak{R} \times [0, T]$. Equivalently, the single fuzzy-valued series

$$\mathfrak{F}(\mathfrak{s}, t, \vee) = \sum_{k=0}^{\infty} \mathfrak{F}_k(\mathfrak{s}, t, \vee)$$

is uniformly convergent, and the finite $\mathcal{LRPS}$ sum

$$\mathfrak{F}_M(\mathfrak{s}, t, \vee) = \sum_{k=0}^{M} \mathfrak{F}_k(\mathfrak{s}, t, \vee)$$

provides a valid approximate fuzzy solution of the NLTFFCRWPE.

7. Ulam-Hyers stability of the NLTFFCRWPE

Definition 7.1. *The NLTFFCRWPE, Eq (3.2), is said to be Ulam-Hyers stable if there exists a constant* $\Lambda_H > 0$ *such that, for every* $\varepsilon > 0$*, whenever a fuzzy function*

$$\mathfrak{F}(\mathfrak{s}, t, \vee) \in C([0, T], \mathbb{F}_R)$$

satisfies the inequality

$$\left\| {}^{C}D_t^{\varpi} \mathfrak{F}(\mathfrak{s}, t, \vee) + \mathfrak{N}(\mathfrak{F})(\mathfrak{s}, t, \vee) \right\| \leq \varepsilon, \tag{7.1}$$

there exists a unique solution

$$(\mathfrak{T})(\mathfrak{s}, t, \vee) \in C([0, T], \mathbb{F}_R)$$

of Eq (3.2) such that

$$\|\mathfrak{F} - \mathfrak{T}\| \leq \Lambda_H \varepsilon. \tag{7.2}$$

Here, $\mathfrak{F}$ is called an approximate fuzzy solution, and $\mathfrak{T}$ is the corresponding exact fuzzy solution.

Theorem 7.1. *Assume that the nonlinear operator $\mathfrak{N}$ follows the Lipschitz condition*

$$\|\mathfrak{N}(\mathfrak{F}) - \mathfrak{N}(\mathfrak{T})\| \leq L_{\mathfrak{N}} \|\mathfrak{F} - \mathfrak{T}\|, \tag{7.3}$$

for all admissible fuzzy functions $\mathfrak{F}, \mathfrak{T} \in C([0,T], \mathbb{F}_R)$, where $L_{\mathfrak{N}} > 0$. If

$$\delta = \frac{T^{\varpi} L_{\mathfrak{N}}}{\Gamma(\varpi + 1)} < 1, \tag{7.4}$$

then the NLTFFCRWPE, Eq (3.2), is Ulam-Hyers stable.

Proof. Let $\varepsilon > 0$, and let

$$\mathfrak{F}(\mathfrak{s}, t, \vee) \in C([0,T], \mathbb{F}_R)$$

be an approximate solution of Eq (3.2) satisfying Eq (7.1). Then there exists a perturbation function $\tilde{\psi}(\mathfrak{s}, t, \vee) \in C([0,T], \mathbb{F}_R)$, such that

$$\|\tilde{\psi}(\mathfrak{s}, t, \vee)\| \leq \varepsilon, \tag{7.5}$$

and

$${}^{C}D_t^{\varpi} \mathfrak{F}(\mathfrak{s}, t, \vee) = -\mathfrak{N}(\mathfrak{F})(\mathfrak{s}, t, \vee) + \tilde{\psi}(\mathfrak{s}, t, \vee). \tag{7.6}$$

Applying the RL fractional integral operator I_t^{ϖ}, the following equation can be obtained as

$$\mathfrak{F}(\mathfrak{s}, t, \vee) = \mathfrak{F}(\mathfrak{s}, 0, \vee) - \frac{1}{\Gamma(\varpi)} \int_0^t (t-\tau)^{\varpi-1} \mathfrak{N}(\mathfrak{F})(\mathfrak{s}, \tau, \vee)\, d\tau + \frac{1}{\Gamma(\varpi)} \int_0^t (t-\tau)^{\varpi-1} \tilde{\psi}(\mathfrak{s}, \tau, \vee)\, d\tau. \tag{7.7}$$

Let $\mathfrak{T}(\mathfrak{s}, t, \vee)$ be the exact solution with the same initial condition

$$\mathfrak{T}(\mathfrak{s}, 0, \vee) = \mathfrak{F}(\mathfrak{s}, 0, \vee) = \mathfrak{F}_0(\mathfrak{s}, \vee).$$

Then,

$$\mathfrak{T}(\mathfrak{s}, t, \vee) = \mathfrak{F}_0(\mathfrak{s}, \vee) - \frac{1}{\Gamma(\varpi)} \int_0^t (t-\tau)^{\varpi-1} \mathfrak{N}(\mathfrak{T})(\mathfrak{s}, \tau, \vee)\, d\tau. \tag{7.8}$$

Subtracting Eqs (7.7) and (7.8),

$$\mathfrak{F} - \mathfrak{T} = -\frac{1}{\Gamma(\varpi)} \int_0^t (t-\tau)^{\varpi-1} \left[\mathfrak{N}(\mathfrak{F}) - \mathfrak{N}(\mathfrak{T})\right] d\tau + \frac{1}{\Gamma(\varpi)} \int_0^t (t-\tau)^{\varpi-1} \tilde{\psi}\, d\tau.$$

Taking norms and using the Lipschitz condition

$$\|\mathfrak{N}(\mathfrak{F}) - \mathfrak{N}(\mathfrak{T})\| \leq L_{\mathfrak{N}} \|(\mathfrak{F} - \mathfrak{T})\|,$$

we obtain

$$\|\mathfrak{F} - \mathfrak{T}\| \leq \frac{L_{\mathfrak{N}}}{\Gamma(\varpi)} \int_0^t (t-\tau)^{\varpi-1} \|\mathfrak{F} - \mathfrak{T}\| d\tau + \frac{\varepsilon}{\Gamma(\varpi)} \int_0^t (t-\tau)^{\varpi-1} d\tau.$$

Since

$$\int_0^t (t-\tau)^{\varpi-1} d\tau = \frac{t^{\varpi}}{\varpi}, \qquad \Gamma(\varpi + 1) = \varpi \Gamma(\varpi),$$

we get

$$\|\mathfrak{F} - \mathfrak{T}\| \leq \frac{L_{\mathfrak{N}} t^{\varpi}}{\Gamma(\varpi + 1)} \|\mathfrak{F} - \mathfrak{T}\| + \frac{\varepsilon t^{\varpi}}{\Gamma(\varpi + 1)}.$$

Taking the supremum over $[0, T]$:

$$\|\mathfrak{F} - \mathfrak{T}\| \leq \delta \|\mathfrak{F} - \mathfrak{T}\| + \frac{\varepsilon T^{\varpi}}{\Gamma(\varpi + 1)},$$

where

$$\delta = \frac{T^{\varpi} L_{\mathfrak{N}}}{\Gamma(\varpi + 1)}.$$

which implies that

$$T < T_* = \left(\frac{\Gamma(\varpi + 1)}{L_{\mathfrak{N}}}\right)^{1/\varpi}.$$

Thus,

$$\|\mathfrak{F} - \mathfrak{T}\| \leq \frac{T^{\varpi}}{\Gamma(\varpi + 1)(1 - \delta)} \varepsilon.$$

Hence, Ulam-Hyers stability holds with

$$\Lambda_H = \frac{T^{\varpi}}{\Gamma(\varpi + 1)\left(1 - \frac{T^{\varpi} L_{\mathfrak{N}}}{\Gamma(\varpi+1)}\right)}. \tag{7.9}$$

From Eq (7.9), the stability constant Λ_H increases with the time horizon T as long as $\frac{T^{\varpi} L_{\mathfrak{N}}}{\Gamma(\varpi+1)} < 1$. Defining the admissible threshold by $T_* = \left(\frac{\Gamma(\varpi+1)}{L_{\mathfrak{N}}}\right)^{1/\varpi}$, the contraction condition becomes $T < T_*$. Hence, Λ_H increases as T increases within this admissible interval and satisfies $\Lambda_H \to +\infty$ as $T \to T_*^-$. □

8. Illustrative examples

Example 1. *Consider a fractional-order NLTFFCRWP problem given by*

$$\begin{cases} \frac{\partial^{\varpi}}{\partial t^{\varpi}} \mathfrak{F}(\mathfrak{s}, t) + \alpha \frac{\partial}{\partial \mathfrak{s}} \mathfrak{F}(\mathfrak{s}, t) + \beta \mathfrak{F}(\mathfrak{s}, t) \left(\frac{\partial}{\partial \mathfrak{s}} \mathfrak{F}(\mathfrak{s}, t)\right) + \gamma \frac{\partial^2}{\partial \mathfrak{s}^2} \mathfrak{F}(\mathfrak{s}, t) = 0, \qquad \varpi \in (0, 1], \\ \mathfrak{F}(\mathfrak{s}, 0) = (\curlyvee, 2 - \curlyvee)\left(e^{-(\mathfrak{s}-1)^2} + e^{-(\mathfrak{s}+1)^2}\right), \quad \mathfrak{s} \in \mathfrak{R}, \ \ t \in (0, T]. \end{cases} \tag{8.1}$$

Case 1. *Let $\mathfrak{F}(\mathfrak{s}, t)$ be $[(\diamond) - \varpi]$-differentiable. After applying the FLT and substituting the FICs, Eq (8.1) takes the form*

$$\begin{cases} \mathfrak{Q}\left[\underline{\mathfrak{F}}(\mathfrak{s}, t)\right] = \frac{1}{q}(\curlyvee)\left(e^{-(\mathfrak{s}-1)^2} + e^{-(\mathfrak{s}+1)^2}\right) - \frac{1}{q^{\varpi}} \mathfrak{Q}\left[\alpha \frac{\partial}{\partial \mathfrak{s}} \underline{\mathfrak{F}}(\mathfrak{s}, t) + \beta \underline{\mathfrak{F}}(\mathfrak{s}, t)\left(\frac{\partial}{\partial \mathfrak{s}} \underline{\mathfrak{F}}(\mathfrak{s}, t)\right) + \gamma \frac{\partial^2}{\partial \mathfrak{s}^2} \underline{\mathfrak{F}}(\mathfrak{s}, t)\right], \\ \mathfrak{Q}\left[\overline{\mathfrak{F}}(\mathfrak{s}, t)\right] = \frac{1}{q}(2 - \curlyvee)\left(e^{-(\mathfrak{s}-1)^2} + e^{-(\mathfrak{s}+1)^2}\right) - \frac{1}{q^{\varpi}} \mathfrak{Q}\left[\alpha \frac{\partial}{\partial \mathfrak{s}} \overline{\mathfrak{F}}(\mathfrak{s}, t) + \beta \overline{\mathfrak{F}}(\mathfrak{s}, t)\left(\frac{\partial}{\partial \mathfrak{s}} \overline{\mathfrak{F}}(\mathfrak{s}, t)\right) + \gamma \frac{\partial^2}{\partial \mathfrak{s}^2} \overline{\mathfrak{F}}(\mathfrak{s}, t)\right]. \end{cases} \tag{8.2}$$

The i-th truncated term series form of the solution presented in Eq (5.17) is the following:

$$\begin{cases} \underline{\mathcal{Y}}(\mathfrak{s}, q; \curlyvee) = \frac{1}{q}(\curlyvee)\left(e^{-(\mathfrak{s}-1)^2} + e^{-(\mathfrak{s}+1)^2}\right) + \sum_{k=1}^{i} \frac{\underline{\varphi}_k(\mathfrak{s})}{q^{k\varpi+1}}, \\ \overline{\mathcal{Y}}(\mathfrak{s}, q; \curlyvee) = \frac{1}{q}(2 - \curlyvee)\left(e^{-(\mathfrak{s}-1)^2} + e^{-(\mathfrak{s}+1)^2}\right) + \sum_{k=1}^{i} \frac{\overline{\varphi}_k(\mathfrak{s})}{q^{k\varpi+1}}. \end{cases} \tag{8.3}$$

The i-Laplace residual functions of Eq (8.3) are expressed by

$$\begin{cases} \mathfrak{L}\Big[Res_{\underline{\mathcal{Y}_i}}\Big] = \underline{\mathcal{Y}}(\mathfrak{s},q;\curlyvee) - \dfrac{1}{q}(\curlyvee)\left(e^{-(\mathfrak{s}-1)^2}+e^{-(\mathfrak{s}+1)^2}\right) \\ \qquad\qquad + \dfrac{1}{q^{\varpi}}\mathfrak{L}\left[\alpha\dfrac{\partial}{\partial\mathfrak{s}}\underline{\mathfrak{F}}(\mathfrak{s},t)+\beta\underline{\mathfrak{F}}(\mathfrak{s},t)\left(\dfrac{\partial}{\partial\mathfrak{s}}\underline{\mathfrak{F}}(\mathfrak{s},t)\right)+\gamma\dfrac{\partial^2}{\partial\mathfrak{s}^2}\underline{\mathfrak{F}}(\mathfrak{s},t)\right], \\ \mathfrak{L}\Big[Res_{\overline{\mathcal{Y}_i}}\Big] = \overline{\mathcal{Y}}(\mathfrak{s},q;\curlyvee) - \dfrac{1}{q}(2-\curlyvee)\left(e^{-(\mathfrak{s}-1)^2}+e^{-(\mathfrak{s}+1)^2}\right) \\ \qquad\qquad + \dfrac{1}{q^{\varpi}}\mathfrak{L}\left[\alpha\dfrac{\partial}{\partial\mathfrak{s}}\overline{\mathfrak{F}}(\mathfrak{s},t)+\beta\overline{\mathfrak{F}}(\mathfrak{s},t)\left(\dfrac{\partial}{\partial\mathfrak{s}}\overline{\mathfrak{F}}(\mathfrak{s},t)\right)+\gamma\dfrac{\partial^2}{\partial\mathfrak{s}^2}\overline{\mathfrak{F}}(\mathfrak{s},t)\right]. \end{cases} \tag{8.4}$$

Substituting Eq (8.3) into Eq (8.4), and then solving the relations $\lim_{q\to\infty} q^{k\varpi+1}\mathfrak{L}[Res_{\underline{\mathcal{Y}_i}}(\mathfrak{s},q;\curlyvee)]=0$ *and* $\lim_{q\to\infty} q^{k\varpi+1}\mathfrak{L}[Res_{\overline{\mathcal{Y}_i}}(\mathfrak{s},q;\curlyvee)] = 0$ *recursively, the following terms of the lower and upper solutions can be presented as*

$$\begin{cases} \underline{\varphi}_0(\mathfrak{s};\curlyvee) = (\curlyvee)\left(e^{-(\mathfrak{s}-1)^2}+e^{-(\mathfrak{s}+1)^2}\right), \\ \overline{\varphi}_0(\mathfrak{s};\curlyvee) = (2-\curlyvee)\left(e^{-(\mathfrak{s}-1)^2}+e^{-(\mathfrak{s}+1)^2}\right). \end{cases} \tag{8.5}$$

$$\begin{cases} \underline{\varphi_1} = \quad \curlyvee\Big(e^{-(\mathfrak{s}-1)^2}(2\mathfrak{s}-4(\mathfrak{s}-1)^2)+e^{-(\mathfrak{s}+1)^2}(2\mathfrak{s}+4-4(\mathfrak{s}+1)^2)\Big) \\ \qquad\quad +2\curlyvee^2(e^{-(\mathfrak{s}-1)^2}+e^{-(\mathfrak{s}+1)^2})\Big(e^{-(\mathfrak{s}-1)^2}(\mathfrak{s}-1)+e^{-(\mathfrak{s}+1)^2}(\mathfrak{s}+1)\Big), \\ \overline{\varphi_1} = \quad (2-\curlyvee)\Big(e^{-(\mathfrak{s}-1)^2}(2\mathfrak{s}-4(\mathfrak{s}-1)^2)+e^{-(\mathfrak{s}+1)^2}(2\mathfrak{s}+4-4(\mathfrak{s}+1)^2)\Big) \\ \qquad\quad +2(2-\curlyvee)^2(e^{-(\mathfrak{s}-1)^2}+e^{-(\mathfrak{s}+1)^2})\Big(e^{-(\mathfrak{s}-1)^2}(\mathfrak{s}-1)+e^{-(\mathfrak{s}+1)^2}(\mathfrak{s}+1)\Big). \end{cases}$$

Putting $\varphi_j(\mathfrak{s},\curlyvee)$, $j=0,1,\ldots$ *in Eq (8.3), the following expression is obtained as*

$$\begin{cases} \underline{\mathcal{Y}}(\mathfrak{s},q;\curlyvee) = \dfrac{1}{q}(\curlyvee)\left(e^{-(\mathfrak{s}-1)^2}+e^{-(\mathfrak{s}+1)^2}\right) \\ \qquad\qquad + \dfrac{1}{q^{\varpi+1}}\Big[\curlyvee\left(e^{-(\mathfrak{s}-1)^2}(2\mathfrak{s}-4(\mathfrak{s}-1)^2)+e^{-(\mathfrak{s}+1)^2}(2\mathfrak{s}+4-4(\mathfrak{s}+1)^2)\right) \\ \qquad\qquad + 2\curlyvee^2(e^{-(\mathfrak{s}-1)^2}+e^{-(\mathfrak{s}+1)^2})\Big(e^{-(\mathfrak{s}-1)^2}(\mathfrak{s}-1)+e^{-(\mathfrak{s}+1)^2}(\mathfrak{s}+1)\Big)\Big]+..., \\ \overline{\mathcal{Y}}(\mathfrak{s},q;\curlyvee) = \dfrac{1}{q}(2-\curlyvee)\left(e^{-(\mathfrak{s}-1)^2}+e^{-(\mathfrak{s}+1)^2}\right) \\ \qquad\qquad + \dfrac{1}{q^{\varpi+1}}\Big[(2-\curlyvee)\Big(e^{-(\mathfrak{s}-1)^2}(2\mathfrak{s}-4(\mathfrak{s}-1)^2)+e^{-(\mathfrak{s}+1)^2}(2\mathfrak{s}+4-4(\mathfrak{s}+1)^2)\Big) \\ \qquad\qquad + 2(2-\curlyvee)^2(e^{-(\mathfrak{s}-1)^2}+e^{-(\mathfrak{s}+1)^2})\Big(e^{-(\mathfrak{s}-1)^2}(\mathfrak{s}-1)+e^{-(\mathfrak{s}+1)^2}(\mathfrak{s}+1)\Big)\Big]+.... \end{cases} \tag{8.6}$$

Applying the inverse FLT to Eq (8.6), the obtained results are as follows:

$$\begin{cases} \underline{\mathfrak{F}}(\mathfrak{s},t,\gamma) = (\gamma)\left(e^{-(\mathfrak{s}-1)^2}+e^{-(\mathfrak{s}+1)^2}\right)+\Big[\ \gamma\left(e^{-(\mathfrak{s}-1)^2}(2\mathfrak{s}-4(\mathfrak{s}-1)^2)+e^{-(\mathfrak{s}+1)^2}(2\mathfrak{s}+4-4(\mathfrak{s}+1)^2)\right) \\ \qquad +2\,\gamma^2\,(e^{-(\mathfrak{s}-1)^2}+e^{-(\mathfrak{s}+1)^2})\left(e^{-(\mathfrak{s}-1)^2}(\mathfrak{s}-1)+e^{-(\mathfrak{s}+1)^2}(\mathfrak{s}+1)\right)\Big]\dfrac{t^{\varpi}}{\Gamma[1+\varpi]}+..., \\ \overline{\mathfrak{F}}(\mathfrak{s},t,\gamma) = (2-\gamma)\left(e^{-(\mathfrak{s}-1)^2}+e^{-(\mathfrak{s}+1)^2}\right)+\Big[(2-\gamma)\Big(e^{-(\mathfrak{s}-1)^2}(2\mathfrak{s}-4(\mathfrak{s}-1)^2) \\ \qquad +e^{-(\mathfrak{s}+1)^2}(2\mathfrak{s}+4-4(\mathfrak{s}+1)^2)\Big)+2(2-\gamma)^2(e^{-(\mathfrak{s}-1)^2}+e^{-(\mathfrak{s}+1)^2}) \\ \qquad \left(e^{-(\mathfrak{s}-1)^2}(\mathfrak{s}-1)+e^{-(\mathfrak{s}+1)^2}(\mathfrak{s}+1)\right)\Big]\dfrac{t^{\varpi}}{\Gamma[1+\varpi]}+.... \end{cases} \tag{8.7}$$

Consequently, the truncated fuzzy solution of Eq (8.1) can be presented as

$$\begin{aligned} \mathfrak{F}(\mathfrak{s},t,\gamma) = \Bigg[& (\gamma)\left(e^{-(\mathfrak{s}-1)^2}+e^{-(\mathfrak{s}+1)^2}\right)+\Big(\ \gamma\left(e^{-(\mathfrak{s}-1)^2}(2\mathfrak{s}-4(\mathfrak{s}-1)^2)+e^{-(\mathfrak{s}+1)^2}(2\mathfrak{s}+4-4(\mathfrak{s}+1)^2)\right) \\ & +2\,\gamma^2\,(e^{-(\mathfrak{s}-1)^2}+e^{-(\mathfrak{s}+1)^2})\left(e^{-(\mathfrak{s}-1)^2}(\mathfrak{s}-1)+e^{-(\mathfrak{s}+1)^2}(\mathfrak{s}+1)\right)\Big)\dfrac{t^{\varpi}}{\Gamma[1+\varpi]}, \\ & (2-\gamma)\left(e^{-(\mathfrak{s}-1)^2}+e^{-(\mathfrak{s}+1)^2}\right)+\Big((2-\gamma)\left(e^{-(\mathfrak{s}-1)^2}(2\mathfrak{s}-4(\mathfrak{s}-1)^2)+e^{-(\mathfrak{s}+1)^2}(2\mathfrak{s}+4-4(\mathfrak{s}+1)^2)\right) \\ & +2(2-\gamma)^2(e^{-(\mathfrak{s}-1)^2}+e^{-(\mathfrak{s}+1)^2})\left(e^{-(\mathfrak{s}-1)^2}(\mathfrak{s}-1)+e^{-(\mathfrak{s}+1)^2}(\mathfrak{s}+1)\right)\Big)\dfrac{t^{\varpi}}{\Gamma[1+\varpi]}\Bigg]. \end{aligned} \tag{8.8}$$

Case 2. *Let $\mathfrak{F}(\mathfrak{s},t)$ be $[(\diamond\diamond)-\varpi]$-differentiable. Then, following Eq (5.14), similar results can be obtained.*

Case 3. *Let $\mathfrak{F}(\mathfrak{s},t)$ be $[(\diamond)-\varpi]$-differentiable and $\frac{\partial}{\partial t}\mathfrak{F}(\mathfrak{s},t)$ be $[(\diamond\diamond)-\varpi]$-differentiable, respectively. By following the similar methodology as in Case 1, the obtained fuzzy solution for Case 3 can be represented as*

$$\begin{cases} \underline{\mathfrak{F}}(\mathfrak{s},t,\gamma) = (\gamma)\left(e^{-(\mathfrak{s}-1)^2}+e^{-(\mathfrak{s}+1)^2}\right)+\Big[(2-\gamma)\Big(e^{-(\mathfrak{s}-1)^2}(2\mathfrak{s}-4(\mathfrak{s}-1)^2)+e^{-(\mathfrak{s}+1)^2}(2\mathfrak{s}+4-4(\mathfrak{s}+1)^2)\Big) \\ \qquad +2(2-\gamma)^2(e^{-(\mathfrak{s}-1)^2}+e^{-(\mathfrak{s}+1)^2})\left(e^{-(\mathfrak{s}-1)^2}(\mathfrak{s}-1)+e^{-(\mathfrak{s}+1)^2}(\mathfrak{s}+1)\right)\Big]\dfrac{t^{\varpi}}{\Gamma[1+\varpi]}+..., \\ \overline{\mathfrak{F}}(\mathfrak{s},t,\gamma) = (2-\gamma)\left(e^{-(\mathfrak{s}-1)^2}+e^{-(\mathfrak{s}+1)^2}\right)+\Big[\ \gamma\left(e^{-(\mathfrak{s}-1)^2}(2\mathfrak{s}-4(\mathfrak{s}-1)^2)+e^{-(\mathfrak{s}+1)^2}(2\mathfrak{s}+4-4(\mathfrak{s}+1)^2)\right) \\ \qquad +2\,\gamma^2\,(e^{-(\mathfrak{s}-1)^2}+e^{-(\mathfrak{s}+1)^2})\left(e^{-(\mathfrak{s}-1)^2}(\mathfrak{s}-1)+e^{-(\mathfrak{s}+1)^2}(\mathfrak{s}+1)\right)\Big]\dfrac{t^{\varpi}}{\Gamma[1+\varpi]}+.... \end{cases} \tag{8.9}$$

Thus, the truncated fuzzy solution to Eq (8.1) for Case 3 is given as follows:

$$\begin{aligned}\mathfrak{F}(\mathfrak{s},t,\gamma)=\Bigg[&(\gamma)\left(e^{-(\mathfrak{s}-1)^2}+e^{-(\mathfrak{s}+1)^2}\right)+\Big((2-\gamma)\Big(e^{-(\mathfrak{s}-1)^2}(2\mathfrak{s}-4(\mathfrak{s}-1)^2)+e^{-(\mathfrak{s}+1)^2}(2\mathfrak{s}+4-4(\mathfrak{s}+1)^2)\Big)\\&+2(2-\gamma)^2(e^{-(\mathfrak{s}-1)^2}+e^{-(\mathfrak{s}+1)^2})\Big(e^{-(\mathfrak{s}-1)^2}(\mathfrak{s}-1)+e^{-(\mathfrak{s}+1)^2}(\mathfrak{s}+1)\Big)\Big)\frac{t^{\varpi}}{\Gamma[1+\varpi]},\\&(2-\gamma)\left(e^{-(\mathfrak{s}-1)^2}+e^{-(\mathfrak{s}+1)^2}\right)+\Big(\gamma\left(e^{-(\mathfrak{s}-1)^2}(2\mathfrak{s}-4(\mathfrak{s}-1)^2)+e^{-(\mathfrak{s}+1)^2}(2\mathfrak{s}+4-4(\mathfrak{s}+1)^2)\right)\\&+2\gamma^2(e^{-(\mathfrak{s}-1)^2}+e^{-(\mathfrak{s}+1)^2})\Big(e^{-(\mathfrak{s}-1)^2}(\mathfrak{s}-1)+e^{-(\mathfrak{s}+1)^2}(\mathfrak{s}+1)\Big)\Big)\frac{t^{\varpi}}{\Gamma[1+\varpi]}\Bigg].\end{aligned}\tag{8.10}$$

To substantiate the convergence condition imposed in Theorem 6.1, we verify the component-wise convergence criterion for problem (8.1) with

$$\alpha=\beta=\gamma=1,\qquad 0<\varpi\leq 1,\qquad \mathfrak{s}\in\mathfrak{R}.$$

For the convergence analysis, we consider a finite time interval $0\leq t\leq T$. *Thus, the domain used for establishing uniform convergence is taken as* $W_T=\mathfrak{R}\times[0,T]$. *Now define*

$$G(\mathfrak{s})=e^{-(\mathfrak{s}-1)^2}+e^{-(\mathfrak{s}+1)^2}.$$

Then, the zeroth LRPSM component corresponding to the FICs of problem (8.1) is given by

$$\mathfrak{F}_0(\mathfrak{s},\gamma)=[\gamma G(\mathfrak{s}),\ (2-\gamma)G(\mathfrak{s})],\qquad 0\leq\gamma\leq 1.\tag{8.11}$$

Consequently, according to the fuzzy norm defined in Theorem 6.1,

$$\|\mathfrak{F}_0\|=2\sup_{\mathfrak{s}\in\mathbb{R}}|G(\mathfrak{s})|\approx 2.0397316.$$

Thus, the constant appearing in the initial bound can be selected as $N=2.0397316$.

For the first LRPSM coefficient, let

$$F_0(\mathfrak{s},\tilde{c})=\tilde{c}G(\mathfrak{s}),$$

where $\tilde{c}=[\gamma,2-\gamma]$ *stands for the lower and upper fuzzy endpoints, respectively. We have*

$$G_{\mathfrak{s}}=-2(\mathfrak{s}-1)e^{-(\mathfrak{s}-1)^2}-2(\mathfrak{s}+1)e^{-(\mathfrak{s}+1)^2},$$

and

$$G_{\mathfrak{s}\mathfrak{s}}=\left[4(\mathfrak{s}-1)^2-2\right]e^{-(\mathfrak{s}-1)^2}+\left[4(\mathfrak{s}+1)^2-2\right]e^{-(\mathfrak{s}+1)^2}.$$

Using $\alpha=\beta=\gamma=1$, *the first LRPSM coefficient is obtained as*

$$\phi_1(\mathfrak{s},\tilde{c})=-\tilde{c}G_{\mathfrak{s}}-\tilde{c}G(\mathfrak{s})G_{\mathfrak{s}}-\tilde{c}G_{\mathfrak{s}\mathfrak{s}}^2.\tag{8.12}$$

Hence, the first fuzzy LRPSM component can be expressed as

$$\mathfrak{F}_1(\mathfrak{s}, t, \vee) = [\phi_1(\mathfrak{s}, \vee), \phi_1(\mathfrak{s}, 2 - \vee)] \frac{t^{\varpi}}{\Gamma(1 + \varpi)}.$$

Consequently, by $\sup|\phi_1(s, \vartheta)| \approx 6.06512$,

$$\|\mathfrak{F}_1\| \leq \frac{6.06512\, T^{\varpi}}{\Gamma(1 + \varpi)}.$$

Therefore, the ratio of the first two successive LRPSM components satisfies

$$\rho_1 = \frac{\|\mathfrak{F}_1\|}{\|\mathfrak{F}_0\|} \leq 2.97343 \frac{T^{\varpi}}{\Gamma(1 + \varpi)}.$$

Thus, the contraction condition $\rho_1 < 1$ *is satisfied whenever*

$$T < \left[\frac{\Gamma(1 + \varpi)}{2.97343}\right]^{1/\varpi}.$$

The successive LRPSM components are then examined through the ratio

$$\rho_k = \frac{\|\mathfrak{F}_k\|}{\|\mathfrak{F}_{k-1}\|}, \qquad k \geq 1.$$

If there exists a constant $\rho < 1$ *such that* $\rho_k \leq \rho < 1, \ \ k \geq 1$, *then*

$$\|\mathfrak{F}_k\| \leq \rho^k \|\mathfrak{F}_0\| \leq N\rho^k.$$

Therefore,

$$\sum_{k=0}^{\infty} \|\mathfrak{F}_k\| \leq N \sum_{k=0}^{\infty} \rho^k = \frac{N}{1 - \rho} < \infty.$$

Hence, by the Weierstrass M-test, the fuzzy LRPSM series

$$\mathfrak{F}(\mathfrak{s}, t, \vee) = \sum_{k=0}^{\infty} \mathfrak{F}_k(\mathfrak{s}, t, \vee) \tag{8.13}$$

converges uniformly on W_T. *Furthermore, for the M-term approximation*

$$\mathfrak{F}_M(\mathfrak{s}, t, \vee) = \sum_{k=0}^{M} \mathfrak{F}_k(\mathfrak{s}, t, \vee), \tag{8.14}$$

the truncation error satisfies

$$\|\mathfrak{F} - \mathfrak{F}_M\| \leq \sum_{k=M+1}^{\infty} \|\mathfrak{F}_k\| \leq N \sum_{k=M+1}^{\infty} \rho^k = \frac{N\rho^{M+1}}{1 - \rho}.$$

Using $N = 2.0397316$*, this becomes*

$$\|\mathfrak{F} - \mathfrak{F}_M\| \leq \frac{2.0397316\,\rho^{M+1}}{1-\rho},$$

which leads to zero when $M \to 0$ *for* $\rho \in (0,1)$*. Thus, the LRPSM approximation converges uniformly to the fuzzy solution of problem (8.1) on* W_T*.*

For a numerical verification of the theoretical truncation-error estimate, we consider $\varpi = 0.75$ *on the finite time interval* $0 \leq t \leq 0.1$*. The first component ratio satisfies* $\rho_1 \approx 0.575324 < 1$*.*

Thus, the contraction condition is satisfied on the selected time interval. Using $\rho = 0.575324$ *in the theoretical estimate*

$$E_M \leq \frac{2.0397316\,\rho^{M+1}}{1-\rho},$$

the resulting truncation-error bounds are reported in Table 2. The error bound decreases progressively as the number of LRPSM terms increases, tending to zero as $M \to \infty$*, which numerically supports the theoretical convergence result established in Theorem 6.1.*

Table 2. Truncation-error bound E_M with $\varpi = 0.75$, $T = 0.1$, $N = 2.0397316$, and ρ=0.575324 for problem (8.1).

Number of terms M	Truncation-error bound E_M
0	2.763301
1	1.589794
2	0.914647
3	0.526219
4	0.302746
5	0.174177
6	0.100208

The fractional order ϖ *explicitly governs the temporal structure of the LRPSM solution as presented in Eq (6.1) through the fractional powers* $t^{k\varpi}$ *and the Gamma-function factors* $\Gamma(k\varpi+1)$*. Furthermore, the relationship clearly indicates that the temporal interval on which convergence is guaranteed by the contraction analysis depends upon the fractional order* ϖ*. Consequently,* ϖ *influences both the fractional temporal framework of the LRPSM solution and the sufficient temporal interval on which convergence is guaranteed, as determined by the contraction principle. If* $L_{\mathfrak{N}}$ *denotes the Lipschitz constant of the nonlinear operator* $\mathfrak{N}$*, the fractional integral estimate yields the sufficient contraction condition*

$$\frac{T^{\varpi} L_{\mathfrak{N}}}{\Gamma(\varpi+1)} < 1.$$

As a result, the permissible time frame in which convergence is guaranteed by the contraction principle is restricted by

$$T < T_*(\varpi) = \left[\frac{\Gamma(\varpi+1)}{L_{\mathfrak{N}}}\right]^{1/\varpi}.$$

Therefore, the fractional order does not merely modify the form of the LRPSM series; it also explicitly enters the sufficient temporal convergence bound through both $\Gamma(\varpi+1)$ *and the exponent* $1/\varpi$*.*

Example 2. *Consider a fractional-order NLTFFCRWPE given by*

$$\begin{cases} \frac{\partial^{\varpi}}{\partial t^{\varpi}}\mathfrak{F}(\mathfrak{s},t)+\alpha\frac{\partial}{\partial \mathfrak{s}}\mathfrak{F}(\mathfrak{s},t)+\beta\mathfrak{F}(\mathfrak{s},t)\left(\frac{\partial}{\partial \mathfrak{s}}\mathfrak{F}(\mathfrak{s},t)\right)+\gamma\frac{\partial^2}{\partial \mathfrak{s}^2}\mathfrak{F}(\mathfrak{s},t)=0, \qquad \varpi\in(0,1],\\ \mathfrak{F}(\mathfrak{s},0)=(\curlyvee-1,1-\curlyvee)(\operatorname{sech}\mathfrak{s}^2), \quad \mathfrak{s}\in\mathfrak{R}, \quad t\in(0,T]. \end{cases} \tag{8.15}$$

Case 1. *Let $\mathfrak{F}(\mathfrak{s},t)$ be $[(\diamond)-\varpi]$-differentiable. The truncated fuzzy solutions of Eq (8.15) can be presented as*

$$\begin{cases} \underline{\mathfrak{F}}(\mathfrak{s},t,\curlyvee) &= (\curlyvee-1)\operatorname{sech}^2(\mathfrak{s})+2(\curlyvee-1)\operatorname{sech}^2(\mathfrak{s})\frac{t^{\varpi}}{\Gamma(1+\varpi)}\underline{\mathbb{F}}_1(\mathfrak{s})+2(\curlyvee-1)\operatorname{sech}^2(\mathfrak{s})\frac{t^{2\varpi}}{\Gamma(1+2\varpi)}\underline{\mathbb{F}}_2(\mathfrak{s}),\\ \overline{\mathfrak{F}}(\mathfrak{s},t,\curlyvee) &= (1-\curlyvee)\operatorname{sech}^2(\mathfrak{s})+2(1-\curlyvee)\operatorname{sech}^2(\mathfrak{s})\frac{t^{\varpi}}{\Gamma(1+\varpi)}\overline{\mathbb{F}}_1(\mathfrak{s})+2(1-\curlyvee)\operatorname{sech}^2(\mathfrak{s})\frac{t^{2\varpi}}{\Gamma(1+2\varpi)}\overline{\mathbb{F}}_2(\mathfrak{s}), \end{cases} \tag{8.16}$$

where

$$\begin{aligned} \underline{\mathbb{F}}_1(\mathfrak{s}) &= \tanh(\mathfrak{s})+(\curlyvee-1)\operatorname{sech}^2(\mathfrak{s})\tanh(\mathfrak{s})+\operatorname{sech}^2(\mathfrak{s})-2\tanh^2(\mathfrak{s}),\\ \underline{\mathbb{F}}_2(\mathfrak{s}) &= \tanh(\mathfrak{s})-2\tanh^2(\mathfrak{s})-\operatorname{sech}^2(\mathfrak{s})+4(\curlyvee-1)\operatorname{sech}^2(\mathfrak{s})\tanh^2(\mathfrak{s})-(\curlyvee-1)\operatorname{sech}^4(\mathfrak{s}),\\ \overline{\mathbb{F}}_1(\mathfrak{s}) &= \tanh(\mathfrak{s})+(1-\curlyvee)\operatorname{sech}^2(\mathfrak{s})\tanh(\mathfrak{s})+\operatorname{sech}^2(\mathfrak{s})-2\tanh^2(\mathfrak{s}),\\ \overline{\mathbb{F}}_2(\mathfrak{s}) &= \tanh(\mathfrak{s})-2\tanh^2(\mathfrak{s})-\operatorname{sech}^2(\mathfrak{s})+4(1-\curlyvee)\operatorname{sech}^2(\mathfrak{s})\tanh^2(\mathfrak{s})-(1-\curlyvee)\operatorname{sech}^4(\mathfrak{s}). \end{aligned}$$

Case 2. *Let $\mathfrak{F}(\mathfrak{s},t)$ be $[(\diamond\diamond)-\varpi]$-differentiable. Then, following Eq (8.15), similar results can be obtained.*

Case 3. *Let $\mathfrak{F}(\mathfrak{s},t)$ be $[(\diamond)-\varpi]$-differentiable and $\frac{\partial}{\partial t}\mathfrak{F}(\mathfrak{s},t)$ be $[(\diamond\diamond)-\varpi]$-differentiable, respectively. By following the procedure as explained in the methodology for Case 3, the truncated solutions can be depicted as*

$$\begin{cases} \underline{\mathfrak{F}}(\mathfrak{s},t,\curlyvee) &= (\curlyvee-1)\operatorname{sech}^2(\mathfrak{s})+2(1-\curlyvee)\operatorname{sech}^2(\mathfrak{s})\frac{t^{\varpi}}{\Gamma(1+\varpi)}\overline{\mathbb{F}}_1(\mathfrak{s})+2(1-\curlyvee)\operatorname{sech}^2(\mathfrak{s})\frac{t^{2\varpi}}{\Gamma(1+2\varpi)}\overline{\mathbb{F}}_2(\mathfrak{s}),\\ \overline{\mathfrak{F}}(\mathfrak{s},t,\curlyvee) &= (1-\curlyvee)\operatorname{sech}^2(\mathfrak{s})+2(\curlyvee-1)\operatorname{sech}^2(\mathfrak{s})\frac{t^{\varpi}}{\Gamma(1+\varpi)}\underline{\mathbb{F}}_1(\mathfrak{s})+2(\curlyvee-1)\operatorname{sech}^2(\mathfrak{s})\frac{t^{2\varpi}}{\Gamma(1+2\varpi)}\underline{\mathbb{F}}_2(\mathfrak{s}), \end{cases} \tag{8.17}$$

where

$$\begin{aligned} \overline{\mathbb{F}}_1(\mathfrak{s}) &= \tanh(\mathfrak{s})+(1-\curlyvee)\operatorname{sech}^2(\mathfrak{s})\tanh(\mathfrak{s})+\operatorname{sech}^2(\mathfrak{s})-2\tanh^2(\mathfrak{s}),\\ \overline{\mathbb{F}}_2(\mathfrak{s}) &= \tanh(\mathfrak{s})-2\tanh^2(\mathfrak{s})-\operatorname{sech}^2(\mathfrak{s})+4(1-\curlyvee)\operatorname{sech}^2(\mathfrak{s})\tanh^2(\mathfrak{s})-(1-\curlyvee)\operatorname{sech}^4(\mathfrak{s}),\\ \underline{\mathbb{F}}_1(\mathfrak{s}) &= \tanh(\mathfrak{s})+(\curlyvee-1)\operatorname{sech}^2(\mathfrak{s})\tanh(\mathfrak{s})+\operatorname{sech}^2(\mathfrak{s})-2\tanh^2(\mathfrak{s}),\\ \underline{\mathbb{F}}_2(\mathfrak{s}) &= \tanh(\mathfrak{s})-2\tanh^2(\mathfrak{s})-\operatorname{sech}^2(\mathfrak{s})+4(\curlyvee-1)\operatorname{sech}^2(\mathfrak{s})\tanh^2(\mathfrak{s})-(\curlyvee-1)\operatorname{sech}^4(\mathfrak{s}). \end{aligned}$$

9. Application of the NLTFFCRWPE in the wound healing process

Wound healing is a highly structured biological process by which damaged tissue recovers its appearance and function after injury. Numerous biological processes, including cell migration, tissue regeneration, inflammation, nutrition transport, fibroblast activity, collagen deposition, and epithelial repair, interact with one another. Because such systems evolve over time and space, mathematical modeling provides a useful foundation for studying healing dynamics quantitatively. Wound healing does not occur uniformly in biological contexts. Healing rates might vary depending on the patient's health, age, infection, oxygen supply, immunological response, and therapy effects.

Fuzzy mathematical models are therefore helpful, since they take into consideration variability in the biological parameters or the initial wound profile. Further, fractional-order models are crucial since traditional integer-order derivatives are unable to adequately capture the memory and inherited behavior found in real tissues. Therefore, the NLTFFCRWPE model under consideration can be considered as a nonlinear wave-type biological transport model that describes the evolution and spread of healing activity in damaged tissue under uncertain biological circumstances.

The considered NLTFFCRWP problem is given by

$$\begin{cases} \frac{\partial^{\varpi}}{\partial t^{\varpi}}\mathfrak{F}(\mathfrak{s},t) + \alpha\frac{\partial}{\partial \mathfrak{s}}\mathfrak{F}(\mathfrak{s},t) + \beta\mathfrak{F}(\mathfrak{s},t)\left(\frac{\partial}{\partial \mathfrak{s}}\mathfrak{F}(\mathfrak{s},t)\right) + \gamma\frac{\partial^2}{\partial \mathfrak{s}^2}\mathfrak{F}(\mathfrak{s},t) = 0, \qquad \varpi \in (0,1], \\ \mathfrak{F}(\mathfrak{s},0) = (\curlyvee - 1, 1 - \curlyvee)\left(\frac{\mathfrak{F}_0+\epsilon}{2}\left[1 - \tanh(\urcorner(\mathfrak{s}+\mathbb{L}))\right] + \left[1 + \tanh(\urcorner(\mathfrak{s}-\mathbb{L}))\right]\right), \end{cases} \tag{9.1}$$

where $\frac{\partial^{\varpi}}{\partial t^{\varpi}}\mathfrak{F}(\mathfrak{s},t)$ illustrates the biological activity concentration profile or healing condition at time $t \in (0,T]$ and spatial point $\mathfrak{s} \in \mathfrak{R}$, and the fractional derivative $\frac{\partial^{\varpi}}{\partial t^{\varpi}}$ stands for the memory effect of biological tissue; $\alpha\frac{\partial}{\partial \mathfrak{s}}\mathfrak{F}(\mathfrak{s},t)$ depicts the linear transport; $\beta\mathfrak{F}(\mathfrak{s},t)\left(\frac{\partial}{\partial \mathfrak{s}}\mathfrak{F}(\mathfrak{s},t)\right)$ stands for nonlinear biological interaction; and dispersion or spreading effects inside tissue are described by the term $\gamma\frac{\partial^2}{\partial \mathfrak{s}^2}\mathfrak{F}(\mathfrak{s},t)$. The FICs demonstrate the uncertainty in the wound recovery process. The hyperbolic-tangent function in the FICs is utilized to create a smooth spatial transition between the damaged area and its surrounding tissue. The parameter $\urcorner$ controls the steepness of the transition in the initial wound profile, and the parameter $\mathbb{L}$ stands for the characteristic half-width of the damage region. The parameter $\urcorner$ governs the gradient of these transitions and hence influences the sharpness of the wound boundary: higher values of $\urcorner$ yield sharper transitions, while smaller values result in more gradual spatial profiles. The parameter $\mathbb{L}$ defines the typical spatial dimension of the wound by identifying the transition layers at $\mathfrak{s} = \pm\mathbb{L}$; hence, $2\mathbb{L}$ signifies the characteristic width of the wound area in the non-dimensional spatial coordinate. In this study, $\urcorner = \mathbb{L} = 1$ is employed to denote a normalized wound profile characterized by a mild transition steepness and a distinctive wound width of two spatial units. Such parameters thus offer a versatile framework for determining the initial spatial distribution of biological activity or concentration associated with the wound healing process. Moreover, to determine the fuzzy solution for this process using LRPSM, we apply the FLT and substitute the FICs; then Eq (9.1) can be presented as

$$\begin{cases} \mathfrak{L}\left[\underline{\mathfrak{F}}(\mathfrak{s},t)\right] = \frac{1}{q}(\curlyvee - 1)\left(\frac{\mathfrak{F}_0+\epsilon}{2}\left[1 - \tanh(\urcorner(\mathfrak{s}+\mathbb{L}))\right] + \left[1 + \tanh(\urcorner(\mathfrak{s}-\mathbb{L}))\right]\right) \\ \qquad\qquad - \frac{1}{q^{\varpi}}\mathfrak{L}\left[\alpha\frac{\partial}{\partial \mathfrak{s}}\underline{\mathfrak{F}}(\mathfrak{s},t) + \beta\underline{\mathfrak{F}}(\mathfrak{s},t)\left(\frac{\partial}{\partial \mathfrak{s}}\underline{\mathfrak{F}}(\mathfrak{s},t)\right) + \gamma\frac{\partial^2}{\partial \mathfrak{s}^2}\underline{\mathfrak{F}}(\mathfrak{s},t)\right], \\ \mathfrak{L}\left[\overline{\mathfrak{F}}(\mathfrak{s},t)\right] = \frac{1}{q}(1 - \curlyvee)\left(\frac{\mathfrak{F}_0+\epsilon}{2}\left[1 - \tanh(\urcorner(\mathfrak{s}+\mathbb{L}))\right] + \left[1 + \tanh(\urcorner(\mathfrak{s}-\mathbb{L}))\right]\right) \\ \qquad\qquad - \frac{1}{q^{\varpi}}\mathfrak{L}\left[\alpha\frac{\partial}{\partial \mathfrak{s}}\overline{\mathfrak{F}}(\mathfrak{s},t) + \beta\overline{\mathfrak{F}}(\mathfrak{s},t)\left(\frac{\partial}{\partial \mathfrak{s}}\overline{\mathfrak{F}}(\mathfrak{s},t)\right) + \gamma\frac{\partial^2}{\partial \mathfrak{s}^2}\overline{\mathfrak{F}}(\mathfrak{s},t)\right]. \end{cases} \tag{9.2}$$

The i-th truncated term series form of the solution of Eq (9.2) can be represented as

$$\begin{cases} \underline{\mathcal{Y}}(\mathfrak{s},q;\curlyvee) = \dfrac{1}{q}(\curlyvee-1)\Big(\dfrac{\mathfrak{F}_0+\epsilon}{2}\left[1-\tanh(\urcorner(\mathfrak{s}+\mathbb{L}))\right]+\left[1+\tanh(\urcorner(\mathfrak{s}-\mathbb{L}))\right]\Big)+\displaystyle\sum_{k=1}^{i}\frac{\underline{\varphi}_k(\mathfrak{s})}{q^{k\varpi+1}}, \\ \overline{\mathcal{Y}}(\mathfrak{s},q;\curlyvee) = \dfrac{1}{q}(1-\curlyvee)\Big(\dfrac{\mathfrak{F}_0+\epsilon}{2}\left[1-\tanh(\urcorner(\mathfrak{s}+\mathbb{L}))\right]+\left[1+\tanh(\urcorner(\mathfrak{s}-\mathbb{L}))\right]\Big)+\displaystyle\sum_{k=1}^{i}\frac{\overline{\varphi}_k(\mathfrak{s})}{q^{k\varpi+1}}, \end{cases} \tag{9.3}$$

and the i-Laplace residual functions of Eq (9.2) are given by

$$\begin{cases} \mathfrak{Q}\Big[Res_{\underline{\mathcal{Y}}_i}\Big] = \underline{\mathcal{Y}}(\mathfrak{s},q;\curlyvee)-\dfrac{1}{q}(\curlyvee-1)\Big(\dfrac{\mathfrak{F}_0+\epsilon}{2}\left[1-\tanh(\urcorner(\mathfrak{s}+\mathbb{L}))\right]+\left[1+\tanh(\urcorner(\mathfrak{s}-\mathbb{L}))\right]\Big) \\ \qquad\qquad +\dfrac{1}{q^{\varpi}}\mathfrak{Q}\Big[\alpha\dfrac{\partial}{\partial\mathfrak{s}}\underline{\mathfrak{F}}(\mathfrak{s},t)+\beta\underline{\mathfrak{F}}(\mathfrak{s},t)\Big(\dfrac{\partial}{\partial\mathfrak{s}}\underline{\mathfrak{F}}(\mathfrak{s},t)\Big)+\gamma\dfrac{\partial^2}{\partial\mathfrak{s}^2}\underline{\mathfrak{F}}(\mathfrak{s},t)\Big], \\ \mathfrak{Q}\Big[Res_{\overline{\mathcal{Y}}_i}\Big] = \overline{\mathcal{Y}}(\mathfrak{s},q;\curlyvee)-\dfrac{1}{q}(1-\curlyvee)\Big(\dfrac{\mathfrak{F}_0+\epsilon}{2}\left[1-\tanh(\urcorner(\mathfrak{s}+\mathbb{L}))\right]+\left[1+\tanh(\urcorner(\mathfrak{s}-\mathbb{L}))\right]\Big) \\ \qquad\qquad +\dfrac{1}{q^{\varpi}}\mathfrak{Q}\Big[\alpha\dfrac{\partial}{\partial\mathfrak{s}}\overline{\mathfrak{F}}(\mathfrak{s},t)+\beta\overline{\mathfrak{F}}(\mathfrak{s},t)\Big(\dfrac{\partial}{\partial\mathfrak{s}}\overline{\mathfrak{F}}(\mathfrak{s},t)\Big)+\gamma\dfrac{\partial^2}{\partial\mathfrak{s}^2}\overline{\mathfrak{F}}(\mathfrak{s},t)\Big]. \end{cases} \tag{9.4}$$

Substituting Eq (9.3) into Eq (9.4), and then solving the relations $\lim_{q\to\infty} q^{k\varpi+1}\mathfrak{Q}[Res_{\underline{\mathcal{Y}}_i}(\mathfrak{s},q;\curlyvee)] = 0$ and $\lim_{q\to\infty} q^{k\varpi+1}\mathfrak{Q}[Res_{\overline{\mathcal{Y}}_i}(\mathfrak{s},q;\curlyvee)] = 0$ recursively, the following terms of the lower and upper solutions can be written as

$$\begin{gathered} \underline{\mathfrak{A}} = \mathfrak{F}_0+\epsilon(\curlyvee-1), \\ \overline{\mathfrak{A}} = \mathfrak{F}_0+\epsilon(1-\curlyvee), \\ \begin{cases} \underline{\varphi}_0(\mathfrak{s};\curlyvee) = \underline{\mathfrak{A}}+\dfrac{\underline{\mathfrak{A}}}{2}\Big[\tanh(\urcorner(\mathfrak{s}-\mathbb{L}))-\tanh(\urcorner(\mathfrak{s}+\mathbb{L}))\Big], \\ \overline{\varphi}_0(\mathfrak{s};\curlyvee) = \overline{\mathfrak{A}}+\dfrac{\overline{\mathfrak{A}}}{2}\left[\tanh\left(\urcorner(\mathfrak{s}-\mathbb{L})\right)-\tanh\left(\urcorner(\mathfrak{s}+\mathbb{L})\right)\right], \end{cases} \end{gathered} \tag{9.5}$$

$$\begin{aligned} \underline{\varphi}_1(\mathfrak{s};\curlyvee) = {} & \frac{\underline{\mathfrak{A}}\urcorner}{2}\Big[-\operatorname{sech}^2(\urcorner(\mathfrak{s}-\mathbb{L}))+\operatorname{sech}^2(\urcorner(\mathfrak{s}+\mathbb{L}))\Big] \\ & +\underline{\mathfrak{A}}\urcorner^2\Big[\operatorname{sech}^2(\urcorner(\mathfrak{s}-\mathbb{L}))\tanh(\urcorner(\mathfrak{s}-\mathbb{L}))-\operatorname{sech}^2(\urcorner(\mathfrak{s}+\mathbb{L}))\tanh(\urcorner(\mathfrak{s}+\mathbb{L}))\Big] \\ & -\frac{\underline{\mathfrak{A}}^2\urcorner}{2}\Big[\operatorname{sech}^2(\urcorner(\mathfrak{s}-\mathbb{L}))-\operatorname{sech}^2(\urcorner(\mathfrak{s}+\mathbb{L}))\Big]\times\Big[1+\frac{1}{2}(\tanh(\urcorner(\mathfrak{s}-\mathbb{L}))-\tanh(\urcorner(\mathfrak{s}+\mathbb{L})))\Big], \end{aligned}$$

$$\begin{aligned} \overline{\varphi}_1(\mathfrak{s};\curlyvee) = {} & \frac{\overline{\mathfrak{A}}\urcorner}{2}\left[\operatorname{sech}^2\left(\urcorner(\mathfrak{s}+\mathbb{L})\right)-\operatorname{sech}^2\left(\urcorner(\mathfrak{s}-\mathbb{L})\right)\right] \\ & +\overline{\mathfrak{A}}\urcorner^2\left[\operatorname{sech}^2\left(\urcorner(\mathfrak{s}-\mathbb{L})\right)\tanh\left(\urcorner(\mathfrak{s}-\mathbb{L})\right)-\operatorname{sech}^2\left(\urcorner(\mathfrak{s}+\mathbb{L})\right)\tanh\left(\urcorner(\mathfrak{s}+\mathbb{L})\right)\right] \\ & -\frac{\overline{\mathfrak{A}}^2\urcorner}{2}\left[\operatorname{sech}^2\left(\urcorner(\mathfrak{s}-\mathbb{L})\right)-\operatorname{sech}^2\left(\urcorner(\mathfrak{s}+\mathbb{L})\right)\right]\times\left[1+\frac{1}{2}\left(\tanh\left(\urcorner(\mathfrak{s}-\mathbb{L})\right)-\tanh\left(\urcorner(\mathfrak{s}+\mathbb{L})\right)\right)\right]. \end{aligned}$$

Putting $\varphi_j(\mathfrak{s},\curlyvee)$, $j = 0,1,\ldots$ in Eq (9.3), the following expression is obtained as

$$\begin{cases} \underline{\mathcal{Y}}(\mathfrak{s},q;\vee)=\dfrac{1}{q}\Big[\underline{\mathfrak{A}}+\dfrac{\underline{\underline{\mathfrak{A}}}}{2}\Big(\tanh(\urcorner(\mathfrak{s}-\mathbb{L}))-\tanh(\urcorner(\mathfrak{s}+\mathbb{L}))\Big)\Big]+\dfrac{1}{q^{\varpi+1}}\Big[\dfrac{\underline{\mathfrak{A}}\urcorner}{2}\Big[-\operatorname{sech}^2(\urcorner(\mathfrak{s}-\mathbb{L}))+\operatorname{sech}^2(\urcorner(\mathfrak{s}+\mathbb{L}))\Big]\\ \quad+\underline{\mathfrak{A}}\urcorner^2\Big[\operatorname{sech}^2(\urcorner(\mathfrak{s}-\mathbb{L}))\tanh(\urcorner(\mathfrak{s}-\mathbb{L}))-\operatorname{sech}^2(\urcorner(\mathfrak{s}+\mathbb{L}))\tanh(\urcorner(\mathfrak{s}+\mathbb{L}))\Big]\\ \quad-\dfrac{\underline{\underline{\mathfrak{A}}}^2\urcorner}{2}\Big[\operatorname{sech}^2(\urcorner(\mathfrak{s}-\mathbb{L}))-\operatorname{sech}^2(\urcorner(\mathfrak{s}+\mathbb{L}))\Big]\\ \quad\times\Big[1+\dfrac{1}{2}(\tanh(\urcorner(\mathfrak{s}-\mathbb{L}))-\tanh(\urcorner(\mathfrak{s}+\mathbb{L})))\Big]\Big]+\ldots,\\ \overline{\mathcal{Y}}(\mathfrak{s},q;\vee)=\dfrac{1}{q}\overline{\mathfrak{A}}+\dfrac{\overline{\mathfrak{A}}}{2}\left[\tanh\left(\urcorner(\mathfrak{s}-\mathbb{L})\right)-\tanh\left(\urcorner(\mathfrak{s}+\mathbb{L})\right)\right]+\dfrac{1}{q^{\varpi+1}}\Big[\dfrac{\overline{\mathfrak{A}}\urcorner}{2}\Big[\operatorname{sech}^2\left(\urcorner(\mathfrak{s}+\mathbb{L})\right)-\operatorname{sech}^2\left(\urcorner(\mathfrak{s}-\mathbb{L})\right)\Big]\\ \quad+\overline{\mathfrak{A}}\urcorner^2\Big[\operatorname{sech}^2\left(\urcorner(\mathfrak{s}-\mathbb{L})\right)\tanh\left(\urcorner(\mathfrak{s}-\mathbb{L})\right)-\operatorname{sech}^2\left(\urcorner(\mathfrak{s}+\mathbb{L})\right)\tanh\left(\urcorner(\mathfrak{s}+\mathbb{L})\right)\Big]\\ \quad-\dfrac{\overline{\mathfrak{A}}^2\urcorner}{2}\Big[\operatorname{sech}^2\left(\urcorner(\mathfrak{s}-\mathbb{L})\right)-\operatorname{sech}^2\left(\urcorner(\mathfrak{s}+\mathbb{L})\right)\Big]\\ \quad\times\Big[1+\dfrac{1}{2}\left(\tanh\left(\urcorner(\mathfrak{s}-\mathbb{L})\right)-\tanh\left(\urcorner(\mathfrak{s}+\mathbb{L})\right)\right)\Big]\Big]+\ldots. \end{cases} \tag{9.6}$$

Applying the inverse FLT to Eq (9.6), the obtained results are as follows:

$$\begin{cases} \underline{\mathfrak{F}}(\mathfrak{s},t,\vee)=\underline{\mathfrak{A}}+\dfrac{\underline{\underline{\mathfrak{A}}}}{2}\Big(\tanh(\urcorner(\mathfrak{s}-\mathbb{L}))-\tanh(\urcorner(\mathfrak{s}+\mathbb{L}))\Big)+\Big[\dfrac{\underline{\mathfrak{A}}\urcorner}{2}\Big[-\operatorname{sech}^2(\urcorner(\mathfrak{s}-\mathbb{L}))+\operatorname{sech}^2(\urcorner(\mathfrak{s}+\mathbb{L}))\Big]\\ \quad+\underline{\mathfrak{A}}\urcorner^2\Big[\operatorname{sech}^2(\urcorner(\mathfrak{s}-\mathbb{L}))\tanh(\urcorner(\mathfrak{s}-\mathbb{L}))-\operatorname{sech}^2(\urcorner(\mathfrak{s}+\mathbb{L}))\tanh(\urcorner(\mathfrak{s}+\mathbb{L}))\Big]\\ \quad-\dfrac{\underline{\underline{\mathfrak{A}}}^2\urcorner}{2}\Big[\operatorname{sech}^2(\urcorner(\mathfrak{s}-\mathbb{L}))-\operatorname{sech}^2(\urcorner(\mathfrak{s}+\mathbb{L}))\Big]\\ \quad\times\Big[1+\dfrac{1}{2}(\tanh(\urcorner(\mathfrak{s}-\mathbb{L}))-\tanh(\urcorner(\mathfrak{s}+\mathbb{L})))\Big]\Big]\dfrac{t^{\varpi}}{\Gamma[1+\varpi]}+\ldots,\\ \overline{\mathfrak{F}}(\mathfrak{s},t,\vee)=\overline{\mathfrak{A}}+\dfrac{\overline{\mathfrak{A}}}{2}\left[\tanh\left(\urcorner(\mathfrak{s}-\mathbb{L})\right)-\tanh\left(\urcorner(\mathfrak{s}+\mathbb{L})\right)\right]+\Big[\dfrac{\overline{\mathfrak{A}}\urcorner}{2}\Big[\operatorname{sech}^2\left(\urcorner(\mathfrak{s}+\mathbb{L})\right)-\operatorname{sech}^2\left(\urcorner(\mathfrak{s}-\mathbb{L})\right)\Big]\\ \quad+\overline{\mathfrak{A}}\urcorner^2\Big[\operatorname{sech}^2\left(\urcorner(\mathfrak{s}-\mathbb{L})\right)\tanh\left(\urcorner(\mathfrak{s}-\mathbb{L})\right)-\operatorname{sech}^2\left(\urcorner(\mathfrak{s}+\mathbb{L})\right)\tanh\left(\urcorner(\mathfrak{s}+\mathbb{L})\right)\Big]\\ \quad-\dfrac{\overline{\mathfrak{A}}^2\urcorner}{2}\Big[\operatorname{sech}^2\left(\urcorner(\mathfrak{s}-\mathbb{L})\right)-\operatorname{sech}^2\left(\urcorner(\mathfrak{s}+\mathbb{L})\right)\Big]\\ \quad\times\Big[1+\dfrac{1}{2}\left(\tanh\left(\urcorner(\mathfrak{s}-\mathbb{L})\right)-\tanh\left(\urcorner(\mathfrak{s}+\mathbb{L})\right)\right)\Big]\Big]\dfrac{t^{\varpi}}{\Gamma[1+\varpi]}+\ldots. \end{cases} \tag{9.7}$$

Thus, the truncated fuzzy solution of Eq (9.1) can be presented as

$$
\begin{aligned}
\mathfrak{F}(\mathfrak{s},t,\vee) =& \Bigg[\underline{\mathfrak{A}} + \frac{\underline{\mathfrak{A}}}{2}\Big(\tanh(\urcorner(\mathfrak{s}-\mathbb{L})) - \tanh(\urcorner(\mathfrak{s}+\mathbb{L}))\Big) + \Bigg[\frac{\underline{\mathfrak{A}}\urcorner}{2}\Big[-\operatorname{sech}^2(\urcorner(\mathfrak{s}-\mathbb{L})) + \operatorname{sech}^2(\urcorner(\mathfrak{s}+\mathbb{L}))\Big] \\
&+ \underline{\mathfrak{A}}\urcorner^2\Big[\operatorname{sech}^2(\urcorner(\mathfrak{s}-\mathbb{L}))\tanh(\urcorner(\mathfrak{s}-\mathbb{L})) - \operatorname{sech}^2(\urcorner(\mathfrak{s}+\mathbb{L}))\tanh(\urcorner(\mathfrak{s}+\mathbb{L}))\Big] \\
&- \frac{\underline{\mathfrak{A}}^2\urcorner}{2}\Big[\operatorname{sech}^2(\urcorner(\mathfrak{s}-\mathbb{L})) - \operatorname{sech}^2(\urcorner(\mathfrak{s}+\mathbb{L}))\Big] \\
&\times\Big[1+\frac{1}{2}(\tanh(\urcorner(\mathfrak{s}-\mathbb{L})) - \tanh(\urcorner(\mathfrak{s}+\mathbb{L})))\Big]\Bigg]\frac{t^{\varpi}}{\Gamma[1+\varpi]}, \\
\overline{\mathfrak{A}} + \frac{\overline{\mathfrak{A}}}{2}&\left[\tanh\left(\urcorner(\mathfrak{s}-\mathbb{L})\right) - \tanh\left(\urcorner(\mathfrak{s}+\mathbb{L})\right)\right] + \left[\frac{\overline{\mathfrak{A}}\urcorner}{2}\left[\operatorname{sech}^2\left(\urcorner(\mathfrak{s}+\mathbb{L})\right) - \operatorname{sech}^2\left(\urcorner(\mathfrak{s}-\mathbb{L})\right)\right]\right. \\
&+ \overline{\mathfrak{A}}\urcorner^2\left[\operatorname{sech}^2\left(\urcorner(\mathfrak{s}-\mathbb{L})\right)\tanh\left(\urcorner(\mathfrak{s}-\mathbb{L})\right) - \operatorname{sech}^2\left(\urcorner(\mathfrak{s}+\mathbb{L})\right)\tanh\left(\urcorner(\mathfrak{s}+\mathbb{L})\right)\right] \\
&- \frac{\overline{\mathfrak{A}}^2\urcorner}{2}\left[\operatorname{sech}^2\left(\urcorner(\mathfrak{s}-\mathbb{L})\right) - \operatorname{sech}^2\left(\urcorner(\mathfrak{s}+\mathbb{L})\right)\right] \\
&\left.\times\left[1+\frac{1}{2}\left(\tanh\left(\urcorner(\mathfrak{s}-\mathbb{L})\right) - \tanh\left(\urcorner(\mathfrak{s}+\mathbb{L})\right)\right)\right]\right]\frac{t^{\varpi}}{\Gamma[1+\varpi]}\Bigg].
\end{aligned}
\tag{9.8}
$$

10. Results and discussion

The behavior of the resulting fuzzy approximate solution $\mathfrak{F}(\mathfrak{s},t)$ of the proposed NLTFFCRWPE under Caputo $g\mathbb{H}$-differentiability via LRPSM is displayed in three-dimensional surface plots and their corresponding two-dimensional plots. The lower and upper $\vee$-cut branches of the fuzzy solution $(\underline{\mathfrak{F}}(\mathfrak{s},t),\ \overline{\mathfrak{F}}(\mathfrak{s},t))$ describe the fuzzy solution's uncertainty band by two surfaces. In Figure 1, the lower and upper fuzzy solutions $(\underline{\mathfrak{F}}(\mathfrak{s},t),\ \overline{\mathfrak{F}}(\mathfrak{s},t))$ are plotted by taking the value $\varpi = 0.75$ and $\vee = 0.5$. A smooth wave-like profile with a bounded amplitude can be seen in this plot. The upper fuzzy surface $(\overline{\mathfrak{F}}(\mathfrak{s},t))$ reaches larger values, approximately around 1.5, while the lower fuzzy surface $(\underline{\mathfrak{F}}(\mathfrak{s},t))$ stays relatively modest. This shows that the uncertainty introduced by the fuzzy initial condition or fuzzy parameters results in a vertical spread in the solution. The broadness between the two surfaces indicates the degree of uncertainty in the wave amplitude. A larger distance between the surfaces implies that the fuzzy effect is more prominent, whereas a smaller distance suggests that the solution approaches the crisp case. This result is consistent with the $\mathcal{CRWP}$ model's projected nonlinear wave propagation. Furthermore, the surfaces are smooth with respect to both $\mathfrak{s}$ and t, which contributes to the stability of the LRPSM approximation. There are no rapid numerical fluctuations, discontinuities, or erratic jumps on the surface. In Figure 2, the corresponding two-dimensional plots for different fractional orders ϖ, fixing the value $\vee = 0.5$ and $t = 0.05$, govern the system's memory effect for the prescribed model. When the fractional order is smaller, the system has more memory and evolves more slowly. As the fractional order ϖ approaches 1, the NLTFFCRWP model converges to conventional integer-order behavior. The curves for different values of the fractional-order derivative ϖ are clearly distinguished, which proves that the memory effect exerts a more noticeable influence on the model's dynamics.

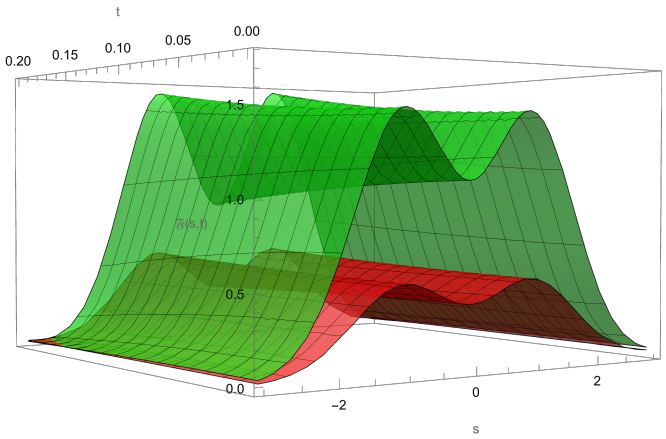


Figure 1. 3D plot of lower and upper bounds of $\mathfrak{F}(\mathfrak{s}, t)$ for $\curlyvee = 0.5$ and $\varpi = 0.75$.

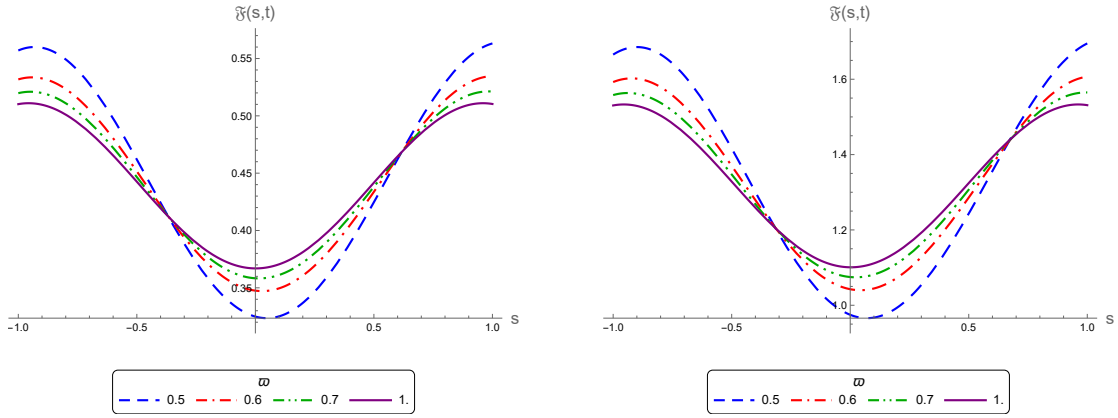


Figure 2. 2D plots of $\underline{\mathfrak{F}}(\mathfrak{s}, t)$ and $\overline{\mathfrak{F}}(\mathfrak{s}, t)$ for $\curlyvee = 0.5$ and $t = 0.05$, respectively (from left to right).

In Figure 3, the three-dimensional plot illustrates a distinctly significant hazy behavior. In this particular case, the upper solution $\overline{\mathfrak{F}}(\mathfrak{s}, t)$ predominantly retains a positive value, whereas the lower solution $\underline{\mathfrak{F}}(\mathfrak{s}, t)$ transitions into the negative region for certain values of $\mathfrak{s}$ and t. This suggests that the fuzzy solution band may intersect the zero level based on the lower boundary of the uncertainty range. In this plot, the value of the fractional derivative is taken as $\varpi = 0.6$ and $\curlyvee = 0.5$. $\overline{\mathfrak{F}}(\mathfrak{s}, t)$ creates a profile that resembles a crest, while $\underline{\mathfrak{F}}(\mathfrak{s}, t)$ forms a depressed shape. This signifies that the NLTFFCRWP model's solution is susceptible to uncertainty in some domains of study. Despite this, both surfaces remain smooth and confined, so verifying that the LRPSM approximation does not produce unstable or nonphysical numerical behavior inside the aforementioned domain. Further, in Figure 4, their corresponding two-dimensional plots with different values of ϖ, considering the values $\curlyvee = 0.5$ and fixing $t = 0.1$. The two-dimensional visualizations further validate the uniformity of the LRPSM solution. The continuity of the curves and their consistent variation over the fractional order suggest that the derived series solution is stable and convergent within the specified region. The findings reveal that uncertainty $\curlyvee$ mostly impacts the amplitude of the solution, whereas the fractional order ϖ affects the rate of temporal evolution and wave propagation.

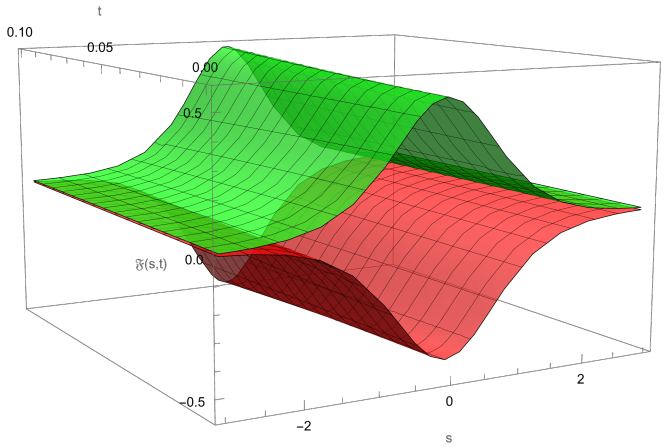


Figure 3. 3D plot of lower and upper bounds of $\mathfrak{F}(\mathfrak{s}, t)$ for $\Upsilon = 0.5$ and $\varpi = 0.6$.

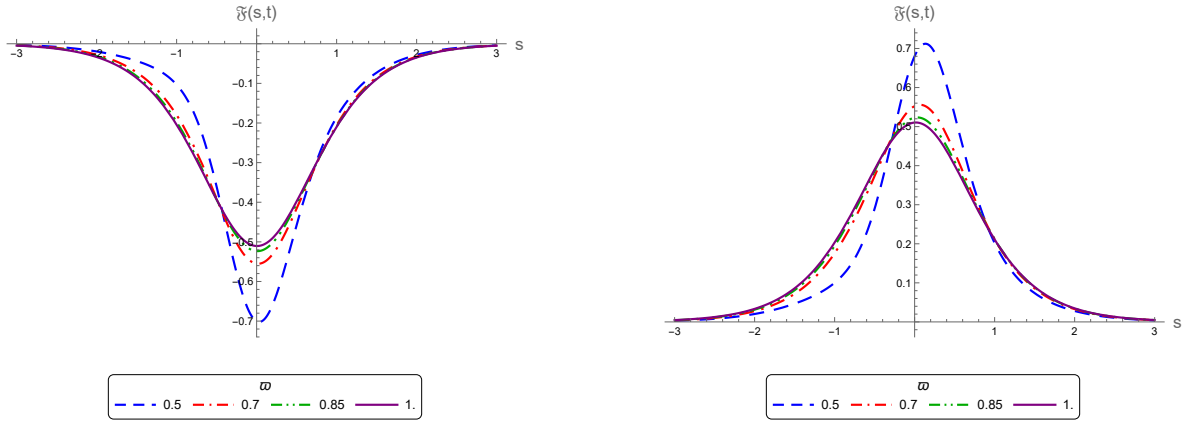


Figure 4. 2D plots of $\underline{\mathfrak{F}}(\mathfrak{s}, t)$ and $\overline{\mathfrak{F}}(\mathfrak{s}, t)$ for $\Upsilon = 0.5$ and $t = 0.1$, respectively (from left to right).

In Figure 5, the fuzzy healing response is represented by $\mathfrak{F}(\mathfrak{s}, t)$, which, depending on the biological interpretation of the NLTFFCRWP model, can be understood as the concentration of active healing cells, tissue recovery profile, or wound-healing density. The fuzzy uncertainty band of the wound-healing process is formed by the lower and upper surfaces. To plot the obtained fuzzy solutions for this healing process, the steepness K and width L are taken as 1, $\epsilon = 0.3$, $\mathfrak{s}_0 = 1$, the fractional derivative $\varpi = 0.7$, and $\Upsilon = 0.5$. The graph clearly depicts a localized decline at the middle of the spatial region. This depression indicates the wound area, where the healing reaction is slower than in the surrounding healthy tissue. Away from the wound center, the solution steadily rises and approaches a higher level, indicating that tissue away from the damaged area is less impacted and has a stronger biological reaction. This behavior has physical significance because, in wound-healing dynamics, the surrounding tissue supports the healing process through migration, proliferation, and diffusion-like spreading, while the central injured region typically has decreased cell density or decreased recovery activity at the initial stage. Moreover, the smooth valley-shaped structure is an important feature of the graph. This smoothness suggests that the LRPSM solution does not exhibit artificial oscillations, sudden jumps, or erratic numerical behaviour. As a result, the graphical results confirm the proposed approximate scheme's accuracy and stability within the chosen spatial and temporal domains. In

Figure 6, the impact of memory on the wound-healing process is further explained by the related two-dimensional graphs for various fractional order values. The model's memory strength is determined by the fractional order ϖ. The memory impact is greater, and the healing process proceeds more slowly, when ϖ is less. The healing reaction gets quicker and more straightforward as $\varpi \to 1$, bringing the fractional model closer to the traditional integer-order model. Further, the two-dimensional plots make it easier to see the upper and lower fuzzy bands. The lower solution $\underline{\mathfrak{F}}(\mathfrak{s}, t)$ describes the least favourable healing response, while the upper solution $\overline{\mathfrak{F}}(\mathfrak{s}, t)$ describes the most favourable healing response. If the band becomes narrow, the fuzzy solution approaches the crisp solution. If the band widens, uncertainty has a greater impact on the healing process.

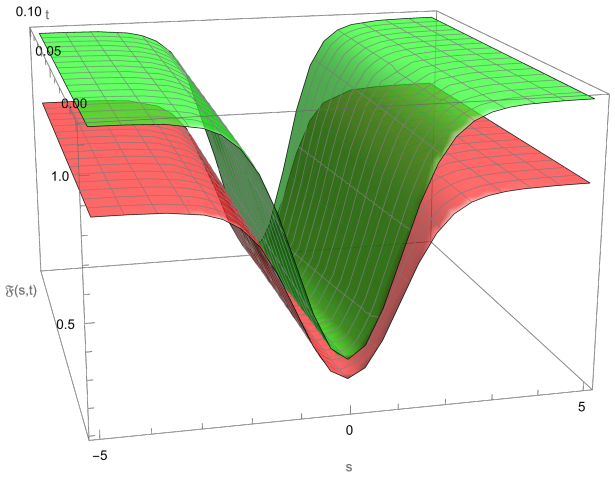


Figure 5. 3D plot of lower and upper bounds of the graph of $\mathfrak{F}(\mathfrak{s}, t)$ for $\Upsilon = 0.5$ and $\varpi = 0.7$.

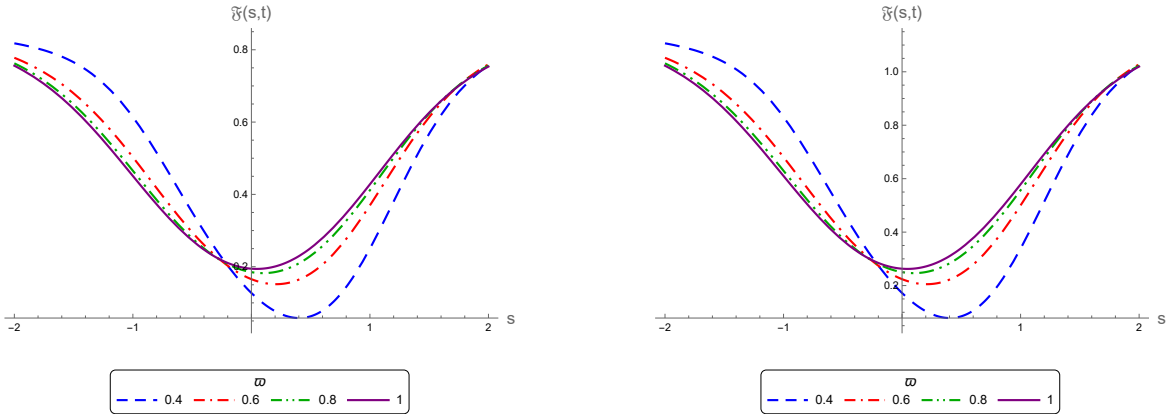


Figure 6. 2D plots of $\underline{\mathfrak{F}}(\mathfrak{s}, t)$ and $\overline{\mathfrak{F}}(\mathfrak{s}, t)$ for $\Upsilon = 0.5$ and $t = 0.1$, respectively (from left to right).

Table 3 demonstrates the numerical characteristics of the lower and upper fuzzy solutions of the proposed NLTFFCRWP model for different values of the fractional-order derivative ϖ and the Υ-cut level, where $\Upsilon \in [0, 1]$. Each pair $(\underline{\mathfrak{F}}(\mathfrak{s}, t), \overline{\mathfrak{F}}(\mathfrak{s}, t))$ denotes the respective lower and upper bounds of the fuzzy solution, which accurately illustrates the uncertainty propagation throughout the system. For each prescribed Υ-cut, the lower and higher endpoints typically rise as the fractional order ϖ ascends from 0.4 to 1. This behavior suggests that the fractional order markedly affects the extent

of the wound-healing profile, with elevated values of ϖ yielding relatively greater solution values for the specified parameter range. Furthermore, the width of the fuzzy interval varies correspondingly with the $\curlyvee$-cut level. As $\curlyvee$ approaches one, the lower and upper limits converge, indicating a decrease in uncertainty signified by higher-order fuzzy cuts. In particular, for $\curlyvee = 1$, the lower and upper bounds converge for each evaluated value of ϖ. This equality arises directly from the definition of the 1-cut of a fuzzy number, which reduces the fuzzy interval to its crisp core, rather than being a consequence of the integer-order case $\varpi = 1$. Consequently, the detected endpoint coincidence at $\curlyvee = 1$ should be regarded as a characteristic of the fuzzy representation, whereas the fluctuation of the solution's magnitude with ϖ signifies the impact of the fractional temporal dynamics. Moreover, to investigate the numerical stability and physical robustness of the proposed LRPSM formulation, the convection-diffusion parameters α, β, and γ are systematically changed from their reference values to 0.7, 0.3, and 0.1, respectively. The corresponding two-dimensional lower and upper solution profiles along with their numerical values are displayed in Figure 7 and Table 4. The obtained results show that the LRPSM approximation is numerically stable under these parameter fluctuations, and the solution profiles preserve their qualitative characteristics over the examined parameter regimes. From a physical perspective, α is a parameter that controls the strength of the directed transport or convection in the wound environment. Thus, decreasing α corresponds to a decrease in the strength of spatial transport associated with the redistribution or migration of the healing-related quantity. The parameter β governs the nonlinear interaction and the state-dependent transport mechanism, and hence its reduction correlates to a reduced nonlinear contribution to the evolution of the wound-healing profile. In contrast, γ is the diffusion or spatial-spreading process, and decreasing γ means less diffusive redistribution in the tissue. Despite these substantial variations in parameters, the lower and upper fuzzy solutions are well-defined and have consistent numerical behavior. Thus, the proposed LRPSM framework can provide stable approximations under different convection, nonlinear interaction, and diffusion-dominated regimes. This parameter-variation analysis therefore provides additional numerical evidence of the robustness of the proposed methodology and shows its applicability to wound-healing scenarios with different relative strengths of directed transport, nonlinear interaction, and spatial diffusion. The numerical findings further indicate that the fractional parameter serves as an effective means of regulating memory-dependent dynamics, while the fuzzy framework efficiently addresses the intrinsic uncertainties of the CRWP system. The obtained results confirm the efficiency of the suggested methodology for explaining complex biological processes influenced by fractional dynamics in uncertain circumstances.

From a computational perspective, the LRPSM offers a relatively systematic recursive approach for developing the approximate solution. During each iteration, the procedure necessitates the assessment of the residual components and corresponding recursive coefficients, while the fractional-order component is integrated via the LTmethodology. In contrast to the Adomian decomposition approach, LRPSM avoids the explicit formulation of Adomian polynomials, which may become progressively complex for highly nonlinear terms. In contrast to the variational iteration method, it also avoids the repetitive development and enhancement of correction functionals. As a result, the computing demands of LRPSM primarily involve the synthesis of recursive coefficients and the assessment of residuals, making the method appropriate for deriving truncated analytical approximations of the suggested fuzzy fractional model. However, the actual computational cost depends on the quantity of preserved terms, the complexity of the nonlinear operator, and the necessary accuracy of the approximation.

Besides implementing semi-analytical solution methodologies, intermittent and impulsive control strategies offer effective frameworks for managing nonlinear dynamical systems. Intermittent pinning impulsive control exerts impulses on designated nodes or spatial areas at predetermined intervals, whereas event-triggered intermittent impulsive control initiates interventions only when certain state-dependent criteria are achieved, thus minimizing irrelevant control measures. Asynchronous impulsive-based intermittent control facilitates interventions at non-synchronized intervals for various system components. In contrast to standard control-oriented methodologies, the current research emphasizes fuzzy fractional modeling and semi-analytical approximation of wound-healing dynamics based on LRPSM. These control strategies, however, offer encouraging alternatives for future developments in therapeutic interventions or localized treatment methods.

Table 3. Lower and upper fuzzy solutions of problem (9.1) for different γ and ϖ.

$\gamma \backslash \varpi$	0.4	0.6	0.8	1.0
0.0	(0.0812, 0.1509)	(0.1281, 0.2378)	(0.1501, 0.2787)	(0.1604, 0.2979)
0.1	(0.0847, 0.1474)	(0.1336, 0.2323)	(0.1565, 0.2722)	(0.1673, 0.2910)
0.2	(0.0882, 0.1439)	(0.1390, 0.2269)	(0.1629, 0.2658)	(0.1742, 0.2841)
0.3	(0.0917, 0.1404)	(0.1445, 0.2214)	(0.1693, 0.2594)	(0.1810, 0.2773)
0.4	(0.0952, 0.1369)	(0.1500, 0.2159)	(0.1758, 0.2529)	(0.1879, 0.2704)
0.5	(0.0986, 0.1335)	(0.1555, 0.2104)	(0.1822, 0.2465)	(0.1948, 0.2635)
0.6	(0.1021, 0.1300)	(0.1610, 0.2049)	(0.1886, 0.2401)	(0.2016, 0.2566)
0.7	(0.1056, 0.1265)	(0.1665, 0.1994)	(0.1951, 0.2337)	(0.2085, 0.2498)
0.8	(0.1091, 0.1230)	(0.1720, 0.1939)	(0.2015, 0.2272)	(0.2154, 0.2429)
0.9	(0.1126, 0.1195)	(0.1775, 0.1884)	(0.2079, 0.2208)	(0.2223, 0.2360)
1.0	(0.1161, 0.1161)	(0.1830, 0.1830)	(0.2144, 0.2144)	(0.2291, 0.2291)

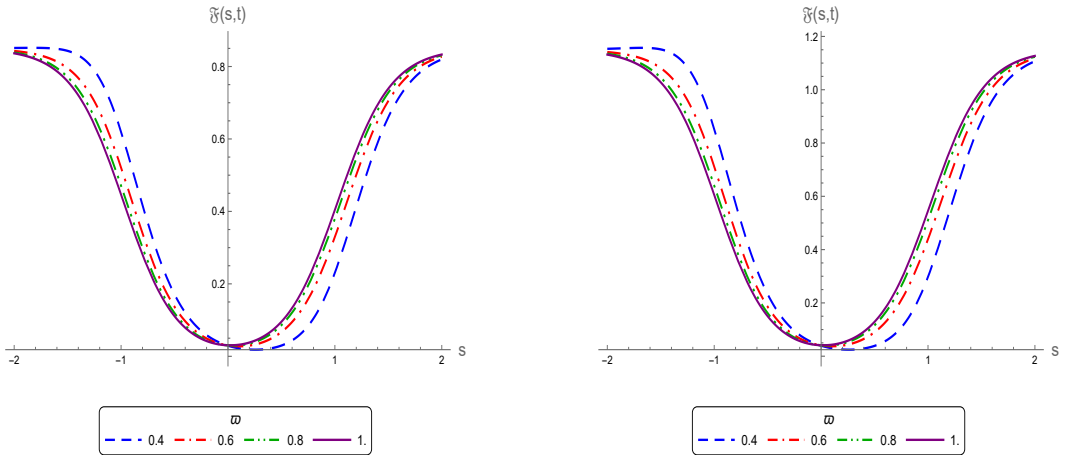


Figure 7. 2D plots of $\underline{\mathfrak{F}}(\mathfrak{s}, t)$ and $\overline{\mathfrak{F}}(\mathfrak{s}, t)$ for $\gamma = 0.5$ and $t = 0.1$, respectively (from left to right).

Table 4. Lower and upper fuzzy solutions of problem (9.1) for different $\curlyvee$ and ϖ.

$\curlyvee \backslash \varpi$	0.4	0.6	0.8	1.0
0.0	(0.018339, 0.033919)	(0.022790, 0.042255)	(0.025053, 0.046495)	(0.026159, 0.048566)
0.1	(0.019122, 0.033143)	(0.023764, 0.041283)	(0.026126, 0.045424)	(0.027280, 0.047446)
0.2	(0.019903, 0.032367)	(0.024739, 0.040311)	(0.027199, 0.044352)	(0.028400, 0.046326)
0.3	(0.020685, 0.031591)	(0.025714, 0.039339)	(0.028272, 0.043281)	(0.029521, 0.045205)
0.4	(0.021466, 0.030814)	(0.026688, 0.038367)	(0.029344, 0.042209)	(0.030641, 0.044085)
0.5	(0.022247, 0.030036)	(0.027662, 0.037395)	(0.030417, 0.041137)	(0.031762, 0.042965)
0.6	(0.023027, 0.029259)	(0.028636, 0.036422)	(0.031489, 0.040066)	(0.032882, 0.041845)
0.7	(0.023807, 0.028481)	(0.029610, 0.035449)	(0.032561, 0.038994)	(0.034003, 0.040725)
0.8	(0.024587, 0.027703)	(0.030583, 0.034476)	(0.033634, 0.037922)	(0.035123, 0.039605)
0.9	(0.025366, 0.026924)	(0.031557, 0.033503)	(0.034706, 0.036850)	(0.036244, 0.038484)
1.0	(0.026145, 0.026145)	(0.032530, 0.032530)	(0.035778, 0.035778)	(0.037364, 0.037364)

11. Conclusions

The current study emphasizes the significant challenge of solving nonlinear biological models in which complex interactions such as population dynamics, disease transmission, and metabolic processes add substantial nonlinearities into the governing equations. In this work, an enhanced NLTFFCRWP model is developed utilizing the fuzzy fractional Caputo $g\mathbb{H}$-derivative to represent a range of possible biological behaviour rather than a single fixed response. The suggested technique offers a mathematically rigorous extension of classical deterministic models by integrating memory-dependent fractional dynamics and uncertainty through a fuzzy formulation. The existence and uniqueness of the fuzzy solution for the NLTFFCRWP model, with specified FICs under the Caputo $g\mathbb{H}$-derivative, are demonstrated using Schauder's fixed point theorem and the Banach contraction principle. Furthermore, LRPSM, which combines the LTwith the RPS approach, is utilized to provide an effective approximate fuzzy solution for the suggested model. A comprehensive convergence analysis is conducted for the proposed fuzzy series solution, producing appropriate conditions to guarantee the consistent convergence of the approximate fuzzy solution to the corresponding exact fuzzy solution. The Ulam-Hyers stability of the suggested fractional fuzzy framework is examined using the Caputo $g\mathbb{H}$-derivative, illustrating the robustness and reliability of the derived solutions in terms of perturbations. Moreover, to prove the reliability and validity of the proposed model and suggested methodology, various examples are provided that enhance the novelty of this work. A real-world application of the NLTFFCRWP model along with suitable FICs for the wound healing process is also explained in detail, which demonstrates that healing activity spreads and changes in injured tissues under uncertain biological conditions. The obtained results demonstrate that the proposed methodology offers a reliable analytical framework for modeling nonlinear systems influenced by fractional dynamics in uncertain circumstances for handling real-world challenges across many scientific, biological, and engineering disciplines. Despite its benefits, the suggested fuzzy fractional framework possesses specific constraints. The model offers a basic description of wound-healing processes and does not specifically incorporate intricate immune-cell interactions, vascular development, tissue variability, or individual patient characteristics. Moreover, the parameters lack calibration with extensive experimental data; hence, the outcomes have to be regarded mostly as a

mathematical depiction rather than as direct clinical forecasts. Future study may include parameter estimation informed by experiments, heterogeneous tissue characteristics, and more precise biological mechanisms. However, it may also extend the suggested framework to incorporate multidimensional and diverse wound-healing models, facilitating the inclusion of more authentic tissue geometries and healing patterns. From a computational perspective, a comprehensive comparison of LRPSM with various semi-analytical and numerical approaches in terms of accuracy, rate of convergence, residual error, and computing cost would give further insight into the usefulness of LRPSM for fuzzy fractional biological systems.

Author contributions

Maria Sarfraz: Conceptualization, Methodology, Investigation, Visualization, Software, Writing–original draft; Ghazala Akram: Supervision, Conceptualization, Validation, Visualization, Software, Administration, Writing–Review & Editing; Khurram Shabbir: Validation, Visualization, Software, Review & Editing of the manuscript; Hafiz Abdul Wajid: Validation, Visualization, Software, Review & Editing of the manuscript. All authors have read and agreed to the published version of the manuscript.

Use of Generative-AI tools declaration

The authors declare they have not used Artificial Intelligence (AI) tools in the creation of this article.

Conflict of interest

All authors declare no conflicts of interest in this paper.

References

1. M. B. Abd-el-Malek, M. M. Kassem, M. L. M. Meky, Group theoretic approach for solving the problem of diffusion of a drug through a thin membrane, *J. Comput. Math.*, **14** (2002), 1–11. https://doi.org/10.1016/S0377-0427(01)00516-7
2. S. A. Abdelhafeez, A. A. M. Arafa, Y. H. Zahran, I. S. I. Osman, M. Ramadan, Adapting Laplace residual power series approach to the Caudrey-Dodd-Gibbon equation, *Sci. Rep.*, **14** (2024), 9772. https://doi.org/10.1038/s41598-024-57780-x
3. R. P. Agarwal, V. Lakshmikantham, J. J. Nieto, On the concept of solution for fractional differential equations with uncertainty, *Nonlinear Anal.-Theory*, **72** (2010), 2859–2862. https://doi.org/10.1016/j.na.2009.11.029
4. R. P. Agarwal, S. Arshad, D. O'Regan, V. Lupulescu, A Schauder fixed point theorem in semilinear spaces and applications, *Fixed Point Theory Appl.*, **2013** (2013), 306. https://doi.org/10.1186/1687-1812-2013-306
5. N. Ahmad, A. Ullah, A. Ullah, S. Ahmad, K. Shah, I. Ahmad, On analysis of the fuzzy fractional order Volterra-Fredholm integro-differential equation, *Alex. Eng. J.*, **60** (2021), 1827–1838. https://doi.org/10.1016/j.aej.2020.11.031

6. G. Akram, M. Sarfraz, Multiple optical soliton solutions for CGL equation with Kerr law nonlinearity via extended modified auxiliary equation mapping method, *Optik*, **242** (2021), 167258. https://doi.org/10.1016/j.ijleo.2021.167258
7. G. Akram, M. Sadaf, M. Sarfraz, N. Anum, Dynamics investigation of (1 + 1)-dimensional time-fractional potential Korteweg-de Vries equation, *Alex. Eng. J.*, **61** (2022), 501–509. https://doi.org/10.1016/j.aej.2021.06.023
8. M. Alaroud, M. Al-Smadi, R. R. Ahmad, U. K. Salma Din, An analytical numerical method for solving fuzzy fractional Volterra integro-differential equations, *Symmetry*, **11** (2019), 205. https://doi.org/10.3390/sym11020205
9. R. Alikhani, F. Bahrami, Fuzzy partial differential equations under the cross product of fuzzy numbers, *Inform. Sciences*, **494** (2019), 80–99. https://doi.org/10.1016/j.ins.2019.04.030
10. T. Allahviranloo, A. Armand, Z. Gouyandeh, Fuzzy fractional differential equations under generalized fuzzy Caputo derivative, *J. Intell. Fuzzy Syst.*, **26** (2014), 1481–1490. https://doi.org/10.3233/IFS-130831
11. M. Alinezhad, T. Allahviranloo, On the solution of fuzzy fractional optimal control problems with the Caputo derivative, *Inform. Sciences*, **421** (2017), 218–236. https://doi.org/10.1016/j.ins.2017.08.094
12. T. V. An, N. V. Hoa, The stability of the controlled problem of fuzzy dynamic systems involving the random-order Caputo fractional derivative, *Inform. Sciences*, **612** (2022), 427–452. https://doi.org/10.1016/j.ins.2022.08.076
13. M. Asif, S. Khan, H. Khan, S. Jebran, A computational strategy based on the residual power series method with the help of the Laplace transforms, *Fuzzy Information and Engineering*, **18** (2026), 223–250. https://doi.org/10.26599/FIE.2026.9270013
14. B. Bede, L. Stefanini, Generalized differentiability of fuzzy-valued functions, *Fuzzy Set. Syst.*, **230** (2013), 119–141. https://doi.org/10.1016/j.fss.2012.10.003
15. B. Bede, S. G. Gal, Generalizations of the differentiability of fuzzy-number-valued functions with applications to fuzzy differential equations, *Fuzzy Set. Syst.*, **151** (2005), 581–599. https://doi.org/10.1016/j.fss.2004.08.001
16. Y. C. Cano, H. R. Flores, On new solutions of fuzzy differential equations, *Chaos Soliton. Fract.*, **38** (2008), 112–119. https://doi.org/10.1016/j.chaos.2006.10.043
17. J. Chen, J. R. Holt, E. L. Evans, J. S. Lowengrub, M. M. Pathak, PIEZO1 regulates leader cell formation and cellular coordination during collective keratinocyte migration, *PLoS Comput. Biol.*, **20** (2024), e1011855. https://doi.org/10.1371/journal.pcbi.1011855
18. K. Diethelm, N. J. Ford, Analysis of fractional differential equations, *J. Math. Anal. Appl.*, **265** (2002), 229–248. https://doi.org/10.1006/jmaa.2000.7194
19. D. Dubois, H. Prade, Towards fuzzy differential calculus part 3: differentiation, *Fuzzy Set. Syst.*, **8** (1982), 225–233.
20. A. El Ghazouani, M. Elomari, S. Melliani, Solving higher-order fuzzy differential equations via Laplace residual power series approach, *TWMS J. Appl. Eng. Math.*, **15** (2025), 309–318.

21. T. Eriqat, R. Saadeh, A. El-Ajou, A. Qazza, M. N. Oqielat, A. Ghazal, A new analytical algorithm for uncertain fractional differential equations in the fuzzy conformable sense, *AIMS Mathematics*, **9** (2024), 9641–9681. https://doi.org/10.3934/math.2024472

22. M. Friedman, M. Ming, A. Kandel, Fuzzy derivatives and fuzzy Cauchy problems using LP metric, In: *Fuzzy logic foundations and industrial applications*, Boston: Springer, 1996, 57–72. https://doi.org/10.1007/978-1-4613-1441-7_3

23. D. Ghosh, J. R. Yaron, M. R. Abedin, S. Godeshala, S. Kumar, J. Kilbourne, et al., Bioactive nanomaterials kickstart early repair processes and potentiate temporally modulated healing of healthy and diabetic wounds, *Biomaterials*, **306** (2024), 122496. https://doi.org/10.1016/j.biomaterials.2024.122496

24. P. Guchhait, M. K. Maiti, M. Maiti, A production inventory model with fuzzy production and demand using fuzzy differential equation: an interval compared genetic algorithm approach, *Eng. Appl. Artif. Intel.*, **26** (2013), 766–778. https://doi.org/10.1016/j.engappai.2012.10.017

25. E. U. Haq, Q. M. U. Hassan, J. Ahmad, K. Ehsan, Fuzzy solution of system of fuzzy fractional problems using a reliable method, *Alex. Eng. J.*, **61** (2022), 3051–3058. https://doi.org/10.1016/j.aej.2021.08.034

26. O. Kaleva, Fuzzy differential equations, *Fuzzy Set. Syst.*, **24** (1987), 301–317. https://doi.org/10.1016/0165-0114(87)90029-7

27. E. Khodadadi, E. Çelik, The variational iteration method for fuzzy fractional differential equations with uncertainty, *Fixed Point Theory Appl.*, **2013** (2013), 13. https://doi.org/10.1186/1687-1812-2013-13

28. A. Mohammadzadeh, E. Kayacan, A novel fractional-order type-2 fuzzy control method for online frequency regulation in AC microgrid, *Eng. Appl. Artif. Intel.*, **90** (2020), 103483. https://doi.org/10.1016/j.engappai.2020.103483

29. S. Mukherjee, A. Kumar, S. Kumbhakar, Numerical simulation of fuzzy fractional differential equations using a reliable technique, *Journal of Fuzzy Extension and Applications*, **5** (2024), 159–172. https://doi.org/10.22105/jfea.2024.449034.1418

30. R. G. Nascimento, K. Fricke, F. A. Viana, A tutorial on solving ordinary differential equations using Python and hybrid physics-informed neural network, *Eng. Appl. Artif. Intel.*, **96** (2020), 103996. https://doi.org/10.1016/j.engappai.2020.103996

31. K. Odagiri, H. Fujisaki, H. Takada, R. Ogawa, Mathematical model for promotion of wound closure with ATP release, *Biophysics and Physicobiology*, **20** (2023), e200023. https://doi.org/10.2142/biophysico.bppb-v20.0023

32. M. N. Oqielat, T. Eriqat, O. Ogilat, A. El-Ajou, S. E. Alhazmi, S. Al-Omari, Laplace-residual power series method for solving time-fractional reaction-diffusion model, *Fractal Fract.*, **7** (2023), 309. https://doi.org/10.3390/fractalfract7040309

33. F. S. Pedro, M. M. Lopes, V. F. Wasques, E. Esmi, L. C. D. Barros, Fuzzy fractional differential equations with interactive derivative, *Fuzzy Set. Syst.*, **467** (2023), 108488. https://doi.org/10.1016/j.fss.2023.02.009

34. O. A. Peña, P. Martin, Cellular and molecular mechanisms of skin wound healing, *Nat. Rev. Mol. Cell Biol.*, **25** (2024), 599–616. https://doi.org/10.1038/s41580-024-00715-1

35. A. Puliyanda, K. Srinivasan, Z. Li, V. Prasad, Benchmarking chemical neural ordinary differential equations to obtain reaction network-constrained kinetic models from spectroscopic data, *Eng. Appl. Artif. Intel.*, **125** (2023), 106690. https://doi.org/10.1016/j.engappai.2023.106690

36. M. L. Puri, D. A. Ralescu, Differentials of fuzzy functions, *J. Math. Anal. Appl.*, **91** (1983), 552–558. https://doi.org/10.1016/0022-247X(83)90169-5

37. A. Rivaz, O. S. Fard, T. A. Bidgoli, On the existence and uniqueness of solutions for fuzzy fractional differential equations, *Tbilisi Math. J.*, **10** (2017), 197–205. https://doi.org/10.1515/tmj-2017-0013

38. N. Sajid, G. Akram, Solitary dynamics of longitudinal wave equation arises in magneto-electro-elastic circular rod, *Mod. Phys. Lett. B*, **35** (2021), 2150086. https://doi.org/10.1142/S021798492150086X

39. S. Salahshour, T. Allahviranloo, S. Abbasbandy, D. Baleanu, Existence and uniqueness results for fractional differential equations with uncertainty, *Adv. Differ. Equ.*, **2012** (2012), 112. https://doi.org/10.1186/1687-1847-2012-112

40. M. Sarfraz, G. Akram, Mathematical analysis and numerical simulation of fuzzy fractional generalized SIR epidemic model via powerful strategies, *Math. Comput. Simul.*, **251** (2027), 741–759. https://doi.org/10.1016/j.matcom.2026.08.019

41. K. Shah, A. R. Seadawy, M. Arfan, Evaluation of one dimensional fuzzy fractional partial differential equations, *Alex. Eng. J.*, **59** (2020), 3347–3353. https://doi.org/10.1016/j.aej.2020.05.003

42. M. Shahriyar, F. Ismail, S. Aghabeigi, A. Ahmadian, S. Salahshour, An eigenvalue-eigenvector method for solving a system of fractional differential equations with uncertainty, *Math. Probl. Eng.*, **2013** (2013), 579761. https://doi.org/10.1155/2013/579761

43. M. J. Simpson, K. M. Murphy, S. W. McCue, P. R. Buenzli, Discrete and continuous mathematical models of sharp-fronted collective cell migration and invasion, *R. Soc. Open Sci.*, **11** (2024), 240126. https://doi.org/10.1098/rsos.240126

44. H. N. Van, V. Ho, A survey on the initial value problems of fuzzy implicit fractional differential equations, *Fuzzy Set. Syst.*, **400** (2020), 90–133. https://doi.org/10.1016/j.fss.2019.10.012

45. A. Younus, M. Asif, U. Atta, T. Bashir, T. Abdeljawad, Applications of fuzzy conformable Laplace transforms for solving fuzzy conformable differential equations, *Soft Comput.*, **27** (2023), 8583–8597. https://doi.org/10.1007/s00500-023-08181-1

46. L. A. Zadeh, Fuzzy sets, *Information and Control*, **8** (1965), 338–353. https://doi.org/10.1016/S0019-9958(65)90241-X



AIMS Press

© 2026 the Author(s), licensee AIMS Press. This is an open access article distributed under the terms of the Creative Commons Attribution License (https://creativecommons.org/licenses/by/4.0)